AD-A129 282 NONLINEAR SCATTERING OF ACOUSTIC WAVES BY VIBRATING OBSTACLES(U) NAVAL RESEARCH LAB WASHINGTON DC J C PIQUETTE 01 JUN 83 NRL-MR-5077 1/2

UNCLASSIFIED F/G 20/1 NL

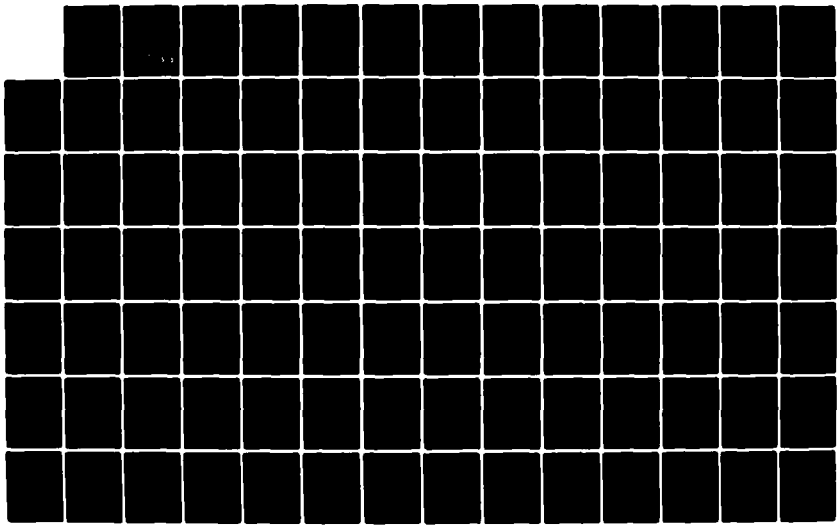

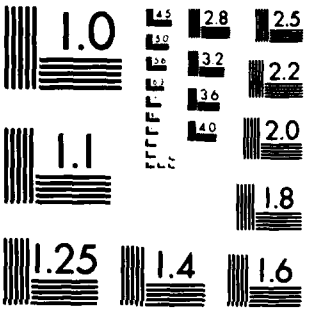

NRL Memorandum Report 5077

Nonlinear Scattering of Acoustic Waves by Vibrating Obstacles

Jean C. Piquette

Underwater Sound Reference Detachment
Naval Research Laboratory
P.O. Box 8337
Orlando, Florida 32856

1 June 1983

NAVAL RESEARCH LABORATORY
Washington, D.C.

UNCLASSIFIED

SECURITY CLASSIFICATION OF THIS PAGE (When Data Entered)

REPORT DOCUMENTATION PAGE		READ INSTRUCTIONS BEFORE COMPLETING FORM
1. REPORT NUMBER NRL MEMORANDUM REPORT 5077	2. GOVT ACCESSION NO. AD-A129 282	3. RECIPIENT'S CATALOG NUMBER
4. TITLE (and Subtitle) Nonlinear Scattering of Acoustic Waves by Vibrating Obstacles		5. TYPE OF REPORT & PERIOD COVERED Interim report on a continuing problem. 6. PERFORMING ORG. REPORT NUMBER
7. AUTHOR(s) Jean C. Piquette*		8. CONTRACT OR GRANT NUMBER(s)
9. PERFORMING ORGANIZATION NAME AND ADDRESS Naval Research Laboratory Underwater Sound Reference Detachment PO Box 8337, Orlando, Florida 32856		10. PROGRAM ELEMENT, PROJECT, TASK AREA & WORK UNIT NUMBERS 61153N, RR011-08-42 (59)-0589-00
11. CONTROLLING OFFICE NAME AND ADDRESS Office of Naval Research Direct Funding to Naval Res. Lab., Code 6500		12. REPORT DATE 1 June 1983 13. NUMBER OF PAGES 167
14. MONITORING AGENCY NAME & ADDRESS(if different from Controlling Office)		15. SECURITY CLASS. (of this report) UNCLASSIFIED 15a. DECLASSIFICATION/DOWNGRADING SCHEDULE

16. DISTRIBUTION STATEMENT (of this Report)

Approved for public release; distribution unlimited.

17. DISTRIBUTION STATEMENT (of the abstract entered in Block 20, if different from Report)

18. SUPPLEMENTARY NOTES

*This report is based on the author's doctoral dissertation submitted to the Stevens Institute of Technology in partial fulfillment of the degree requirements.

19. KEY WORDS (Continue on reverse side if necessary and identify by block number)

Scattering
Nonlinear acoustics
Calibration methods
Parametric phenomena
Integrals

20. ABSTRACT (Continue on reverse side if necessary and identify by block number)

The problem of the generation of sum- and difference-frequency waves produced via the scattering of an acoustic wave by an obstacle whose surface vibrates harmonically was studied both theoretically and experimentally. The theoretical approach involved solving the nonlinear wave equation, subject to appropriate boundary conditions, by use of a perturbation expansion of the fields and a Green's function method. This problem was previously studied theoretically by D. Censor (J. Sound & Vib. 25, 101-110, 1972), who solved the linear (over)

DD FORM 1 JAN 73 1473 EDITION OF 1 NOV 65 IS OBSOLETE
S/N 0102-LF-014-6601

cont
i

UNCLASSIFIED
SECURITY CLASSIFICATION OF THIS PAGE (When Data Entered)

20. Abstract (cont'd.)

wave equation with nonlinear boundary conditions. In addition to ordinary rigid-body scattering, Censor predicted nongrowing waves at frequencies equal to the sum and to the difference of the frequencies of the primary waves. The solution to the nonlinear wave equation also yields scattered waves at the sum and difference frequencies. However, the nonlinearity of the medium causes these waves to grow with increasing distance from the scatterer's surface and, after a very small distance, dominate those predicted by Censor.

The simple-source formulation of the second-order nonlinear wave equation for a lossless fluid medium has been derived for arbitrary primary wave fields. (Westevelt's original derivation in J. Acoust. Soc. Am. 35, 535-537, 1963) of this particular form of the nonlinear wave equation was restricted to plane waves.) This equation was used to solve the problem of nonlinear scattering of acoustic waves by a vibrating obstacle for three geometries: 1) a plane-wave scattering by a vibrating plane, 2) cylindrical-wave scattering by a vibrating cylinder, and 3) plane-wave scattering by a vibrating cylinder. A new technique of integration useful for solving definite integrals arising from physical problems is developed.

Successful experimental validation of the theory was inhibited by previously unexpected levels of nonlinearity in the hydrophones used. Such high levels of hydrophone nonlinearity appeared in hydrophones that, by their geometry of construction, were expected to be fairly linear. It appears that this is a rather general problem with hydrophones. A new technique for measuring this hydrophone nonlinearity is presented.

CONTENTS

Symbol List

a = particle rest position

a = radius of cylinder

$a(\nu)$ = Censor's expansion coefficient

A = radiated acoustic pressure amplitude of cylinder vibrating at angular frequency ω'

A' = radiated acoustic pressure amplitude of cylinder vibrating at angular frequency ω''

A_m = rigid-body scattering coefficients

$A(\nu)$ = Censor first-order expansion coefficient

b = cylinder-cylinder separation distance

B_n = expansion coefficient for $\rho_o(\partial q/\partial t)$

$B(\nu)$ = Censor second-order expansion coefficient

c = wave speed

c_o = infinitesimal wave speed

c_p = specific heat at constant pressure

$f^E(x,t)$ = arbitrary Eulerian function

$f^L(a,t)$ = arbitrary Lagrangian function

$g_n(r,r')$ = cylindrical Green's function

$H_m^{(1)}$ = Hankel function of the first kind

J_m = Bessel function of the first kind

k = thermal conductivity

k_c = ω_c/c_o

k_- = $(\omega'-\omega'')/c_o$

N_m = Bessel function of the second kind

P = pressure in fluid

P = second-order pressure in fluid

P_c = acoustic pressure amplitude radiated by cylinder frequency ω_c

$P^E(x,t)$ = Eulerian acoustic pressure

P_i = incident plane-wave acoustic pressure

$P^L(a,t)$ = Lagrangian acoustic pressure

P_n = pressure in fluid associated with frequency n

P_p = acoustic pressure amplitude of plane wave

P_r = radiated plane-wave acoustic pressure

P_{tot} = total first-order acoustic pressure for cylindrical wave scattering from a vibrating cylinder

P_1 = first-order pressure in fluid

$P_{2\pm}$ = second-order particle pressure due to sum and difference frequencies

q = simple source strength

r = magnitude of cylindrical radius vector

$r_{>(<)}$ = the greater(lesser) of r and b

s = mass source term

S = entropy

T = Stress-Tensor

T_{ij} = components of Stress-Tensor

u = particle velocity

u_i = component of particle velocity

u_i = Censor incident pressure

u_{inc} = incident particle velocity wave

u_s = Censor scattered pressure

u_{scatt} = scattered particle velocity wave

u_1 = first-order particle velocity

u_2 = second-order particle velocity

x = position of point in space

Γ = nonlinearity fluid parameter

δ_{nm} = Kronecker delta

$\delta(\vec{r}-\vec{r}')$ = Dirac delta function

ε = Censor small expansion parameter

ε = expansion parameter of order Mach number

θ = Censor operator $\equiv \nu^{-2}(\partial/\partial x)$

ξ = displacement

ν = frequency

ξ_1 = first-order particle displacement

$\xi_{2\pm}$ = second-order particle displacement due to sum and difference frequencies

ρ = variable fluid mass density

ρ_o = ambient fluid mass density

ρ_1 = first-order mass density

ρ_2 = second-order mass density

ϕ = velocity potential

$\phi_{(1)}$ = first-order velocity potential

ω = angular frequency = $2\pi\nu$

ω' = angular frequency of cylinder vibration

$\omega_\pm$ = sum- and difference-angular frequencies

Ω = angular frequency of deformation of surface

$\Box^2$ = D'Alembertian operator = $\nabla^2 - [(1/c_o^2)(\partial^2/\partial t^2)]$

1. INTRODUCTION

This thesis addresses the problem of the nonlinear scattering of acoustic waves with harmonic time dependence by a vibrating obstacle. The obstacle is immersed in an infinite homogeneous fluid medium, and its surface deforms uniformly with harmonic time dependence. The case in which the surrounding fluid medium is water is of primary interest.

The problem of the scattering of a plane wave incident on acoustically rigid spherical and cylindrical obstacles surrounded by an infinite homogeneous fluid medium was first solved by Rayleigh [1] using linear, lossless theory. To obtain numerical values for the rather complicated mathematical solutions, he considered only the limiting case where the radius of the scatterer is much smaller than a wavelength. These results were extended by Morse [2], who obtained a solution in a form more readily evaluated. He provided tables of calculated values, including values when the obstacle is not small compared to a wavelength. Faran [3] obtained a solution in the case where the scattering obstacles are not acoustically rigid. In addition to studying the problem theoretically, Faran performed an experimental investigation of the cylindrical case. Agreement between theory and experiment was excellent and resulted in the establishment of a proper criterion under which a scattering object could be considered acoustically rigid; namely, that the frequency of the incident plane wave be well below that of the lowest mechanical resonance of the scatterer. The non-rigid spherical case was studied experimentally by Hampton and McKinney [4].

All of the studies mentioned above assumed that the linear wave equation was sufficient to describe the situation of interest. However, the exact equations describing acoustic wave propagation in a fluid (as well as for solids and plasmas) are actually nonlinear. The linear wave equation is only an approximation that is valid for small amplitude behavior. Deviations in behavior from that predicted by the linear wave equation can become significant when the Mach number (ratio of particle velocity to phase velocity or, equivalently, the ratio of the change in mass density to the density of the undisturbed fluid) is not much less than unity [5]. In this case, the nonlinear wave equation is required to accurately represent the behavior. The study of acoustical behavior requiring use of the nonlinear wave equation is called nonlinear or finite-amplitude acoustics.

Most solutions of the nonlinear wave equation for fluids have been restricted o plane waves in homogeneous infinite media. In 1860, Earnshaw [6] obtained an implicit solution to the lossless, one-dimensional, nonlinear wave equation subject to a boundary condition at the origin. That solution is valid at propagation distances small relative to the plane-wave discontinuity distance (that propagation distance at which the solution to the lossless nonlinear wave equation for a wave sinusoidal at its origin becomes multiple-valued. This occurs because points of high particle velocity in the wave also have higher propagation velocities and hence tend to overtake the points of low particle velocity, causing the waveform to approach a sawtooth shape. It is proportional to the Mach number and is a convenient measure of the nonlinearity of the problem.*) Earnshaw's solution illustrated that points of high particle velocity/pressure in the time waveform (i.e., the variation with time of the particle velocity/pressure at a fixed position) move more rapidly than points of low particle velocity/pressure. This causes the time waveform of a finite amplitude wave to change its shape (i.e., distort) as the wave propagates. Investigators of this problem usually assume an acoustic wave that is sinusoidal (i.e., harmonic) at its point of origin and utilize a harmonic time analysis of the waveform to describe the subsequent propagation of the wave. The distortion of the waveform from its initial state manifests itself in the generation of harmonic component waves. In effect, a wave of angular frequency ω generates waves of angular frequencies 2ω, 3ω, etc. as it propagates. These harmonic components usually gain energy at the expense of the fundamental component of angular frequency ω.

- - - - - - - - - - -

*In a real situation, the solution never actually becomes multiple valued. It is prevented from doing so due to energy loss due to the viscous terms that are no longer negligible when the discontinuity distance is approached. (Nonetheless, the onset of shock-wave formulation occurs near the discontinuity distance.) In higher-dimensioned problems there is no corresponding discontinuity distance since geometric spreading is sufficient to prevent this catastrophic growth of the nonlinearly generated wave. Nonetheless, it represents a conservative estimate of the distance to which the lossless theory may be applied. It is given by Beyer (Reference 5, p. 104) as:

$$(1/\ell) \approx [1+(B/2A)][(\omega u_o)/c_o^2],$$

where $A = \rho_o(\partial P/\partial \rho)_{S,\rho=\rho_o} = \rho_o c_o^2$, $B = \rho_o^2(\partial^2 P/\partial \rho^2)_{S,\rho=\rho_o}$, ℓ = discontinuity distance. For water at 20°C, B/A is approximately 5.0.

In 1935, Fubini-Ghiron [7] obtained an explicit form for Earnshaw's implicit solution for the case of an initially harmonic wave. He expressed his solution as a Fourier harmonic series with Bessel function coefficients.

In 1960, Kech and Beyer [8] obtained a solution to the problem of the propagation of an initially harmonic plane wave including linear absorptive losses. To obtain this solution, they assumed that each of the acoustic variables can be written in a perturbation series in which the order of magnitude of each term is smaller than that of the preceding term by a factor equal to the Mach number. They then calculated in succession the first six terms of the perturbation series solution for the particle displacement. This gives an approximation to the exact solution that is useful for distances of propagation somewhat less than the plane-wave discontinuity distance.

In 1958, Hayes [9] succeeded in putting the equations of motion (including thermoviscous losses) into the form of a Burgers' equation [10]. Hayes does not make clear in this derivation to what order in Mach number this equation is valid. In 1963, however, Blackstock [11] again put the equations of motion, including thermoviscous losses, into the form of a Burgers' equation. This treatment makes it quite clear that the equation is valid to second order in Mach number. In Reference 11, Blackstock introduces the term "substitution corollary" for the standard procedure used to identify the ordering of terms. In essence, this corollary states that in obtaining a second-order approximation, the individual acoustic variables involved in forming any term comprised of a product of acoustic variables may freely be replaced by their first-order equivalents. A more precise substitution would generate terms higher than second order. This formulation has great utility in that exact solutions of Burgers' equation exist. Blackstock [11,12] succeeded in obtaining such a solution for an initially harmonic plane wave.

In 1964, Blackstock [13] showed that when the spatial coordinate is large relative to a wavelength, Burgers' equation can also be used to solve the problem of propagation of spherical and cylindrical waves in a lossless medium (if the frequency is not large, losses may still be ignored large propagation distances). In 1981, Trivett and Van Buren [14] developed a numerical method of solving the Burgers' equation for plane, cylindrical, and spherical waves including losses.

Significant nonlinear generation of acoustic waves can also occur when two waves of different frequency are present simultaneously in a fluid medium. In 1948, Eckart [15] derived a second-order nonlinear wave equation (re-derived by Westervelt [16] in 1957) useful in obtaining solutions to this type of problem. In 1963, Westervelt [17] considered the problem of two colinear plane waves (called primaries) with different initial harmonic time dependences at the origin. He started with Lighthill's [18] equations of motion and retained terms up to the quadratic in Mach number. In addition to the harmonics of the primaries predicted when a plane wave propagates and distorts in a fluid medium, waves at frequencies equal to the sum and difference of the primary-wave frequencies were also predicted. These sum- and difference-frequency waves tend to grow with increasing distance from the origin. In this paper, Westervelt essentially transformed Eckart's second-order nonlinear wave equation into a form known as the simple-source formulation. This transformation, however, was restricted to the case of plane wave primaries.

Westervelt's theory was confirmed experimentally by Bellin and Beyer [19], who produced a 1-MHz difference-frequency wave by driving a 2.54-cm-diam circular piston source at the primary frequencies 13 and 14 MHz. Agreement between theory and experiment was good.

In 1962, Dean [20] presented a solution for the sum-frequency wave produced by two outgoing, concentric cylindrical waves. He again started from the basic conservation equations and derived a coupled set of differential equations (accurate to second order in Mach number) in terms of a new set of variables (defined in terms of operations on the first- and second-order acoustic quantities). Dean stated that the solution he presented to these equations for this particular case was exact. Lauvstad [21] later stated that Dean's solution to this problem was incorrect except in the farfield. He stated that direct substitution of Dean's solution into the equations demonstrated their incorrectness except, as previously mentioned, in the asymptotic limit approaching the farfield. This, however, is not so. Dean later performed measurements that were in fair agreement with the qualitative aspects of his theory [22]. (No attempt was made to demonstrate quantitative agreement with the theory.) These measurements were performed under farfield conditions. Lauvstad offered his own general expression for the sum-frequency component; however, he used the Green's function corresponding to the

unphysical case of a soft boundary. A correct expression for the difference-frequency pressure for this case will be obtained in this report.

In 1972, Censor [23] solved the linear wave equation for the problem of the scattering of an acoustic plane wave (of angular frequency ω) by an obstacle whose surface deforms harmonically (at angular frequency Ω). In his calculation, Censor included nonlinearities only in the boundary conditions he imposed. He predicted that in addition to the usual rigid-body scattered field, waves at angular frequency $\omega_{\pm} = \omega \pm \Omega$ would be created at the boundary. These waves would then propagate outward from the boundary with a behavior described by the linear wave equation.

Shortly after the appearance of Censor's article, Rogers [24] pointed out that waves at angular frequencies $\omega_{\pm}$ arising from medium nonlinearities would also be predicted by the nonlinear wave equation. Rogers also stated that the effects predicted by Censor depend on the Mach number in the same way as the effects arising from nonlinear theory. Hence, the propagation problem cannot be linearized in any physically meaningful way without also eliminating the boundary effect predicted by Censor. In other words, a solution to the problem of the generation of sum- and difference-frequency waves must necessarily involve solving the nonlinear wave equation.

In the present study, the simple-source formulation of the second-order, nonlinear wave equation for a lossless medium is derived for arbitrary primary wave fields of harmonic time dependence. This equation was previously derived by Westervelt [25]; however, his treatment, as previously mentioned, was restricted to plane-wave primaries. The assumption that no linear losses, such as those due to viscosity or heat conduction, exist in the fluid medium places restrictions on the subsequent solution. These restrictions tend to increase with increasing viscosity and frequency. However, the restrictions are not expected to be significant for the case of a water medium and the frequencies to which the solution will be normally applied (less than about 200 kHz). In obtaining this equation, all terms up to the quadratic in Mach number are retained in the acoustic variables. A perturbation approach is not used until the final step in the derivation; hence, the equation upon which the simple-source formulation is based remains valid even when the second-order effects cause a significant energy drain on the primaries (which invalidates a perturbation-series approach).

In obtaining solutions to this equation, a Born-approximation type of perturbation analysis is used. Here, first-order acoustic wave fields are calculated as solutions to the linear wave equation and then used to determine the inhomogeneous term of the second-order equation. The perturbation analysis is in terms of the Mach number. (Perturbation expansions in terms of Mach number to solve acoustic problems have been used extensively before [15,16,26,27].)

The problem of the generation of sum- and difference-frequency waves via the nonlinear scattering of acoustic waves by vibrating obstacles is then addressed for three geometries:

1. Plane wave normally incident on a uniformly vibrating infinite plane.

2. Cylindrical wave incident on an infinitely long cylinder vibrating uniformly in the radial direction. (The symmetry axes of the incident wave and the scattering cylinder are assumed parallel but not coincident.)

3. Plane wave normally incident on an infinitely long cylinder vibrating uniformly in the radial direction.

The first case above is readily solved after expressing the second-order nonlinear wave equation in one-dimensional form, due to the resulting simplicity of the calculations. Solution of the last two cases is much more difficult. The approach taken is to formulate the solutions in terms of a Green's function. Care must be taken to choose the proper Green's function for evaluating the appropriate Born integral; i.e., the one corresponding to the boundary surfaces involved (this requirement has been discussed previously in a paper presented by the author [28]). The resulting expressions for the acoustic pressure of the sum- and difference-frequency components involve some rather complicated integrals. A new integration procedure was developed that allows the evaluation of these integrals in closed form for the case of two high-frequency primaries. This procedure is described in the Appendix. Numerical results are obtained by Gaussian quadrature integration for the more general case.

The results obtained by the Censor-method approach are also calculated and presented for the two cases for which his theory are applicable--those involving incident plane waves. It is demonstrated that Censor's prediction is of the same order as pseudosound*.

For the case of a plane wave incident on a vibrating cylinder, the results are presented graphically for both the Censor theory and the nonlinear theory.

An experimental investigation was undertaken to confirm the theoretical prediction for the difference-frequency pressure produced in the case in which a plane wave is incident on a vibrating cylindrical surface. Although the experiment was unsuccessful in confirming the theoretical predictions, it was nonetheless successful in identifying several of the difficulties that arise in nearfield, nonlinear difference-frequency experiments and solving all but one of those identified. The most significant of these difficulties (not encountered in previously published work) are:

•Inadvertent direct radiation of the sources at the difference frequency: This will tend to be a greater source of error when the measuring hydrophone is near the sources (since difference-frequency pressures produced by medium nonlinearities tend to grow with distance while directly radiated different-frequency pressure tends to decay with distance).

•Electrical filtering problems due to experimental constraints: The difference frequency was only about one half the lowest primary

- - - - - - - - - - -

*Pseudosound is an effect arising from the uncertainty in the motion of the measuring hydrophone; i.e., the uncertainty in the motion of the hydrophone is of the same order as the difference between Langrangian and Eulerian coordinates. Although pseudosound is of second-order in Mach number (as are the source terms of the second-order nonlinear wave equation), it nonetheless remains a minor component of the second-order field. This is because contributions to the pressure predicted by the acoustic second-order nonlinear wave equation are cumulative with respect to propagation distance and hence tend to overwhelm pseudosound (which is a function only of the magnitude of the acoustic variables at the observation point) within propagation distances that are a fraction of a wavelength. Example calculations of pseudosound relevant to the current research are provided in Sections II. E. 3 and IV. F.

frequency. In addition, the pulse lengths had to be less than about 10 cycles at the difference frequency to avoid interfering reflections from neighboring surfaces. Hence the usual passive methods employed for electrical filtering in previous farfield, nonlinear measurements were inappropriate.

•Difference-frequency voltage generated nonlinearly in the hydrophone: This effect, due to nonlinear mixing of the primaries in the hydrophone, provided larger difference-frequency voltages than those produced by the difference-frequency pressure generated by nonlinearities of the fluid medium. The effect was observed for a wide range of available hydrophones.

Solutions found to the first two of the above difficulties will be discussed in the section concerning experimental results. Although the third difficulty has not been resolved, several valuable observations were made and are presented in the section on the determination of hydrophone nonlinearity (Section IV. F).

In light of the insights gained by these hydrophone nonlinearity measurements, the program at the Underwater Sound Reference Detachment (USRD) of the Naval Research Laboratory has been significantly expanded. The technique to measure hydrophone nonlinearity developed during this research represents a substantial improvement over the technique originally intended to be used by USRD to analyze the linearity of their standard hydrophones. In the current development program, it is intended to use the nonlinearity measurement technique of this research to develop a hydrophone nonlinearity standard.

Chapter II will present the nonlinear theory as well as Censor's theory. The numerical results of each theory will be given in graphical form in Chapter III, along with a discussion of the numerical techniques used. Chapter IV will discuss the experiment, including the choice of experiment and resolution of experimental difficulties, and will present a new technique for determining hydrophone nonlinearity. Lastly, Chapter V will give the conclusions. The new technique of integration developed during the course of this research is presented in the Appendix.

II. THEORY

A. Introduction

This chapter presents some concepts useful in finite-amplitude acoustics, gives the derivation of the simple-source formulation of the second-order acoustic wave equation in a manner that is of quite general applicability to problems involving interacting acoustic pressure fields, and presents the theoretical development of the problem of the nonlinear scattering of acoustic waves from vibrating obstacles for certain specific geometries.

Section II. B discusses the two reference frames used in acoustics--namely, the Lagrangian (or material) coordinates and the Eulerian (or spatial) coordinates. Section II. C discusses the orders of acoustic variables and expressions.

In 1963, Westervelt [17] obtained a simple-source formulation of the second-order nonlinear wave equation. This formulation is an analogy to the simple-source wave equation of linear acoustics, which is essentially the inhomogeneous wave equation for a volumetric distribution of monopole point sources of sound [29].

The analogy drawn by Westervelt is that each elementary volume element in a fluid in which two waves of different frequency are simultaneously present may be viewed as an elementary source of nonlinearly generated waves. The mathematical form of Westervelt's second-order nonlinear wave equation is similar to that of the simple-source equation of linear acoustics if the proper identification of variables is made.

Westervelt's derivation of this equation is based on the assumption that the interacting waves are planar. Hence, it is unclear that his equation is applicable to any other wave geometry.

The inhomogeneous term is quadratic in nature. Hence, if one attempts to obtain the solution for arbitrary wave fields by decomposing the individual waves contributing to the source term into sums of plane waves, the solution must be represented as a sum over pairs of waves. It is often more convenient to use a closed-form representation of the source term (but this requires a demonstration that the equation is valid for non-planar primaries). In the current work, the simple-source formulation of the second-order nonlinear wave

equation is re-derived for primary waves of arbitrary geometry. This derivation is given in Section II. D.

Sections II. E, F, and G present the solutions to the second-order nonlinear wave equation for three specific geometries:

•Plane-wave scattering from a vibrating planar surface.

•Cylindrical-wave scattering from a vibrating cylindrical surface.

•Plane-wave scattering from a vibrating cylindrical surface.

In solving the case of plane-wave scattering from an infinite uniformly vibrating planar surface, the one-dimensional form of the nonlinear wave equation is used. This equation is expressed in terms of Lagrangian coordinates since the first-order boundary conditions can most naturally be satisfied in this reference frame. The equation is solved by a substitution of perturbation-series expansions in Mach number for the acoustic variables such that the solution is accurate to second order (in the sense normally associated with perturbation approximations). As noted by Beyer [30], such an expansion was first considered historically by Airy in 1845 in studying tidal motion. A careful analysis of the results of Censor's theory is presented for the planar case. (Although Censor presented no solution for this case, his method can be applied in a straightforward manner to obtain one.) It is shown that Censor's theory predicts sum- and difference-frequency pressures that are of the same order as pseudosound.

In obtaining a solution to the second-order nonlinear wave equation for the two cases considered involving cylindrical geometry, again the method of expanding the acoustic variables in a perturbation series in Mach number is used.

The actual second-order sum- and difference-frequency pressures are calculated by solving a related Green's function equation. It has been noted [28] that care must be exercised in the choice of Green's function. This is discussed in detail in the paragraphs following Eq. (47) of Section II. D.

Finally, both Censor's theoretical results and the results of the nonlinear theory are presented graphically to facilitate comparison of the two

theories. (Although Censor gave analytical expressions for the scattered sum- and difference-frequency pressures, no numerical values were presented.)

In obtaining the numerical results for the nonlinear theory, the integrals were performed on a high-speed computer (TI-ASC-11) using the method of Gauss Quadrature [32]. (Closed-form solutions to these integrals were obtained in the high-frequency limit based on the new integration technique presented in the Appendix.) The sums obtained from the theory were also carried out on this computer until three significant figures were obtained.

B. Coordinate Systems of Finite-Amplitude Acoustics

Two different kinds of coordinate systems are used to specify acoustic wave fields in fluids--namely, Lagrangian (or material) coordinates that move with the fluid and Eulerian (or spatial) coordinates that are fixed in space. The relationship between these two systems is illustrated in Fig. 1.

When displacement is expressed in terms of Eulerian coordinates, the displacement is that of the fluid element that happens to be located at x at the time of observation. On the other hand, when the displacement is expressed in terms of Lagrangian coordinates a, it refers to a fluid element that had the initial rest position a.

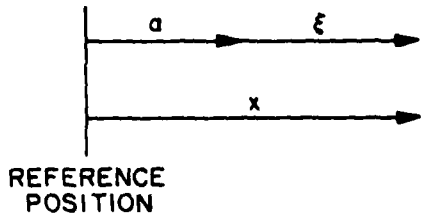

$x = a + \xi$

a = LAGRANGIAN COORDINATE
= REST POSITION OF AN INDIVIDUAL PARTICLE

x = EULERIAN COORDINATE
= POSITION OF A FIXED POINT IN SPACE

ξ = DISPLACEMENT OF THE PARTICLE FROM ITS REST POSITION

Fig. 1 - Geometry of Lagrangian and Eulerian Coordinates

C. The Order of Acoustic Variables and Expressions

Careful consideration must be given to the meaning of "orders" of acoustic variables and expressions. In nonlinear acoustics, the appropriate parameter to determine this order is the Mach number. (This will be justified presently.) Important dimensionless quantities arise when the relevant equation/s are put into dimensionless form. The resulting equation was given for the acoustical case by Blackstock [13]. A relationship (analogous to the Reynolds number) was obtained by Blackstock in this report, which may be used to determine whether the loss terms are significant for a nonlinear propagation problem for initially plane waves. This criterion involves a quantity Γ, where

$$\Gamma = \beta\varepsilon c_o x_c/(1/2)\nu[V + (\gamma-1)/P_r]$$

(β is a measure of medium nonlinearity and is approximately 3.5 for water at 20°C, V is the viscosity number, γ is the ratio of specific heats, ν is the kinematic viscosity, P_r is the Prandtl number, ε is the Mach number, and x_c is a characteristic length). Blackstock noted that for initially sinusoidal waves, x_c may be taken to be $x_c = c_o/\omega = \lambda$, and showed that (at low frequencies) $\Gamma = \beta\varepsilon/\alpha\lambda$, where α = the attenuation coefficient. Blackstock noted that the quantity $\beta\varepsilon/\alpha\lambda$ has been referred to as the Reynolds number in the Russian literature. (He further noted that this quantity is certainly not a measure of inertial to viscous effects, which is the traditional interpretation of the Reynolds number. Instead, Blackstock interprets this quantity as a measure of the importance of nonlinearity to dissipation). The determination of whether a given frequency is "low" can be ascertained using yet another dimensionless quantity known as the "frequency parameter" [33], $X = (\omega\eta V)/\rho_o c_o^2$, where V = viscosity number = $2 + \eta'/\eta$, η = shear coefficient of viscosity, η' = volume coefficient of viscosity. Using a typical frequency of interest of 100 kHz along with the approximate expression $\eta' \approx 3\eta$ for water [34], we get a value $X = 1.4\times10^{-6}$, clearly indicating that this frequency may properly be considered "low" (and hence Blackstock's low-frequency expression for Γ is appropriate).

An important criterion established by Blackstock in Reference 13 is that the results of the propagation of a plane wave that would be obtained via the

inclusion of loss in the equations will closely approach the results obtained excluding loss when $\Gamma>10$. Using typical values of interest in the current research ($\beta \approx 3.5$, $\varepsilon \approx 5\times10^{-4}$, $\alpha \approx 10^{-4}m^{-1}$, and $\lambda \approx 10^{-2}m$), we obtain $\Gamma \approx 1100$. Although Blackstock's expressions are actually valid only for initially plane waves, it is fairly clear, due to this rather substantial value, that losses are relatively unimportant here.

The negligibility of viscous effects for the frequencies and propagation distances of interest in this report can also be demonstrated by computation of the Reynold's number in the two physical regions of concern: 1) the region close to the scatterer's surface (where a viscous boundary layer forms), and 2) the propagation region wherein (at some point) the primary fields will start to form shock waves.

Consider first the required thickness of a viscous boundary layer. We define this thickness as corresponding to a Reynold's number of unity. The Reynold's number (R) can be computed using $R = UL\rho/\mu$ or $R = \omega L^2\rho/\mu$, where U = characteristic velocity, L = characteristic length, ρ = coefficient of viscosity, and ω = characteristic angular frequency. Using a frequency of 100 kHz, a Reynold's number of unity corresponds to a characteristic (boundary layer) thickness of about 10^{-4} cm. This result makes clear the fact that at positions near the scatterer's surface viscous effects may reasonably be neglected (since this distance is $<<\lambda/2\pi$ for the frequencies of interest here).

At larger distances from the scatterer's surface, this analysis breaks down, and a more suitable interpretation of the Reynold's number is needed. As an initially sinusoidally shaped acoustic wave propagates, the nonlinear distortion it suffers causes its waveform to approach the shape of a sawtooth wave. If viscous effects are completely neglected, the waveform becomes a triangular wave at a propagation distance equal to the discontinuity distance (see the discussion of this matter in Chapter I). Using this effect as a guide, it is clear that a convenient choice for the characteristic length L used to compute the Reynold's number is the spatial distance separating the point of maximum particle velocity and adjacent point of zero particle velocity. This "adjacent" point of zero particle velocity is the one occuring ahead of the point of maximum particle velocity (in the sense of the direction of propagation). This characteristic length, as defined here, is initially equal to one quarter of a primary wavelength and approaches zero as the

propagation distance approaches the discontinuity distance. Such a definition makes clear the fact that viscosity can properly be neglected in the propagation region only at propagation distances small relative to the discontinuity distance (since the Reynold's number will approach zero at that point). Hence, we conclude that within a region farther than a fraction of a millimeter from the scatterer's surface and yet not closely approaching the discontinuity distance, viscous effects may safely be neglected and the Mach number taken as the appropriate dimensionless parameter to identify the order of acoustic variables and expressions.

Due to the extremely complex nature of the equations of nonlinear acoustics, some type of approximation method is usually required to obtain a solution. There are two primary approximations that are traditionally used:

- The exact equations can be put into an approximate form more readily solvable. It is the local Mach number dependence of the acoustic variables (discussed above) that forms the basis for this approximation.

- Alternatively, the acoustic variables can be expanded directly in a formal perturbation series in Mach number, which may then be substituted into the exact equations. In such a series, "ordering" is determined by where the boundary conditions are imposed (i.e., the "Mach number" is not the local Mach number but rather the Mach number at the point at which the boundary conditions are imposed). This process results in an infinite set of differential equations (one equation associated with each term, i.e. order of the expansion). Each of these equations can then be individually solved, starting with the first-order equation and ending at whatever order yields the required degree of accuracy.

Let us first consider the approximation involved in obtaining the second-order nonlinear wave equation from the exact fundamental equations. Although this equation is an approximate one, when it is applied to problems involving sound propagation in water, no measurable difference between the pressure predicted by it and that predicted by the exact equations results. This is because in such problems the contributions to the sound field by terms of third and higher orders are negligible. Justification for the negligibility of third-order terms is given in Appendix A of Reference 35, which considers the

consequences of retaining higher-order terms in the fundamental equations and third-order terms in the equation of state. In Reference 36, the equation of state was expressed as

$$p = p_o + A\left(\frac{\rho-\rho_o}{\rho_o}\right) + \frac{B}{2}\left(\frac{\rho-\rho_o}{\rho_o}\right)^2 + \frac{C}{6}\left(\frac{\rho-\rho_o}{\rho_o}\right)^3 .$$

As reported in Reference 35, Van Buren wrote a computer program that computed the distortion occurring during the propagation of an initially sinusoidal wave of amplitude 0.7×10^5 Pa and frequency 2 MHz. (The program included the effects of all orders in the fundamental equations and in the equation of state to third order. Absorption effects were also included.) The wave was allowed to propagate 104 cm (one discontinuity distance). The results of this program were compared to results obtained when only terms up to second order were retained in both the fundamental equations and in the equation of state. The results of comparing these two solutions were: With $C/A = 10^5$, the second harmonic deviated by about -0.2%, the third harmonic by -1.3%, fourth harmonic by +0.06%, etc. In liquids, C/A is approximately [36] $3/2\ (B/A)^2$, which gives $C/A \simeq 40$ for water. It becomes clear from these numerical results that the effects of the higher-order terms (at least in water) are completely negligible.

Although additional effects may arise in non-planar geometries, the plane-wave should represent the worst case (since higher-dimensioned geometries result in spreading of the waves and a reduction in field amplitude).

One last argument can be advanced regarding the negligibility of third-order terms: If one starts with the exact wave equation in Lagrangian coordinates for plane waves and performs straightforward Taylor-Series expansions, one can demonstrate that the third-order source terms are a Mach number smaller than the second-order source terms. Hence, even if third-order source terms result in cumulative effects (as do the second-order terms), the contributions to the answer from the third-order terms will be a Mach number lower than contributions from second-order terms (the Mach number in water is rarely greater than 10^{-4}). This holds as long as dispersion is negligible, which it is in fresh water for frequencies up to 10^{14} Hz. Again, the plane-wave case may be regarded as a worst-case situation, since geometrical spreading will dilute the effects in higher-order geometries.

We begin this discussion by referring to the exact wave equation in Lagrangian coordinates [see Reference 37, Eq. (35)]

$$\ddot{\xi} = c^2[1+\xi_a]^{-2}\xi_{aa} \ .$$

An expansion for the wavespeed c, accurate to third order, has been given by Van Buren [38]. It is

$$c = c_o[1 + (\frac{B}{2A} + 1)\ \frac{u}{c_o} + (\frac{c}{4A} - \frac{B^2}{4A^2} + \frac{B}{2A} + \frac{1}{2})\ \frac{u^2}{c_o^2}].$$

In this equation A, B, and C have their usual meanings--namely,

$$A = \rho_o(\frac{\partial P}{\partial \rho})_{S,\rho=\rho_o} = \rho_o c_o^2, \qquad B = \rho_o^2(\frac{\partial^2 P}{\partial \rho^2})_{S,\rho=\rho_o} ,$$

and $$C = \rho_o^3(\frac{\partial^3 P}{\partial \rho^3})_{S,\rho,\rho_o}.$$

Substituting this expansion for the wavespeed into the exact wave equation in Lagrangian coordinates, expanding the term $(1+\xi_a)^{-2}$, and retaining only terms of third order or less yields:

$$\begin{aligned}\ddot{\xi} - c_o^2\xi_{aa} = {} & c_o^2[2(\frac{B}{2A} + 1)\ \frac{u}{c_o} - 2\xi_a]\xi_{aa} \\ & + c_o^2[(\frac{B}{2A} + 1)\ \frac{u^2}{c_o^2} + 2\ (\frac{c}{4A} - \frac{B^2}{4A^2} - \frac{B}{2A} + \frac{1}{2})\ \frac{u^2}{c_o^2} \\ & - 4\ (\frac{B}{2A} + 1)\ \frac{u}{c_o}\ \xi_a + 3(\xi_a)^2]\xi_{aa}.\end{aligned}$$

The quantities (u/c_o), ξ_a, and ξ_{aa} may all be regarded as being of the order of the Mach number. Hence, the above form of the wave equation can be interpreted as follows: The first set of square brackets (with its coefficients) may be regarded as a source of second-order waves. The second set of square brackets may be regarded as a third-order source expression. As previously mentioned, since the third-order source terms are all a Mach number smaller than the second-order source terms, their contributions will always be a Mach number smaller than the contributions from the second-order terms. Hence, even if these third-order contributions are cumulative (as are the second-order contributions), they will always remain small relative to the

second-order contributions. Hence, for all practical purposes, a solution to the second-order nonlinear wave equation may be regarded as sufficient for specifying a solution to a nonlinear underwater sound propagation problem*. It is frequently the case, however, that exact solutions to even this more simplified equation are too difficult to obtain. In such cases, a solution is usually obtained by using a perturbation-series expansion in Mach number of the acoustic pressure. This expansion is generally substituted directly into the second-order nonlinear wave equation (rather than returning to the still more complicated fundamental equations). Such a substitution can be used to obtain what is known as the simple-source formulation of the second-order nonlinear wave equation.

When one uses a perturbation expansion, however, one must proceed with extreme caution. Although the starting equations may be regarded as sufficiently accurate (whether starting from the fundamental equations or the second-order nonlinear wave equation), the solution obtained by a perturbation series may become inaccurate if the series is truncated too early. In fact, most such perturbation analyses are carried only to second order (since higher orders become exceedingly complicated). In this case, inaccuracies arise due to the failure of the fundamental assumption made in such treatments, namely that the second-order field remains small relative to the first-order field. Since the Mach number is rarely greater than 10^{-4} in water, it might appear this assumption would never become questionable (in fact, it may appear peculiar that second-order effects ever become measurable). The reason they do so is that such effects tend to act cumulatively with propagation distance. Hence, the second-order pressure (for example) at a given observation point is not simply a consequence of the value of the Mach number at that point. Rather, it is a consequence of the entire integrated history of the fields between the sources and the observation point.

In essence, this means that the important second-order contributions to the pressure are not themselves second order (ε^2), but rather of the order of ε^2 times an enhancement factor. What this factor is can be determined for plane, cylindrical, and spherical geometries due to the fortuitous

---

*Hydrophones can rarely be calibrated more accurately than to within 1 dB of relative error. This corresponds to more than 12% experimental error.

circumstance that the Bessel function expansion used by Fubini-Ghiron in the planar case [7] can also be used (when thermoviscous losses are negligible) to solve the higher dimensional cases [see Reference 13, eq. (13)]. After Fubini-Ghiron, we can use the first terms of this series to estimate the growth behavior of the nonlinear fields. In order to do so conveniently, we introduce notation similar to Blackstock's in Reference 13:

$$\sigma = \frac{x}{X}$$

$$f = \begin{cases} \sigma & \text{(plane)} \\ 2\sqrt{\sigma_o}\,(\sqrt{\sigma} - \sqrt{\sigma_o}) & \text{(cylindrical)} \\ \sigma_o \log(\sigma/\sigma_o) & \text{(spherical)} \end{cases}$$

where again ε = Mach number, X = discontinuity distance, and x = propagation distance. (This choice of Blackstock's dimensionless quantity σ is made in order to render his Bessel-function expansion equivalent to that of Fubini-Ghiron.) We can estimate the appropriate "enhancement factor" via the ratio of the second-order to the first-order contributions to the field from this Bessel-function series. This ratio is equal to $[J_2(2f)]/[2\,J_1(f)]$, which (for small arguments of the Bessel function) is approximately equal to $\frac{1}{2}$ f. Hence, the enhancement factors for each of the three geometries becomes:

$$\begin{cases} \frac{1}{2}\frac{x}{X} & \text{(plane)} \\ \sqrt{\frac{x_o}{X}}\left(\sqrt{\frac{x}{X}} - \sqrt{\frac{x_o}{X}}\right) & \text{(cylindrical)} \\ \frac{1}{2}\frac{x_o}{X}\log\left(\frac{x}{x_o}\right) & \text{(spherical)} \end{cases}$$

where x_o represents the location of the scatterer's surface in the nonlinear scattering problem of interest here.

Confirmation of the growth of the second-order fields relative to the primary fields is provided by the many successful measurements of nonlinearly generated field effects described in Chapter I. Therefore, it is seen that in an underwater nonlinear propagation problem, the primary fields tend to <u>decay</u> (due to geometrical spreading, energy loss to secondary field generation, and energy loss due to absorption when high frequencies and/or large propagation

distances are involved) while the secondary fields tend to grow. Eventually, the secondary fields can become comparable to or even exceed the primary fields. When this occurs, solutions based on second-order perturbation methods are no longer valid.

In the following section, the second-order nonlinear wave equation is derived from the fundamental equations. The acoustic pressure is then expanded in a perturbation series to second order. This perturbation expansion is used to obtain the simple-source formulation of the second-order non-linear wave equation. This equation together with the first-order equation of linear acoustics constitutes essentially a type of Born-approximation. It is used to solve the problem of the nonlinear scattering of acoustic waves for vibrating obstacles for three different geometries in Chapter II, Sections E, F, and G. Since these solutions are obtained via a perturbation method, their validity is restricted to small propagation distances from the scatterer's surface.

D. Second-Order Nonlinear Wave Equation

Any investigation of the behavior of finite-amplitude acoustic waves in a fluid begins with the basic equations of motion. These can readily be derived by applying mass and momentum conservation laws to the fluid under consideration. The resulting equations are expressed below in Eulerian coordinates:

1. The Equation of Continuity (Mass Conservation)

$$\frac{\partial \rho}{\partial t} + \vec{\nabla} \cdot (\rho \vec{u}) = S. \qquad (1)$$

In this equation, S is a mass source term representing the rate at which mass is introduced into the region of interest. It can be used to represent monopole sources of sound as well [39]. In the current work, however, sources of sound will be handled instead via specification of appropriate boundary conditions (i.e., by specifying the normal velocity of the surface of the source), and the solutions will be restricted to regions outside the surface of the sources. Hence, the term S will be taken to be zero.

2. The Equation of Momentum Conservation

$$\frac{\partial}{\partial t}(\rho\vec{u}) + \vec{\nabla} \cdot (\rho\vec{u}\vec{u}) = -\vec{\nabla} \cdot \vec{\vec{p}} \tag{2}$$

where ρ is the mass density, $\vec{u}$ is the particle velocity, and $\vec{\vec{p}}$ is the stress tensor whose components are:

$$P_{ij} = P\delta_{ij} + \mu \left(-\frac{\partial u_i}{\partial x_j} - \frac{\partial u_j}{\partial x_i} + \frac{2}{3}\delta_{ij}\sum_k \frac{\partial u_k}{\partial x_k}\right)$$

where μ is the coefficient of viscosity and P is the pressure.

Lighthill [18] combined Eqs. (1) and (2) to produce the following equation of motion for the mass density

$$-c_o^2 \Box^2 \rho = \sum_{i,j} \frac{\partial^2 T_{ij}}{\partial x_i \partial x_j} \tag{3}$$

where $\Box^2$ = D'Alembertian Operator = $\nabla^2 - \frac{1}{c_o^2}\frac{\partial^2}{\partial t^2}$,

with c_o = infinitesimal wave speed = $(\partial P/\partial \rho)^{1/2}_{S,\rho=\rho_o}$, (4)

and the Lighthill stress tensor $\vec{\vec{T}}$ is defined by

$$T_{ij} = \rho u_i u_j + P_{ij} - \rho c_o^2 \delta_{ij} \tag{5}$$

where P_{ij} is as defined above.

In the present work, frequencies on the order of 100 kHz and propagation distances on the order of 100 cm in fresh water will be considered. The effects of viscous attenuation (for a plane wave) may be summarized by the equation $P = P_o e^{-\alpha x}$. At a frequency of 100 kHz in fresh water, the constant α has a value of $\sim 10^{-4}$ m^{-1}. It is clear, then, that viscous losses for the present work are completely negligible and P_{ij} may be replaced by $P\delta_{ij}$. (In fact, the equations for sound propagation in fresh water need not include the effects of viscosity until frequencies approaching 1 MHz or distances on the order of kilometers are considered. Hence, the equations herein derived have a broad applicability; however, viscous effects will be important in the boundary layer.

Substituting T_{ij} into Eq. (3) yields:

$$\frac{\partial^2 \rho}{\partial t^2} = \sum_{i,j} \frac{\partial^2 (\rho u_i u_j)}{\partial x_i \partial x_j} + \nabla^2 P \tag{6}$$

which may be used to show that*

$$\Box^2 P = \frac{\partial^2}{\partial t^2} (\Delta\rho - c_o^2 \Delta P) - \sum_{i,j} \frac{\partial^2 (\rho u_i u_j)}{\partial x_i \partial x_j} . \tag{7}$$

The usual wave equation of linear acoustics, $\Box^2 P = 0$, follows if we only retain terms that are linear in the field variables. On the other hand, we need to retain terms up to the quadratic in the field variables in order to obtain a nonlinear wave equation that is accurate to second order. As stated earlier, third and higher order terms in the wave equation do not measurably contribute to nonlinear acoustic behavior in liquids (such as water) where these results will be applied. Thus the term $\rho u_i u_j$ can be replaced by its second-order approximation $\rho_o u_i u_j$, thereby neglecting the third-order term $(\rho - \rho_o) u_i u_j$. The last term in Eq. (7) can now be written:

$$\sum_{i,j} \frac{\partial^2 (\rho u_i u_j)}{\partial x_i \partial x_j} \approx \rho_o \{ (\vec{u}\cdot\vec{\nabla})(\vec{\nabla}\cdot\vec{u}) + (\vec{\nabla}\cdot\vec{u})^2 + \sum_{i,j} \frac{\partial u_j}{\partial x_i} \frac{\partial u_i}{\partial x_j} \} . \tag{8}$$

Now, it can easily be shown that

$$\sum_{i,j} \frac{\partial u_j}{\partial x_i} \frac{\partial u_i}{\partial x_j} = \vec{\nabla} \cdot [(\vec{u}\cdot\vec{\nabla})\vec{u}] - (\vec{u}\cdot\vec{\nabla})(\vec{\nabla}\cdot\vec{u}) . \tag{9}$$

Also, by vector identity:

$$(\vec{u}\cdot\vec{\nabla})\vec{u} = \frac{1}{2} \vec{\nabla}(u^2) - \vec{u} \times (\vec{\nabla}\times\vec{u}) . \tag{10}$$

- - - - - - - - - - -

*In obtaining Eq. (7) a factor of ρ has been replaced by $\Delta\rho$ and P by ΔP. This may be freely done due to the presence of the differential operators acting on these quantities. This freedom will frequently be used in several of the equations obtained throughout the remainder of the current section.

It can be shown that in linear acoustics the particle velocity field is irrotational; i.e., $\vec{\nabla}\times\vec{u} = 0$ [the validity of this assumption is discussed in Hunt [37] in reference to his Eq. (56)]. Although the particle velocity is irrotational only to first order, Blackstock [40] has pointed out that any factor in a second-order term may be replaced by its first-order equivalent since a more precise substitution will result in terms of third (or higher) order. (Blackstock calls this fact the substitution corrollary.) Since the last term in Eq. (10) is clearly of second order, we may freely use the irrotationality condition in this term.

Combining the equation that results from Eq. (10) by using this substitution with Eqs. (8) and (9), we obtain:

$$\sum_{i,j} \frac{\partial^2(\rho u_i u_j)}{\partial x_i \partial x_j} \approx \rho_o[(\vec{u}\cdot\vec{\nabla})(\vec{\nabla}\cdot\vec{u}) + (\vec{\nabla}\cdot\vec{u})^2 + \nabla^2(\tfrac{1}{2}\vec{u}^2)]. \tag{11}$$

In the first term on the right-hand side of Eq. (11), we may freely replace $\vec{\nabla}\cdot\vec{u}$ by equations accurate to first order, since the overall term will remain accurate to the second order due to the presence of $\vec{u}$ dotted into the remainder of the term. Of use here is the first-order continuity equation as obtained from Eq. (1):

$$\vec{\nabla}\cdot\vec{u} \overset{1}{=} -\frac{1}{\rho_o}\frac{\partial\rho}{\partial t}. \tag{12}$$

(The "1" over the equal sign denotes first-order. This notation shall be adopted for the remainder of this thesis. Similarly, a "2" over the equal sign will denote second order.)

Therefore the first term on the right-hand side of Eq. (11) becomes

$$(\vec{u}\cdot\vec{\nabla})(\vec{\nabla}\cdot\vec{u}) \overset{2}{=} -\frac{(\vec{u})}{\rho_o}\frac{\partial}{\partial t}(\vec{\nabla}\rho). \tag{13}$$

To complete the analysis we need an equation of state for the fluid medium. Since any thermodynamic quantity in systems in which pressure, volume, and temperature are thermodynamic parameters can be represented as a

function of any two state variables, we can obtain an equation of state by expanding the pressure in a Taylor series in the state variables ρ (density) and S (entropy). This yields

$$P = P_o + \left(\frac{\partial P}{\partial \rho}\right)_{S,\rho=\rho_o} (\rho-\rho_o) + \frac{1}{2} \left(\frac{\partial^2 P}{\partial \rho^2}\right)_{S,\rho=\rho_o} (\rho-\rho_o)^2$$

$$+ \ldots + \left(\frac{\partial P}{\partial S}\right)_{S,\rho=\rho_o} (S-S_o) + \ldots \quad . \tag{14}$$

It is usual to simplify Eq. (14) under the assumption of adiabatic compressibility. According to Morse & Ingard [41], adiabatic compressibility is achieved under the condition that the highest frequency component in the acoustic field is significantly less than $(c_o^2 \rho_o c_p)/k$, where k is the thermal conductivity and c_p is the specific heat at constant pressure. For water, this expression gives a frequency of about 10^{13} Hz, a value well above anything of interest in the current work. We will, therefore, neglect contributions to the pressure in Eq. (14) due to changes in entropy, giving (to second order)

$$P \cong P_o + \left(\frac{\partial P}{\partial \rho}\right)_{S,\rho=\rho_o} (\rho-\rho_o) + \frac{1}{2} \left(\frac{\partial^2 P}{\partial \rho^2}\right)_{S,\rho=\rho_o} (\rho-\rho_o)^2. \tag{15}$$

If we solve Eq. (15) for $P - P_o$ to first order, we obtain

$$P - P_o = \Delta P \cong \left(\frac{\partial P}{\partial \rho}\right)_{S,\rho=\rho_o} (\rho-\rho_o) \cong c_o^2 \Delta\rho \tag{16}$$

or, in terms of the "del" operator,

$$\vec{\nabla} P \cong c_o^2 \vec{\nabla} \rho, \tag{17}$$

where Eq. (4) has been used for c_o.

The equation of momentum conservation to first order is

$$-\vec{\nabla}p \triangleq \rho_o \frac{\partial \vec{u}}{\partial t} . \tag{18}$$

Combining Eqs. (13), (17), and (18) yields the following relation, accurate to second order.

$$(\vec{u}\cdot\vec{\nabla})(\vec{\nabla}\cdot\vec{u}) \triangleq \frac{\vec{u}}{c_o^2} \cdot \frac{\partial^2 \vec{u}}{\partial t^2} . \tag{19}$$

Combining the elementary relation

$$\frac{1}{2} \frac{\partial^2}{\partial t^2} (u^2) = \vec{u} \cdot \frac{\partial^2 \vec{u}}{\partial t^2} + \left(\frac{\partial \vec{u}}{\partial t}\right)^2 \tag{20}$$

with Eq. (19) gives

$$(\vec{u}\cdot\vec{\nabla})(\vec{\nabla}\cdot\vec{u}) \triangleq \frac{1}{2c_o^2} \frac{\partial^2 (u)^2}{\partial t^2} - \frac{1}{c_o^2} \left(\frac{\partial \vec{u}}{\partial t}\right)^2 . \tag{21}$$

Also, by definition of the D'Alembertian operator,

$$\frac{1}{c_o^2} \frac{\partial^2 \vec{u}^2}{\partial t^2} = \nabla^2 \vec{u}^2 - \Box^2 \vec{u}^2 . \tag{22}$$

Combining Eqs. (21) and (22) gives

$$(\vec{u}\cdot\vec{\nabla})(\vec{\nabla}\cdot\vec{u}) \triangleq \frac{1}{2} \nabla^2 \vec{u}^2 - \frac{1}{2} \Box^2 \vec{u}^2 - \frac{1}{c_o^2} \left(\frac{\partial \vec{u}}{\partial t}\right)^2 . \tag{23}$$

We now consider the $(\vec{\nabla}\cdot\vec{u})^2$ term in Eq. (11). By using first-order approximation for the equation of continuity [Eq. (12)], we obtain

$$(\vec{\nabla}\cdot\vec{u})^2 \triangleq \frac{1}{\rho_o^2} \left(\frac{\partial \Delta\rho}{\partial t}\right)^2 . \tag{24}$$

Combining Eq. (24) with the elementary relationship

$$\frac{1}{2}\frac{\partial^2(\Delta\rho)^2}{\partial t^2} = \Delta\rho\,\frac{\partial^2\Delta\rho}{\partial t^2} + \left(\frac{\partial\Delta\rho}{\partial t}\right)^2 \tag{25}$$

and with the D'Alembertian operator acting on $(\Delta\rho)^2$,

$$\Box^2(\Delta\rho)^2 = \nabla^2(\Delta\rho)^2 - \frac{1}{c_o^2}\frac{\partial^2(\Delta\rho)^2}{\partial t^2} \tag{26}$$

gives

$$(\vec{\nabla}\cdot\vec{u})^2 \triangleq \frac{c_o^2}{\rho_o^2}\frac{\nabla^2(\Delta\rho)^2}{2} - \frac{c_o^2}{2\rho_o^2}\Box^2(\Delta\rho)^2 - \frac{\Delta\rho}{c_o^2}\frac{\partial^2\Delta\rho}{\partial t^2}. \tag{27}$$

Substituting Eqs. (23) and (27) into Eq. (11) yields

$$\sum_{i,j}\frac{\partial^2(\rho u_i u_j)}{\partial x_i \partial x_j} \triangleq \rho_o\{\nabla^2\frac{\vec{u}^2}{2} - \Box^2\left[\frac{\vec{u}^2}{2} + \frac{c_o^2(\Delta\rho)^2}{2\rho_o^2}\right]$$

$$- \frac{1}{c_o^2}\left(\frac{\partial\vec{u}}{\partial t}\right)^2 + \frac{c_o^2}{2\rho_o^2}\nabla^2(\Delta\rho)^2 - \frac{\Delta\rho}{\rho_o^2}\frac{\partial^2\Delta\rho}{\partial t^2}\}. \tag{28}$$

Using the elementary fact that

$$\frac{1}{2}\nabla^2(\Delta\rho)^2 = \Delta\rho\nabla^2\Delta\rho + (\vec{\nabla}\Delta\rho)^2, \tag{29}$$

we obtain for the last two terms in Eq. (28)

$$\frac{c_o^2}{2\rho_o^2}\nabla^2(\nabla\rho)^2 - \frac{\nabla\rho}{\rho_o^2}\frac{\partial^2\nabla\rho}{\partial t^2}$$

$$= \frac{c_o^2}{\rho_o^2}\Delta\rho\,\nabla^2\Delta\rho + \frac{c_o^2}{\rho_o^2}(\vec{\nabla}\Delta\rho)^2 - \frac{\Delta\rho}{\rho_o}\frac{\partial^2\Delta\rho}{\partial t^2}$$

$$= \frac{c_o^2}{\rho_o^2}(\vec{\nabla}\Delta\rho)^2 + \frac{c_o^2\Delta\rho}{\rho_o^2}\left[\nabla^2\Delta\rho - \frac{1}{c_o^2}\frac{\partial^2\Delta\rho}{\partial t^2}\right]. \tag{30}$$

The term in brackets is equal to zero accurate to first order, so use of the substitution corollary allows simplification of Eq. (30) to give, accurate to second order,

$$\frac{c_o^2}{2\rho_o^2}\nabla^2(\Delta\rho)^2 - \frac{\Delta\rho}{\rho_o^2}\frac{\partial^2\Delta\rho}{\partial t^2} \overset{2}{=} \frac{c_o^2}{\rho_o^2}(\vec{\nabla}\Delta\rho)^2. \tag{31}$$

Now, Eqs. (17) and (18) may be combined to give the first-order approximation

$$\vec{\nabla}\Delta\rho \overset{1}{=} -\frac{\rho_o}{c_o^2}\frac{\partial\vec{u}}{\partial t}. \tag{32}$$

Finally, Eqs. (31) and (32) may be combined to show that the last three terms in Eq. (28) vanish. Hence, Eq. (28) becomes

$$\sum_{i,j}\frac{\partial^2(\Delta\rho u_i u_j)}{\partial x_i \partial x_j} \overset{2}{=} \rho_o\nabla^2\vec{u}^2 - \Box^2[\tfrac{1}{2}\rho_o\vec{u}^2 + \tfrac{1}{2}c_o^2(\Delta\rho)^2/\rho_o]. \tag{33}$$

From Eq. (16) we have the first-order approximation

$$\Delta P \overset{1}{=} c_0^2(\Delta\rho). \tag{34}$$

Using this in Eq. (15) yields, accurate to second order,

$$\Delta P \overset{2}{=} c_o^2\Delta\rho + \tfrac{1}{2}c_o^{-4}\left(\frac{\partial^2 P}{\partial\rho^2}\right)_{S,\rho=\rho_o}(\Delta P)^2, \tag{35}$$

or

$$\Delta\rho - c_o^{-2}\Delta P \overset{2}{=} -\tfrac{1}{2}c_o^{-6}\left(\frac{\partial^2 P}{\partial\rho^2}\right)_{S,\rho=\rho_o}(\Delta P)^2. \tag{36}$$

If Eqs. (33) and (36) are substituted into Eq. (7), the following equation is obtained:

$$\Box^2 \Delta P \cong -\frac{1}{2} c_o^{-6} \left(\frac{\partial^2 P}{\partial \rho^2}\right)_{S,\rho=\rho_o} \frac{\partial^2 (\Delta P)^2}{\partial t^2} +$$

$$\Box^2 \left[\frac{1}{2} \rho_o \vec{u}^2 + \frac{1}{2} c_o^2 (\Delta\rho)^2/\rho_o \right] - \rho_o \nabla^2 u^2. \tag{37}$$

An equation equivalent to Eq. (37) was first derived by Eckart [15] in 1948, and later by Westervelt [16] in 1957. In 1963, Westervelt [17] transformed this equation into what is commonly referred to as the simple-source formulation. However, in so doing, he used an expression valid only for plane waves. In what follows, Eq. (37) will be transformed into the simple-source formulation without recourse to plane wave properties.

In order to carry Eq. (37) further, we require some additional first-order relationships. Since it is irrotational to first order, a scalar function ϕ known as the velocity potential can be assumed such that, accurate to first order,

$$\vec{u} \cong -\vec{\nabla}\phi. \tag{38}$$

The scalar potential ϕ is a solution to the linear homogeneous wave equation $\Box^2 \phi = 0$.

Now, by rearranging the definition of the D'Alembertian operator acting on u^2 and by use of Eq. (38) we obtain, accurate to second order:

$$\nabla^2 u^2 \cong \Box^2 u^2 + c_o^{-2} \frac{\partial^2}{\partial t^2} \left|\vec{\nabla}\phi\right|^2. \tag{39}$$

The last term can be rewritten using the identity

$$\left|\vec{\nabla}\phi\right|^2 = \frac{1}{2} \nabla^2 \phi^2 - \phi \nabla^2 \phi. \tag{40}$$

From the definition of the D'Alembertian we have

$$\nabla^2\phi^2 = \Box^2\phi^2 + c_o^{-2}\frac{\partial^2}{\partial t^2}\phi^2. \tag{41}$$

Also,

$$\nabla^2\phi = \Box^2\phi + c_o^{-2}\frac{\partial^2\phi}{\partial t^2} = c_o^{-2}\frac{\partial^2\phi}{\partial t^2} \tag{42}$$

since $\Box^2\phi = 0$.

Substituting Eqs. (40, 41, & 42) into Eq. (39), the following second-order expression for ∇^2u^2 is obtained:

$$\nabla^2u^2 \triangleq \Box^2u^2 + c_o^{-2}\frac{\partial^2}{\partial t^2}[\tfrac{1}{2}\Box^2\phi^2 + c_o^{-2}(\frac{\partial\phi}{\partial t})^2]. \tag{43}$$

If Eq. (43) is substituted into Eq. (37), the following equation results:

$$\Box^2 p \triangleq -\tfrac{1}{2}c_o^{-6}(\frac{\partial^2 P}{\partial\rho^2})_{S,\rho=\rho_o}\frac{\partial^2(\Delta P)^2}{\partial t^2} - \rho_o c_o^{-2}\frac{\partial^2}{\partial t^2}[c_o^{-2}(\frac{\partial\phi}{\partial t})^2]$$

$$+ \Box^2[\tfrac{1}{2}\rho_o^{-1}c_o^{2}(\Delta\rho)^2 - \tfrac{1}{2}\rho_o u^2 - \tfrac{1}{2}\rho_o c_o^{-2}\frac{\partial^2}{\partial t^2}(\phi^2)]. \tag{44}$$

We next wish to re-express the second term of Eq. (44) in terms of the acoustic pressure. We begin to do so by combining Eqs. (18) and (38) to obtain the first-order approximation

$$\vec{\nabla}p \triangleq \vec{\nabla}(\rho_o\frac{\partial\phi}{\partial t}). \tag{45}$$

Equation (38), which defines the velocity potential, allows a certain freedom in the choice of the function ϕ, since it is only this function's gradient that is therein defined. (This is analogous to the freedom of choice of gauge in electrodynamics.) We choose to impose this additional freedom in such a way as to allow Eq. (45) to possess the "solution", accurate to first order

$$P - P_o = \Delta P \triangleq \rho_o \frac{\partial \phi}{\partial t} . \tag{46}$$

It will be noted that Eq. (46) in no way contradicts Eq. (45) or Eq. (38); so choosing ϕ such that the usual additive constant obtained in solving an equation such as Eq. (45) to be equal to P_o is a consistent, and hence permissible, choice. A second way of viewing this situation is to consider the combination of Eqs. (38) and (46) to constitute a (consistent) definition of ϕ. [Although Eq. (46) is only one of an infinity of possible choices of "gauge".] Using Eq. (46) in Eq. (44) gives

$$\Box^2 \Delta P \cong -c_o^{-4} \rho_o^{-1} \left[1 + \frac{\rho_o}{2} \left(\frac{\partial^2 P}{\partial \rho^2}\right)_{S,\rho=\rho_o} c_o^{-2}\right] \frac{\partial^2 (\Delta P)^2}{\partial t^2}$$

$$+ \Box^2 \left[\frac{1}{2} \rho_o^{-1} c_o^2 (\Delta \rho)^2 - \frac{1}{2} \rho_o u^2 - \frac{1}{2} \rho_o c_o^{-2} \frac{\partial^2}{\partial t^2} (\phi^2)\right]. \tag{47}$$

Now introduce the perturbation expansion* $P - P_0 = \varepsilon P_1 + \varepsilon^2 P_2$ where $\Box^2 P_1 = 0$ + obtain secondary waves as solution to Eq. (47).

Equation (47) may be simplified by moving the terms under the D'Alembertian operator on the right-hand side of this equation to the left-hand side. On the left-hand side of this equation we then have P_2 + additional terms under the D'Alembertian operator. This new equation can now be solved for this new combination, subtracting the additional terms from the solution to obtain P_2. In practice, the terms under the D'Alembertian operator on the right-hand side of this equation are very small and can actually be neglected. In any case, these terms will clearly be non-growing contributions to the solution and will quickly be overwhelmed by the growing contributions.

- - - - - - - - - - -

*It is important to note that up to this point in the derivation no perturbation analysis has been used. Hence, Eq. (47) remains valid even under conditions that invalidate perturbation analyses.

One further remark is worthwhile in discussing the D'Alembertian terms of Eq. (47). If, in fact, these terms are not negligible in comparison to the predicted value for P_2 obtained in solving these equations, the result thus predicted will most likely be in error. This is due to the fact that when the D'Alembertian terms are lumped onto the left-hand side, an appropriate integral term must be included [28] to reflect the fact that they satisfy different boundary conditions than P_2. Hence, in solving Eq. (47) via this "lumping" technique, the values given by the D'Alembertian terms on the right-hand sides must always be compared with the predicted value for P_2 in order to insure consistency of the solution*. This fact has not been previously mentioned in the literature.

At this point, we assume the D'Alembertian terms on the right-hand side of Eq. (47) are negligible.

If we make the definitions:

$$B/A \equiv \frac{\rho_o}{c_o^2} \left(\frac{\partial^2 P}{\partial \rho^2}\right)_{S,\rho=\rho_o}$$

$$\Gamma = \text{nonlinearity parameter} = 1 + \frac{B}{2A}$$

$$q = \text{simple source strength} = \frac{\Gamma}{\rho_0^2 c_o^4} \frac{\partial}{\partial t} (P_1^2),$$

we can cast Eq. (47) into the form

$$\Box^2 P_2' \triangleq -\rho_o \left(\frac{\partial q}{\partial t}\right) . \tag{48}$$

---

*The calculations relevant to the problems considered in this thesis are performed in Chapter IV. B, where estimates of the errors introduced in the relevant surface and volume integrals are discussed.

The prime has been added to the symbol for the second-order pressure to denote that certain second-order quantities have actually been neglected*.

E. Plane-Wave Scattering from a Vibrating Planar Surface

In this section, the problem of the generation of sum- and difference-frequency waves will be addressed for the case of a plane wave normally incident on a surface deforming uniformly and harmonically.

1. Censor-Method Solution

Although he treated several different geometries, Censor never considered the simplest possible case. This case is a plane wave of angular frequency ω normally incident on an infinite plane vibrating uniformly with angular frequency Ω (see Fig. 2). We obtain the solution to this problem following the procedure presented by Censor [23].

We represent the incident plane-wave acoustic pressure as:

$$U_i = P_i e^{-i\omega((x/c_o)+t]}, \tag{49}$$

where x is the Eulerian position coordinate**. The scattered wave is assumed to be of the form:

$$U_S = \int_{-\infty}^{+\infty} d\nu a(\nu) e^{i\nu[(x/c_o)-t]}. \tag{50}$$

U_i+U_s is the total wave field. Using the method of Censor, we require the vanishing of the normal particle displacement at the planar surface x = 0

---

*In solving Eq. (48) in this report, we will not, of course, obtain a solution accurate to second order. P_2' simply reflects corrections to the primary field resulting from the "enhancement" factors discussed in Chapter II, Section C, arising from second-order quantities.

**Censor does not specify that x is the Eulerian position coordinate, but this choice appears consistent with the way he treats this quantity in his paper.

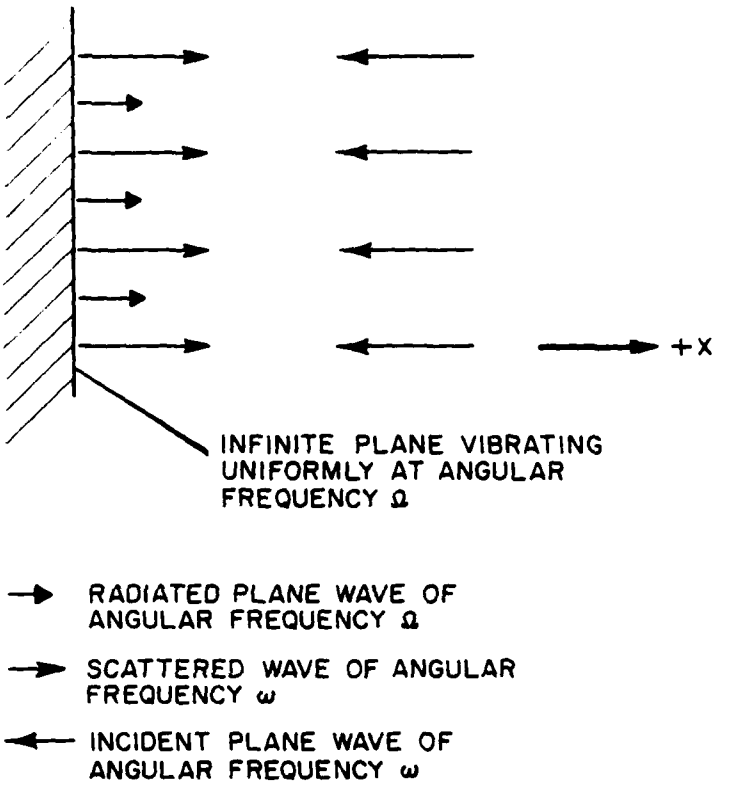

Fig. 2 - Geometry of plane-wave scattering from a vibrating plane

for the rigid-body scattering problem. Since we consider only linear wave fields in the Censor method, the acoustic pressure satisfies the equation

$$-\frac{\partial P}{\partial x} = \rho_o \frac{\partial^2 x}{\partial t^2} . \tag{51}$$

For assumed plane waves, we obtain

$$x = \rho_o(\nu^{-2} \frac{\partial}{\partial x}) P. \tag{52}$$

Hence, the operator Θ used by Censor becomes

$$\Theta = \nu^{-2} \frac{\partial}{\partial x} , \tag{53}$$

and Censor's Eq. (4) for the boundary condition becomes

$$\{-\frac{\omega^{-1}}{c_o} P_i e^{-i\omega[(x/c_o)+t]}$$

$$+ \int_{-\infty}^{+\infty} d\nu a(\nu) \frac{\nu^{-1}}{c_o} e^{i\nu[(x/c_o)-t]}\} = 0. \tag{54}$$

We now let $x = \varepsilon \sin\Omega t$ on the surface and perform the following expansions

$$e^{\pm(i\nu\varepsilon/c_o)\sin\Omega t} \approx 1 \pm i \frac{\nu\varepsilon}{c_o} \sin\Omega t + \ldots \tag{55}$$

$$a(\nu) = A(\nu) + \varepsilon\beta(\nu) + \ldots \quad . \tag{56}$$

We substitute Eqs. (55) and (56) into Eq. (54), retaining terms to zeroth order in ε:

$$-\frac{\omega}{c_o}^{-1} P_i e^{-i\omega t} + \int_{-\infty}^{\infty} d\nu A(\nu) \frac{\nu^{-1}}{c_o} e^{-i\nu t} = 0. \tag{57}$$

Multiplying Eq. (57) by $e^{i\nu' t}$, integrating over t, and letting $\nu' \to \nu$ yields

$$A(\nu) = P_i \delta(\nu-\omega). \tag{58}$$

Taking next the terms of first order in ε when Eq. (55) is substituted into Eq. (54), we obtain

$$\frac{2iP_i}{c_o^2} \sin\Omega t + \int_{-\infty}^{+\infty} d\nu B(\nu) \frac{\nu^{-1}}{c_o} e^{-i\nu t} = 0. \tag{59}$$

Solving Eq. (59) for $B(\nu)$ gives

$$B(\nu) = P_i \frac{\nu}{c_o} [\delta(\nu-\Omega-\omega) - \delta(\nu+\Omega-\omega)]. \tag{60}$$

Substituting Eqs. (60) and (58) into Eq. (56) and using the result in Eq. (50) gives

$$U_S = P_i\{\cos\omega(\frac{x}{c_o} - t) + \varepsilon \frac{(\Omega+\omega)}{c_o} \cos [(\Omega+\omega)(\frac{x}{c_o} - t)]$$

$$+ \frac{\varepsilon(\Omega-\omega)}{c_o} \cos [(-\Omega+\omega)(\frac{x}{c_o} - t)]\}. \qquad (61)$$

We determine the constant ε by requiring that the acoustic pressure for the plane wave radiated from the vibrating plane have the form

$$P = P_r e^{i[(\Omega/c_o)x-\Omega t]}. \qquad (62)$$

Substitution of Eq. (62) and $x = \varepsilon\sin\Omega t$ into Eq. (51) gives

$$\varepsilon = \frac{P_r}{\rho_o c_o \Omega}.$$

Hence, the Censor solution for the scattered acoustic pressure components at angular frequencies $\omega_\pm$ becomes

$$P_\pm = \frac{P_i P_r}{\rho_o c_o^2 \Omega} \omega_\pm e^{i\{\omega_\pm[(x/c_o) - t]\}} \qquad (63)$$

where $\omega_\pm = \omega\pm\Omega$ ($\omega>\Omega$ is assumed) or, taking the real part,

$$P_\pm = \frac{P_i P_r}{\rho_o c_o^2 \Omega} \omega_\pm \cos\{\omega_\pm[(x/c_o) - t]\}. \qquad (64)$$

2. Solution Using One-Dimensional, Second-Order, Nonlinear Wave Equation

In solving the problem of the scattering of a plane wave from a vibrating plane surface, it is convenient to use the one-dimensional, second-order, nonlinear wave equation expressed in Lagrangian coordinates. This equation is shown by Fubini-Ghiron [7] to be

$$\ddot{\xi} - c_o^2 \frac{\partial^2 \xi}{\partial x^2} = -c_o^2(1+\Gamma)\left(\frac{\partial \xi}{\partial x}\right)\left(\frac{\partial^2 \xi}{\partial x^2}\right). \tag{65}$$

[In this section x refers to a Lagrangian coordinate.]

We now represent ξ in a perturbation series $\xi = \varepsilon\xi_1 + \varepsilon^2\xi_2 + \ldots$, where ε is of the order of the Mach number.

We then substitute into Eq. (65) and equate equal orders of ε. This provides the first-order equation

$$\ddot{\xi}_{(1)} - c_o^2 \frac{\partial^2 \xi_{(1)}}{\partial x^2} = 0, \tag{66}$$

(the equation of linear acoustics), and the second-order equation

$$\ddot{\xi}_{(2)} - c_o^2 \frac{\partial^2 \xi_{(2)}}{\partial x^2} = -\frac{c_o^2(1+\Gamma)}{2} \frac{\partial}{\partial x}\left[\frac{\partial \xi_{(1)}}{\partial x}\right]^2. \tag{67}$$

To solve the problem of nonlinear scattering of a plane wave by a vibrating plane using the perturbation approach outlined in Section II. C, we must first solve the first-order (linear) Eq. (66). The physical boundary condition to be met is that there is no relative displacement between the planar surface and the fluid particles in contact with the surface*. This condition can be naturally met in Lagrangian coordinates by equating the displacement of a particle at the surface to the displacement of the surface itself.

The first-order solution is clearly the sum of the incident, scattered, and radiated waves:

$$\xi_{(1)} = \xi_i\left[\sin\omega\left(t + \frac{x}{c_o}\right) - \sin\omega\left(t - \frac{x}{c_o}\right)\right] + \xi_r \sin\Omega\left(t - \frac{x}{c_0}\right). \tag{68}$$

---

*Since we are solving second-order equations here, there should actually be a second boundary condition. In this case this condition takes the form of requiring that, apart from the quantity $\zeta_i \sin\omega[t + (x/c_o)]$, there are no incoming waves.

The first two terms in this expression represent the particle displacement for the rigid-body scattering solution, in which the reflected amplitude is the negative of the incident amplitude to insure the vanishing of the displacement at the rigid-body surface. The third term represents the radiated wave.

The first-order solution ξ_1 is now substituted into the right-hand side of the second-order Eq. (67) and the resulting linear inhomogeneous equation solved for ξ_2. If we retain only those terms that contribute to $\omega_\pm$, we obtain:

$$\ddot{\xi}_{(2)\pm} - c_o^2 \frac{\partial^2 \xi_{(2)\pm}}{\partial x^2} = \frac{(1+\Gamma)\xi_i \xi_r \omega\Omega}{2c_o}$$

$$[-\omega_\mp \sin(\omega_\pm t + \frac{\omega_\mp x}{c_o}) + \omega_\pm \sin\omega_\pm (t - \frac{x}{c_o})] \tag{69}$$

where again $\omega_\pm = \omega \pm \Omega$ (and $\omega > \Omega$ is assumed).

Equation (69) may be solved by the usual methods for ordinary inhomogeneous equations with constant coefficients. The result is:

$$\xi_{(2)\pm} = \frac{-(1+\Gamma)\xi_i \xi_r \omega\Omega}{2c_o} \{\frac{x}{2c_o} \cos(\omega_\pm t - \omega_\pm \frac{x}{c_o})$$

$$+ \frac{\omega_\mp}{\omega_\pm^2 - \omega_\mp^2} [-\sin(\omega_\pm t + \omega_\mp \frac{x}{c_o}) + \sin(\omega_\pm t - \omega_\pm \frac{x}{c_o})]\} \tag{70}$$

where a homogeneous solution has been added that causes $\xi_{2\pm} = 0$ at $x = 0$.

We obtain the corresponding acoustic pressure by performing the integration

$$P_{(2)\pm} = - \int \partial x \rho_o \frac{\partial^2 \xi_{(2)\pm}}{\partial t^2} ,$$

since this relationship is exact to all orders in Lagrangian coordinates. Also, using the fact that the acoustic pressure and displacement amplitudes

(for plane waves) are related to first order by $\xi = P/(\rho_o \omega c_o)$, we obtain the following expression for the sum- and difference-frequency pressure waves

$$P_{(2)\pm} = \frac{(1+\Gamma)P_i P_r}{4\rho_o c_o^2} \{\frac{\omega_\pm x}{c_o} \sin(\omega_\pm t - \omega_\pm \frac{x}{c_o}) - \cos(\omega_\pm t - \omega_\pm \frac{x}{c_o})$$

$$\frac{-2\omega_\pm^2}{\omega_\pm^2 - \omega_\mp^2} [\cos(\omega_\pm t + \omega_\mp \frac{x}{c_o}) + \frac{\omega_\mp}{\omega_\pm} \cos(\omega_\pm t - \omega_\pm \frac{x}{c_o})]\}. \quad (71)$$

It should be noted that Eq. (71) could have been stated in dimensionless form. Specifically, the ratio $P_{2\pm}/\{[(1+\Gamma)P_i P_r]/(\rho_o c_o^2)\}$ depends only on $\tau = \omega_\pm t$, $\zeta = \omega_\pm x/c_o$, the frequency ratio, and the boundary condition.

Comparing Eq. (71) to Censor's solution [Eq. (64)], the most striking distinction between them is the presence of the "x" coefficient in the first term inside the bracket of Eq. (71). Censor's result, being a boundary-effect solution, does not grow with distance from the scattering surface. Contributions from medium nonlinearities, being a cumulative volume effect, do grow with distance from the scattering surface. Hence, the nonlinear effect predicted by Eq. (71) will overwhelm that predicted by Censor within a small distance from the scatterer.

At this point we put these remarks on a more quantitative basis as well as calculate a region of validity for Eq. (71). First we consider relative contribution of the term arising from satisfying the boundary condition to the term representing the growing contribution from the virtual volume sources (i.e., the term with the "x" coefficient). The term that arises from satisfying the boundary condition is the last term in Eq. (71). Hence, a quantitative estimate of the relative contributions can be obtained via the ratio of the coefficients: $(2\omega_\mp c_o)/[(\omega_\pm^2 - \omega_\mp^2)x]$. Using primary frequencies of 160 and 100 kHz (which are of experimental interest later in this thesis), this ratio gives approximately $(1.94\times10^{-3}\text{m})/x$ in the difference-frequency case. Hence, the boundary effect becomes less than 8% of the volume effect at just one difference-frequency wavelength distance from the scattering surface (this wavelength is approximately 2.5 cm).

Also of interest in this problem is the distance to which the solution represented by Eq. (71) remains valid. This can be estimated by comparing the energy density of the secondary waves to the energy density of the primaries. The "secondary waves" include not only the sum- and difference-frequency waves but the second harmonic waves as well.

We can estimate the second-harmonic pressure using the formula obtained by Fubini-Ghiron [7]: $P_{2\omega} = [(P_o^2\omega)/(4\rho_o c_o^3)][2+(B/A)x]$, where the parameter γ of Fubini-Ghiron's original expression has been replaced by $1 + (B/A)$ (see Reference 5, p. 99). We can estimate the sum- and difference-frequency pressures using the coefficient of "x" in Eq. (71). Using 100-kHz primary of 10^5-Pa amplitude, Fubini-Ghiron's formula reduces to $P_{2\omega} = (744\ \text{Pa/m})x$. Similarly, if the second primary is taken to be of 160-kHz frequency and also 10^5-Pa amplitude, the sum- and difference-frequency pressures are $P_+ = (5.46\times10^3\ \text{Pa/m})x$ and $P_- = (1.26\times10^3\ \text{Pa/m})x$. We can estimate the energy densities of each of the relevant waves using the elementary plane-wave energy density formula $P_o^2/(2\rho_o c_o^2)$. We estimate the energy density of the primaries by inserting 10^5 Pa for P_o and multiplying by 3 (to account for the incident, reflected, and radiated waves), giving approximately 6.7 J/m^3 for the primaries. We estimate the energy density of the secondary waves by applying this equation separately to each of the four secondary waves in turn and adding. This gives approximately $[7\times10^{-3}(J/m^5)]x^2$. Hence, the energy density of the secondary waves becomes 1% of the energy density of the primaries at an approximate distance of $x = 3.1$ m. Therefore, it is reasonable to expect the solution to be reliable out to a distance of 3 m.

Finally, to establish the fact that viscous terms do not become important prior to this distance, we calculate the discontinuity distance (see Reference 5, p. 104]: $1/\ell = [(1+(B/2A)][(\omega u_o/c_o^2)]$. For a frequency of 160 kHz and amplitude of 10^5 Pa, this formula gives approximately 9.6 m. Hence, if the solution is restricted to distances less than 3 m, viscous terms can reasonably be expected to play a minor role.

One final comparison of interest is the volume effect term of Eq. (71) relative to the boundary-effect predicted by Censor as represented by Eq. (64). We represent this as

$$\frac{[P_{\pm}]_{\text{Censor}}}{[P_{\pm}]_{\text{nonlinear volume}}} \sim \frac{4c_o}{\Omega(1+\Gamma)x}.$$

For a typical planar surface frequency of 100 kHz, the two effects become equal at a distance x on the order of 0.1 cm. Due to the presence of the "x" factor in the nonlinear volume term, these volume effects continue to grow from this point, while Censor's surface effect remains constant.

One should not be disturbed by the presence of the Ω term in the denominator of this ratio. In the case of low Ω, the relevant factor to scale the distance is the wavelength associated with Ω, which is c_o/Ω. Hence, if we let $x = fc_o/\Omega$, we can determine the fraction (f) of a wavelength at which the nonlinear volume effect overtakes Censor's surface effect. This occurs for $x = 0.89\ (c_o/\Omega)$. Therefore, even in the limiting case in which the frequency of vibration of the planar surface approaches zero (maximizing Censor's effect relative to the nonlinear volume effect), the difference-frequency pressure generated by the fluid medium exceeds that produced by Censor's surface effect within a propagation distance less than the longest wavelength involved in the problem.

3. Some Comments Regarding the Censor Approach to the Problem of the Plane

Censor states in Section (4) of his paper that the fundamental boundary condition for the problem is the vanishing of the normal displacement. It is interesting to note that such a treatment is equivalent to simply recasting the incident wave into Lagrangian coordinates (a system that follows fluid motion), treating the problem as a simple rigid-body scattering, and then transforming the result back into Eulerian or fixed coordinates. We proceed to demonstrate the validity of this interpretation of Censor's approach.

We begin by transforming Censor's incident plane wave (apparently written in Eulerian form) into Lagrangian coordinates. An arbitrary Eulerian function, $f^E(x,t)$, may be transformed into its associated Lagrangian function, $f^L(a,t)$, by an expansion of the form

$$f^L(a,t) = f^E(x,t)\Big|_{x=a+\xi(a,t)} = f^E(x,t)\Big|_{x=a}$$

$$+ \frac{\partial f^E(x,t)}{\partial x}\Big|_{x=a} \xi(a,t) + \ldots, \tag{72}$$

where a = Lagrangian position coordinate

x = Eulerian position coordinate

ξ = displacement (common to both systems).

Letting $f^E(x,t) = P^E(x,t) = P_o e^{-i\omega[(x/c)+t]}$, which is the form of Censor's incident plane wave, and performing the expansion around a = 0 (the boundary surface of the plane), where $\xi(\phi,t) = \varepsilon \sin\Omega t$, one obtains (neglecting terms of order ε^2 or greater)

$$P^L(o,t) = P_o e^{-i\omega t} - \frac{\omega\varepsilon}{2c_o} P_o [e^{-i(\omega-\Omega)t} - e^{-i(\omega+\Omega)t}]. \tag{73}$$

To compare Eq. (73) to Censor's result (Eqs. 63), we must re-express Eq. (73) in Eulerian coordinates. This may be done by constructing the function $P^L(a,t)$, where the Lagrangian coordinate "a" is inserted into the right-hand side of Eq. (73) in the appropriate places to form outgoing plane waves. One can then expand the resulting function $P^L(a,t)$ in a series of the form

$$f^E(x,t) = f^L(a,t)\Big|_{a=x-\xi(x,t)} = f^L(a,t)\Big|_{a=x}$$

$$- \frac{\partial f^L(a,t)}{\partial a}\Big|_{a=x} \xi(x,t). \tag{74}$$

We construct $P^L(a,t)$ from the form of Eq. (73) as

$$P^L(a,t) = P_o e^{i\omega[(a/c_o)-t]} - \frac{\omega\varepsilon P_o}{2c_o}\{e^{i(\omega-\Omega)[(a/c_o)-t]} - e^{i(\omega+\Omega)[(a/c_o)-t]}\}, \quad (75)$$

and now expand $P^L(a,t)$ in a series of the form of Eq. (74) (neglecting terms of order ε^2 or greater) obtaining:

$$P^E(x,t) = P_o e^{i\omega[(x/c_o)-t]} - \frac{\omega\varepsilon P_o}{2c_o}\{e^{i(\omega-\Omega)[(x/c_o)-t]} - e^{i(\omega+\Omega)[(x/c_o)-t]}\} - \{\frac{i\omega P_o}{c_o} e^{i\omega[(x/c_o)-t]} \frac{\omega\varepsilon P_p}{2c_o}[\frac{i(\omega-\Omega)}{c_o} e^{i(\omega-\Omega)[(x/c_o)-t)}] - \frac{i(\omega+\Omega)}{c_o} e^{i(\omega+\Omega)[(x/c_o)-t]}\}\xi(x,t). \quad (76)$$

We now let $\xi = \varepsilon\sin\Omega t$ and again neglect terms of order ε^2 or higher. The result is

$$P^E(x,t) = P_o^{i\omega[(x/c_o)-t)} - \frac{\omega\varepsilon P_o}{2c_o}\{e^{i(\omega-\Omega)[(x/c)-t)} - e^{i(\omega+\Omega)[(x/c_o)+t]}\} - \frac{\varepsilon\omega P_o}{2c_o}\{e^{i[(\omega x/c_o)-(\omega-\Omega)t]} - e^{i[(\omega x/c_o)-(\omega+\Omega)t]}\}. \quad (77)$$

We now recognize that the above expansion is valid only at $x = 0$ (since this is the only place where $\xi = \varepsilon\sin\Omega t$). Evaluating Eq. (77) for $x = 0$ and using the fact that $\varepsilon = P_r/\rho_o c_o \Omega$, we obtain

$$p^E(o,t) = P_o e^{-i\omega t} - \frac{P_o P_r \omega}{P_o c_o^2 \Omega} [e^{-i(\omega-\Omega)t} - e^{-i(\omega+\Omega)t}]. \quad (78)$$

Comparing the sum- and difference-frequency components of Eq. (78) with Censor's result [Eq. (63)], we note that for $\Omega << \omega$, they are identical [P_o of Eq. (78) is equivalent to P_i of Eq. (63)].

Hence, it is seen that Censor's result is clearly of the same order as the difference between Eulerian and Lagrangian coordinates. Such effects normally are not even experimentally measurable, since no presently available measurement hydrophone is either completely rigid (and hence measures in Eulerian coordinates) or moves completely freely with the fluid (and hence measures in Lagrangian coordinates). Any presently available hydrophone will have an uncertainty in its measuring capability, in an experiment design-ed to measure difference-frequency waves, of the order of the difference between the pressure predicted in a Lagrangian frame and the pressure predic-ted in an Eulerian frame. This difference is known as "pseudosound" and is treated more fully in the section describing the experimental results. Hence, the effect predicted by Censor cannot be measured with present-day technology.

F. Cylindrical-Wave Scattering from a Vibrating Cylindrical Surface

The present section considers the problem of the generation of sum- and difference-frequency waves when a cylindrical wave (of angular frequency ω'') is normally incident on a cylinder whose surface deforms radially in a uniform and harmonic fashion. It is assumed that the waves at frequency $\omega_\pm = \omega'' \pm \omega'$ are outwardly propagating waves in the limit $r \to \infty$.

1. Solution Using Second-Order Nonlinear Wave Equation.

We now consider the problem of a vibrating cylindrical surface. The geometry of the problem is indicated in Fig. 3.

In solving the second-order, nonlinear wave Eq. (48), we assume the scattered pressure P_s and the simple-source term $\rho_o(\partial q/\partial t)$ may be represented as*:

$$P_{(2)} = \mathrm{Re} \sum_n P_n(r,\theta)e^{-i\omega_n t} \tag{79}$$

and

$$\rho_o \frac{\partial q}{\partial t} = -\mathrm{Re} \sum_n B_n(r,\theta)e^{-i\omega_n t}, \tag{80}$$

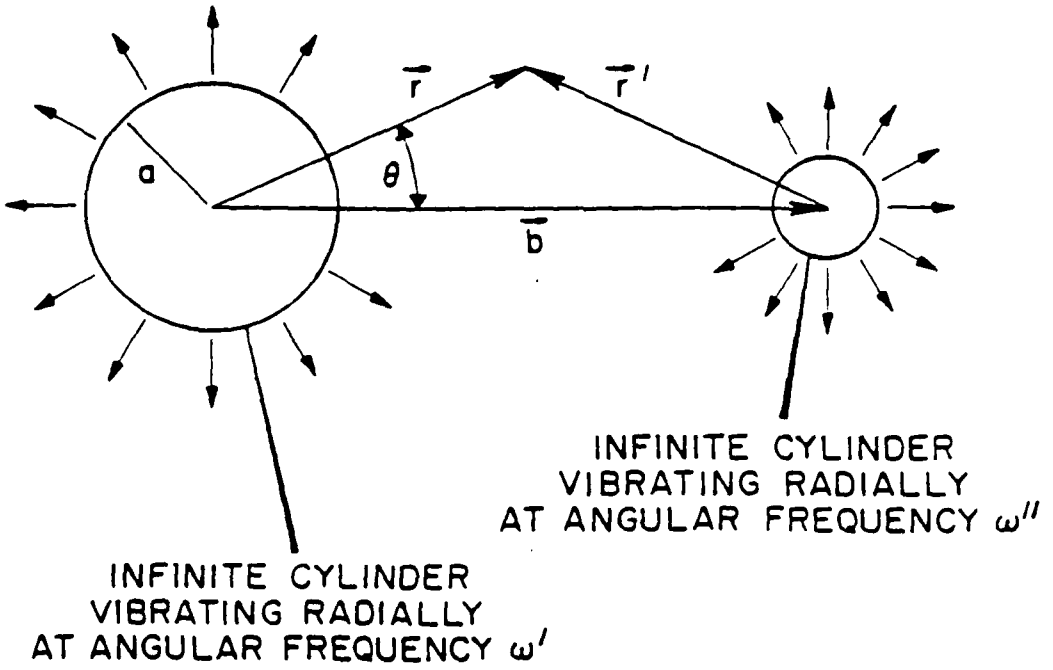

Fig. 3 - Geometry of cylindrical wave scattering from a vibrating cylinder

---

*Specific estimates of errors introduced into the solution of Eq. (48) by the neglect of the D'Alembertian terms of Eq. (47) are provided in Chapter IV. B.

where the subscript n is used to distinguish between sum- and difference-frequency components: n = 1 refers to the sum frequency and n = 2 refers to the difference frequency. Also present in this expansion are terms corresponding to the harmonics of the primaries; but since only the sum and difference frequencies are of interest here, no special notation will be provided for these terms. At the conclusion of this analysis, the numerical subscripts will be replaced by the more descriptive "+" and "-" notation. Hence, for example, $P_1(r,\theta) \to P_+(r)$ and $P_2(r,\theta) \to P_-(\vec{r})$. These replacements will also help avoid confusion between $P_2(r,\theta)$ (the difference-frequency pressure) and $P_2(\vec{r})$ (the perturbation solution accurate to second order).

By substituting Eqs. (79) and (80) into Eq. (48), we obtain the following equation for the time-independent amplitudes

$$\nabla^2 P_n + k_n^2 P_n = B_n \tag{81}$$

with $k_n = \omega_n/c_o$.

We define an associated Green's function $g_n(\vec{r},\vec{r}')$ such that

$$\nabla^2 g_n(\vec{r},\vec{r}') + k_n^2 g_n(\vec{r},\vec{r}') = -\delta(\vec{r}-\vec{r}') \tag{82}$$

subject to the boundary condition $\hat{r} \cdot \vec{\nabla} g_n(r,\vec{r}') = 0$ on the cylindrical surface, where $\hat{r}$ is a unit normal vector, directed outward from that surface. Here $\delta(\vec{r}-\vec{r}')$ is the Dirac delta function. We also have the condition that as $\vec{r} \to \infty$, $g_n \sim (e^{ik_n r}/r^{1/2}) \times$ function of $(\vec{r}', \Theta)$.

A representation of P_n may be obtained by multiplying Eq. (82) by P_n and Eq. (81) by $g_n(r,r')$, subtracting the resulting equations, and integrating over primed variables. The result is:

$$P_n(\vec{r}) = -\int d\tau' B_n(\vec{r}') g_n(\vec{r},\vec{r}') + \iint d\vec{S}' \cdot \vec{\nabla}' P_n(\vec{r}',\theta') g_n(\vec{r}',\vec{r}) \tag{83}$$

in which the vanishing of the normal gradient of the Green's function has been imposed. Formally, the volume integral of Eq. (83) is taken over all space, excluding the volume interior to the cylinder vibrating at angular frequency ω'. The surface integral in this equation represents integrals over the surfaces of both cylinders as well as over the surface at infinity. We will

consider the surface integral over the ω" cylinder later.

In carrying Eq. (83) to a final solution, the surface integral term will actually be dropped, and the volume integral will be analyzed only between r' = a and r' = r (justification for this will be presented shortly as well as in Chapter IV). In summary, what this means is that: 1) the surface integral at r' = a is neglected, 2) the surface integral over the ω" cylinder is neglected, and 3) the volume integral from r' = r to r' = ∞ is neglected. Estimates of the errors arising from some of the neglected terms will be made presently (the rest being postponed until Chapter IV, Section B).

We now consider the surface integral in Eq. (83) in somewhat greater detail. In the current problem we are considering rigid-body scattering, although the surface is permitted to deform harmonically at frequency ω'. The requirement of rigid-body scattering manifests itself in the handling of this surface integral. From the first-order equation of momentum conservation [Eq. (18)], it is clear that for harmonic time dependence, the gradient of the pressure field is proportional to the velocity of the fluid (and hence the velocity of the surface). Therefore, in the surface integral of Eq. (83) the "$\nabla' P_{1.}$" term may be viewed as the component of the surface velocity at the sum and difference frequencies*. We interpret the "rigid-body oscillation" of the surface as constraining the surface to vibrate only at the frequency at which it is being driven (i.e., ω'). Hence this term and the surface integral of Eq. (83) vanish.

We next consider what influences viscosity might have on this surface integral (and hence on the sum- and difference-frequency pressures). We have already demonstrated in Section II. C that effects of viscosity on the propagation of acoustic waves are insignificant in this type of problem. Hence, it is reasonable to separately consider a "boundary region" and a "propagation

---

*This statement is based on the fact that the equation $\dot{\nabla P} = -\rho_o(\partial \dot{u}/\partial t)$ is correct to all orders (in the lossless case) in Lagrangian coordinates. In Eq. (83), of course, the expression $\dot{\nabla}' P_n$ is evaluated in Eulerian coordinates. However, the difference between evaluating a function in these two reference frames is of the order of pseudosound. The validity of this statement, as well as an estimate of the effect of an error of the order of pseudosound on the surface integral of Eq. (83) is provided in Chapter IV. B.

region" (see, for example, the discussion on pages 281-286 of Reference 29). For a frequency of 100 kHz in water, this boundary layer is of approximately 5.6-microns thickness (using equation 6.4.31 of Reference 29). We assume that outside this boundary layer, the lossless equations apply and, hence, the Green's function solution represented in Eq. (83) is appropriate. We note that only the normal velocity component is present in the surface integral. Hence, any tangential velocity component arising from viscous boundary-layer effects will not influence the radiation field in a significant way.

It is assumed, then, that only the volume integral from r' = a to r' = r contributes significantly to the solution. At this point, we neglect the surface integral of Eq. (83) and simply represent P_n as

$$P_n(\vec{r}) = - \int d\tau' B_n(\vec{r}') g_n(\vec{r},\vec{r}') \tag{84}$$

(volume integration only between r' = a and r' = r).

The rigid-body Green's function appropriate to cylindrical geometry is required in Eq. (84). It is well known [42] and is given by

$$g_n(\vec{r},\vec{r}') = \frac{1}{4} \sum_{m=0}^{\infty} (2-\delta_{mo}) \cos m(\phi-\phi') \left[H_m^{(1)}(k_n r) J_m(k_n r') - \frac{J_m'(k_n a)}{H_m^{(1)\prime}(k_n a)} H_m^{(1)}(k_n r) H_m^{(1)}(k_n r') \right]$$

$$r>r' \tag{85}$$

where δ_{mo} is the Kronecker delta. Also, $g_n(\vec{r},\vec{r}') = g_n(\vec{r}',\vec{r})$.

The Green's function $g_n(\vec{r},\vec{r}')$ is not needed for the region r<r' since contributions from this region (which is further from the source than the point of interest) tend to phase cancel against one another and, hence, contribute very little to the overall pressure at the observation point r. Contributions from the region r>r', however, tend to add constructively and give by far the majority of the pressure at the observation point. Hence, in both the current geometry and the one in the next section (involving a plane wave incident on a vibrating cylinder), the contributions to the Green's

function integral between the observation point r and infinity will be assumed negligible.

To complete the solution to the current problem, we must now calculate the functions $B_n(r')$. In order to do so, we refer once again to Fig. 2. From elementary trigonometry we have $r' = (r^2 + b^2 - 2rb\cos\theta)^{1/2}$. We now use the summation theorem (see, for example, Gradshteyn and Ryzhik [43]) to obtain

$$H_o^{(1)}\left(\frac{\omega'' r'}{c_o}\right) = H_o^{(1)}\left(\frac{\omega'' b}{c_o}\right) J_o\left(\frac{\omega'' r}{c_o}\right) + 2 \sum_{m=1}^{\infty} H_m^{(1)}\left(\frac{\omega'' b}{c_o}\right) J_m\left(\frac{\omega'' r}{c_o}\right) \cos m\theta \qquad (86)$$

for $r<b$, and

$$H_o^{(1)}\left(\frac{\omega'' r'}{c_o}\right) = J_o\left(\frac{\omega'' b}{c_o}\right) H_o^{(1)}\left(\frac{\omega'' r}{c_o}\right) + 2 \sum_{m=1}^{\infty} J_m\left(\frac{\omega'' b}{c_o}\right) H_m^{(1)}\left(\frac{\omega'' r}{c_o}\right) \cos m\theta \qquad (87)$$

for $r>b$.

The incident wave is assumed to be of the form of a uniformly diverging cylindrical wave originating at the surface of the cylinder vibrating at an angular frequency ω'' (the interiors of the cylinders are, of course, excluded from the region of interest). Hence, allowing A' to be a pressure amplitude, the incident cylindrical wave may be written in the form $A' H_o^{(1)}(\omega'' r'/c_o)$. Equation (86) is used to re-express $H_o^{(1)}$. Also note that P_{inc} is singular at the origin of the ω'' cylinder.

The corresponding particle velocity may be obtained by use of the first-order equation of momentum conservation [Eq. (18)], expressed in the form $U = [-i/\rho_o \omega][\partial P/\partial r]$ (for the radial component). We thus have for the incident particle velocity wave,

$$U_{inc} = \frac{iA'}{\rho_o c_o} H_o^{(1)}(\frac{\omega'' b}{c_o}) J_1(\frac{\omega'' r}{c_o})$$

$$+ \frac{iA'}{\rho_o c_o} \sum_{m=1}^{\infty} \cos(m\theta)[J_{m+1}(\frac{\omega'' r}{c_o})$$

$$- J_{m-1}(\frac{\omega'' r}{c_o})]H_m^{(1)}(\frac{\omega'' b}{c_o}). \tag{88}$$

We assume the first-order scattered acoustic pressure wave to be of the form:

$$P_{scatt} = \sum_{m=0}^{\infty} A_m \cos m\theta H_m^{(1)}(\frac{\omega'' r}{c_o}) e^{-i\omega'' t}. \tag{89}$$

Hence, the scattered particle velocity wave is

$$U_{scatt} = \{ \frac{iA_o}{\rho_o c_o} H_o^{(1)}(\frac{\omega'' r}{c_o}) + \frac{i}{2\rho_o c_o} \sum_{m=1}^{\infty} A_m \cos m\theta$$

$$\times[H_{m+1}^{(1)}(\frac{\omega'' r}{c_o}) - H_{m-1}^{(1)}(\frac{\omega'' r}{c_o})]\}e^{-i\omega'' t}. \tag{90}$$

We assume the scattering cylinder to be rigid in solving the first-order problem; hence, the boundary condition becomes $U_{inc} = -U_{scatt}$ at $r = a$. This condition yields the scattering amplitudes A_m

$$A_o = -A' \frac{H_o^{(1)}(\frac{\omega'' b}{c_o})}{H_1^{(1)}(\frac{\omega'' a}{c_o})} J_1(\frac{\omega'' a}{c_o})$$

$$A_m = -2A' H_m^{(1)}(\frac{\omega'' b}{c_o}) \frac{[J_{m+1}(\frac{\omega'' a}{c_o}) - J_{m-1}(\frac{\omega'' a}{c_o})]}{[H_{m+1}^{(1)}(\frac{\omega'' a}{c_o}) - H_{m-1}^{(1)}(\frac{\omega'' a}{c_o})]} \quad m > 1. \tag{91}$$

The first-order scattered acoustic pressure for r<b is thus given by Eq. (89) with Eq. (91) substituted for A_m.

The incident acoustic pressure for r>b is given by:

$$P_{inc} = [A' J_o(\frac{\omega" b}{c_o}) H_o^{(1)}(\frac{\omega" r}{c_o}) + 2 \sum_{m=1}^{\infty} J_m(\frac{\omega" b}{c_o}) H_m^{(1)}(\frac{\omega" r}{c_o}) \cos m\theta] x e^{-i\omega" t}. \quad (92)$$

Hence, the general solution to the rigid-body scattering problem to first order is

$$P_{tot} = \{A' H_o^{(1)}(\frac{\omega" b}{c_o}) J_o(\frac{\omega" r}{c_o}) + A_o H_o^{(1)}(\frac{\omega" r}{c_o}) + \sum_{m=1}^{\infty} [A_m H_m^{(1)}(\frac{\omega" r}{c_o}) + 2A' H_m^{(1)}(\frac{\omega" b}{c_o}) J_m(\frac{\omega" r}{c_o})] \cos m\theta\} e^{-i\omega" t} \quad r<b \quad (93)$$

and,

$$P_{tot} = \{A' J_o(\frac{\omega" b}{c_o}) H_o^{(1)}(\frac{\omega" r}{c_o}) + B_o H_o^{(1)}(\frac{\omega" r}{c_o}) + \sum_{m=1}^{\infty} [B_m H_m^{(1)}(\frac{\omega" r}{c_o}) + 2A' J_m(\frac{\omega" b}{c_o}) H_m^{(1)}(\frac{\omega" r}{c_o})] \cos m\theta\} e^{-i\omega" t} \quad r>b. \quad (94)$$

This can be rewritten as

$$P_{tot} = \{A'H_o^{(1)}(\frac{\omega''r_>}{c_o})J_o(\frac{\omega''r_<}{c_o})$$

$$+ A_o H_o^{(1)}(\frac{\omega''r}{c_o}) + \sum_{m=1}^{\infty} [A_m H_m^{(1)}(\frac{\omega''r}{c_o})$$

$$+2A'H_m^{(1)}(\frac{\omega''r_>}{c_o})J_m(\frac{\omega''r_<}{c_o})]\cos m\theta\}e^{-i\omega''t}, \quad (95)$$

where $r_{>(<)}$ is the greater (lesser) of r and b and A_m are given by Eqs. (91).

The primary field P_1 to be used in the simple-source term of the second-order nonlinear differential Eq. (48) is obtained by adding the cylindrically radiated field at frequency ω' to Eq. (95), obtaining:

$$P_{(1)} = AH_o^{(1)}(\frac{\omega'r}{c_o})e^{-i\omega't} + \sum_{m=0}^{\infty} [A_m H_m^{(1)}(\frac{\omega''r}{c_o})$$

$$+ (2-\delta_{mo})A'H_m^{(1)}(\frac{\omega''r_>}{c_o})J_m(\frac{\omega''r_<}{c_o})]\cos m\theta e^{-i\omega''t}, \quad (96)$$

where A = pressure amplitude of the cylinder oscillating at angular frequency ω' and δ_{mo} is the Kronecker delta.

We obtain the real part of P_1 using the fact that $\mathrm{Re}[P_{(1)}] = [P_{(1)}+P_{(1)}^*]/2$. Hence,

$$\mathrm{Re}[P_{(1)}] = \frac{A}{2} H_o^{(1)}(\frac{\omega'r}{c_o})\, e^{-i\omega't}$$

$$+ \sum_{m=0}^{\infty} [\frac{A_m}{2} H_m^{(1)}(\frac{\omega''r}{c_o}) + \frac{2-\delta_{mo}}{2} A'H_m^{(1)}(\frac{\omega''r_>}{c_o})J_m(\frac{\omega''r_<}{c_o})$$

$$\times \cos m\theta e^{-i\omega''t} + \text{c.c.} \quad (97)$$

If we define $[P_{(1)}{}^2]_{\pm}$ as the portions of $P_{(1)}{}^2$ that contribute to the sum- and difference-frequency pressures, we obtain

$$[P_{(1)}{}^2]_+ = \sum_{m=0} \frac{A}{2} H_o{}^{(1)}(\frac{\omega' r}{c_o})[H_m{}^{(1)}(\frac{\omega'' r}{c_o})A_m$$

$$+ (2-\delta_{mo})A' H_m{}^{(1)}(\frac{\omega'' r_>}{c_o})J_m(\frac{\omega'' r_<}{c_o})]$$

$$\times \cos m\Theta e^{-i(\omega'+\omega'')t} + c.c. \qquad (98)$$

and

$$[P_{(1)}{}^2]_- = \sum_{m=0}^{\infty} \frac{A}{2} H_o{}^{(1)}(\frac{\omega' r}{c_o})[H_m{}^{(2)}(\frac{\omega'' r}{c_o})A_m{}^*$$

$$+ (2-\delta_{mo})A' H_m{}^{(2)}(\frac{\omega'' r_>}{c_o})J_m(\frac{\omega'' r_<}{c_o})]$$

$$\times \cos m\Theta e^{-i(\omega'-\omega'')t} + c.c. \qquad (99)$$

The simple source term of Eq. (48) may now be obtained using

$$(\rho_o \frac{\partial q}{\partial t})_{\pm} = \frac{\Gamma}{\rho_o c_o{}^4} \frac{\partial^2}{\partial t^2} [P_{(1)}{}^2]_{\pm}.$$

This results in:

$$(\rho_o \frac{\partial q}{\partial t})_+ = - \frac{\Gamma(\omega'+\omega'')^2}{2\rho_o c_o^4} \sum_{m=0}^{\infty} AH_o^{(1)}(\frac{\omega' r}{c_o})$$

$$[H_m^{(1)}(\frac{\omega'' r}{c_o})A_m + (2 - \delta_{\omega mo})$$

$$\times A'H_m^{(1)}(\frac{\omega'' r_>}{c_o})J_m(\frac{\omega'' r_<}{c_o})]\cos m\Theta e^{-i(\omega'+\omega'')t} + c.c. \qquad (100)$$

and

$$(\rho_o \frac{\partial q}{\partial t})_- = - \frac{\Gamma(\omega'-\omega'')^2}{2\rho_o c_o^4} \sum_{m=0}^{\infty}$$

$$[AH_o^{(1)}(\frac{\omega' r}{c_o})[H_m^{(1)}(\frac{\omega'' r}{c_o})A_m^* + (2-\delta_{mo})$$

$$\times A'H_m^{(2)}(\frac{\omega'' r_>}{c_o})J_m(\frac{\omega'' r_<}{c_o})]\cos m\Theta e^{-i(\omega'-\omega'')t} + c.c. \qquad (101)$$

By Eq. (80),

$$(\rho_o \frac{\partial q}{\partial t})_\pm = \frac{-1}{2}[B_\pm e^{-i\omega_\pm t} + c.c].$$

It should be noted that $\omega_- = |\omega' - \omega''|$ and, therefore, B_- are minus the coefficient of $e^{-i(\omega'-\omega'')t}$, which is explicitly shown in Eq. (101) when $\omega'>\omega''$. It is the complex conjugate of this when $\omega''>\omega'$. For $\omega'>\omega''$,

$$P_{-}(\vec{r}) = -\int_a^r d\tau' B_n(\vec{r}') g_n(\vec{r}', \vec{r})$$

$$= -i \frac{\Gamma(\omega'-\omega'')^2}{4\rho_o c_o^4} \sum_{\ell,m=0}^{\infty} A(2-\delta_{\ell o}) \int_o^{2\pi} d\Theta' \cos m\theta' \cos\ell(\Theta-\Theta')$$

$$\times \int_a^r dr' r' [H_o^{(1)}(\frac{\omega' r'}{c_o}) H_m^{(2)}(\frac{\omega'' r'}{c_o}) H_\ell^{(1)}(k_{-} r) J_\ell(k_{-} r') A_m^*$$

$$- \frac{J_\ell'(k_{-} a)}{H_\ell^{(1)'}(k_\ell a)} H_o^{(1)}(\frac{\omega' r'}{c_o}) H_m^{(2)}(\frac{\omega'' r'}{c_o}) H_\ell^{(1)}(k_{-} r) H_\ell^{(1)}(k_{-} r') A_m^*$$

$$+ A' H_o^{(1)}(\frac{\omega' r'}{c_o})(2-\delta_{mo}) H_m^{(2)}(\frac{\omega'' b}{c_o}) J_m(\frac{\omega'' r'}{c_o}) H_\ell^{(1)}(k_{-} r) J_\ell(k_{-} r')$$

$$- (2-\delta_{mo}) A' H_o^{(1)}(\frac{\omega' r'}{c_o}) H_m^{(2)}(\frac{\omega'' b}{c_o}) J_m(\frac{\omega'' r'}{c_o}) \frac{J_\ell'(k_{-} a)}{H_\ell^{(1)'}(k_{-} a)}$$

$$\times H_\ell^{(1)}(k_{-} r) H_\ell^{(1)}(k_{-} r')] \qquad (102)$$

where $k_{-} = (\omega'-\omega'')/c_o$.

The angular integrals can be performed using the fact that

$$\int_0^{2\pi} d\Theta' \cos m\Theta' \cos\ell(\Theta-\Theta') = \begin{cases} \delta_{\ell m} \pi \cos\ell\Theta & \ell \neq 0 \\ 2\pi & \ell = m = 0. \end{cases}$$

This yields (for r<b):

$$P_-(\vec{r}) = \frac{-i\pi\Gamma(\omega'-\omega'')^2}{2\rho_o c_o^4} \sum_{\ell=0}^{\infty} A\cos(\ell\theta)$$

$$\times\{ \int_a^r dr'r'[H_o^{(1)}(\frac{\omega'r'}{c_o})H_\ell^{(2)}(\frac{\omega''r'}{c_o})H_\ell^{(1)}(k_-r)J_\ell(k_-r')A_\ell^*$$

$$- \frac{J_\ell'(k_-a)}{H_\ell^{(1)\prime}(k_-a)} H_o^{(1)}(\frac{\omega'r'}{c_o})H_\ell^{(2)}(\frac{\omega''r'}{c_o})H_\ell^{(1)}(k_-r)H_\ell^{(1)}(k_-r')A_\ell^*$$

$$+ (2-\delta_{\ell o})A'H_o^{(1)}(\frac{\omega'r'}{c_o})H_\ell^{(2)}(\frac{\omega''b}{c_o})J_\ell(\frac{\omega''r'}{c_o})H_\ell^{(1)}(k_-r)J_\ell(k_-r')$$

$$- (2-\delta_{\ell o})A'H_o^{(1)}(\frac{\omega'r'}{c_o})H_\ell^{(2)}(\frac{\omega''b}{c_o})J_\ell(\frac{\omega''r'}{c_o}) \frac{J_\ell'(k_-a)}{H_\ell^{(1)\prime}(k_-a)}$$

$$\times H_\ell^{(1)}(k_-r)H_\ell^{(1)}(k_-r')]\} \qquad (103)$$

where $r<b$ and $\omega'>\omega''$.

For $r>b$, the integrals in Eq. (103) run from a to b, plus an additional set of integrals to those in Eq. (103) is required in which the roles of r' and b are exchanged for the underlined terms and the limits run from b to r. However, one additional difficulty arises when $r>b$. This is the fact that the source Hankel function has a singularity within the volume of integration. This difficulty can be circumvented by excluding this singular region via the mathematical artifice of enclosing the ω'' cylinder with a surface of radius ε and analyzing the contribution to the solution from the associated surface integral. It is relatively straightforward to demonstrate that this surface contribution is proportional to $\varepsilon\ell n\varepsilon$ and, hence, gives a vanishing contribution in the limit as $\varepsilon \to 0$.

The sum- and difference-frequency pressures can once again be specified in dimensionless form in terms of the parameters $\tau = \omega_\pm t$, $\zeta = \omega_\pm r/c_o$, Θ, $\omega_\pm a/c_o$, $\omega_\pm b/c_o$, as well as the frequency ratio.

At this point we note that estimating a region of validity for Eq. (103) is similar to the case of plane-wave scattering by a vibrating cylinder. Hence, we postpone this calculation until the solution to this latter problem is obtained [see discussion following Eq. (115)].

2. Connection With Previous Research

In 1966, Lauvstad [21] solved the problem of two eccentric cylindrical waves simultaneously present in a fluid medium. The present work differs from Lauvstad's in two important ways. First, Lauvstad solved only the radiation problem; i.e., no scattering of the primaries from the cylindrical surfaces was considered. Secondly, Lauvstad used the Green's function that vanishes at the cylindrical surfaces for the second-order solution. This corresponds to the rather physically unrealizable situation in which the radiating cylindrical surface is acoustically soft. Since the current work used the Green's function whose normal derivative vanishes at the cylindrical surface (corresponding to the more realistic rigid-body case), no limits can be taken to establish correspondence between the results of Lauvstad and the current work.

It is nonetheless of interest to obtain an expression for the difference-frequency pressure for the radiation problem considered by Lauvstad on the basis of the current theory with rigid boundaries replacing Lauvstad's soft boundaries. All that is required is to drop the terms in Eq. (103) containing the scattering coefficients A_ℓ^* (this is equivalent to inhibiting the scattering process in the first-order fields).

This results in:

$$P_-(\vec{r}) = \frac{-i\pi\Gamma(\omega'-\omega'')^2}{4\rho_o c_o^4} AA' \sum_{\ell=0}^{\infty} (2-\delta_{\ell o})\cos(\ell\Theta) H_\ell^{(1)}(k_- r) H_\ell^{(2)}\left(\frac{\omega'' b}{c_o}\right)$$

$$\times \int_a^r dr' r' \left[J_\ell\left(\frac{\omega'' r'}{c_o}\right) H_o^{(1)}\left(\frac{\omega' r}{c_o}\right) \right] \left[J_\ell(k_- r') - \frac{J_\ell'(k_- a)}{H_\ell^{(1)\prime}(k_- a)} H_\ell^{(1)}(k_- r') \right]$$

for $r<b$ and $\omega'>\omega''$.

Although no general correspondence can be made between the results presented above and those of Lauvstad (due to the different choices of Green's functions), it is possible to establish a connection in the asymptotic limit $r \to \infty$. This is due to the physically reasonable result that the effects of the surface contributions in this problem have become negligible at distances far from the surfaces. It is relatively easy to demonstrate in this limit that Lauvstad's Eq. (29) and Eq. (103) above reduce to the same expression in this limit. It is necessary again to discard from Eq. (103) the terms corresponding to surface scattering. It is also necessary to discard the terms which reflect the different boundary conditions satisfied by the Green's functions (namely, the terms with coefficients involving derivatives). It is also necessary in Lauvstad's expression to discard the integrals with infinite limits, which has already been done in producing Eq. (103). Finally, the following correspondence between constants in the two treatments must be made:

Lauvstad's Notation	Notation Used Here
$\Lambda + 2$	2Γ
A_1	$A'/(\rho_o \omega'')$
A_2	$A/(\rho_o \omega')$

When these relations and simplifications are used, Eq. (103) will reduce to

$$P_-(\vec{r}) = \frac{-i\pi(\omega'-\omega'')^2}{2\rho_o c_o^4} \sum_{\ell=0}^{\infty} (2 - \delta_{\ell 0})\cos(\ell\theta) H_\ell^{(1)}(k_- r)$$

$$\times \left[H_\ell^{(2)}\left(\frac{\omega'' b}{c_o}\right) \int_a^b dr' r' \, H_0^{(1)}\left(\frac{\omega' r'}{c_o}\right) J_\ell\left(\frac{\omega'' r'}{c_o}\right) J_\ell(k_- r) \right.$$

$$\left. + J_\ell\left(\frac{\omega'' b}{c_o}\right) \int_b^r dr' r' H_0^{(1)}\left(\frac{\omega' r'}{c_o}\right) H_\ell^{(2)}\left(\frac{\omega'' r'}{c_o}\right) J_\ell(k_- r') \right]$$

for $r \to \infty$ and $r > b$.

Lauvstad's Eq. (29) reduces to $1/2$ times this result. However, an apparent algebraic slip occurred when Lauvstad obtained his Eq. (29) from his Eq.s (26, 27, and 28). [His Eq. (29) should have a divisor of 8, not 16 as listed in Lauvstad's article.]

G. Plane-Wave Scattering from a Vibrating Cylindrical Surface

In the present section, the problem of the generation of sum- and difference-frequency waves arising from the scattering of a plane wave (of angular frequency ω_p) normally incident on a cylinder that deforms radially and uniformly (at angular frequency ω_c) will be considered.

1. Censor-Method Solution

The problem of the scattering of a plane wave of angular frequency ω_p normally incident on a cylinder vibrating radially with angular frequency ω_c (see Fig. 4) was a problem considered by Censor. Substitution of his Eqs. (24) into his Eqs. (10) and (6) results in his solution for the sum- and difference-pressure waves

$$P_{\pm} = -\frac{P_p P_c \left|H_1^{(1)}(k_c a)\right|}{\rho_o c_o^2 \omega_c}\,\omega_{\pm}\left[\frac{H_o^{(1)}\left(\frac{\omega_{\pm} r}{c_o}\right)}{H_o^{(1)\prime}(q) H_o^{(1)}\left(\frac{\omega_{\pm} a}{c_o}\right)}\right.$$

$$\left. + 2\sum_{m=1}^{\infty} i^m \cos m\theta \left(1 - \frac{m^2}{\rho^2}\right) \frac{H_m[\omega_{\pm}(r/c_o)]}{H_m^{(1)\prime}(q) H_m^{(1)\prime}\left(\frac{\omega_{\pm} a}{c_o}\right)}\right], \qquad (104)$$

where $q \equiv \rho\alpha/c_o$, P_p is the plane-wave pressure amplitude and where P_c is the cylindrical-wave pressure amplitude defined by $P = P_c H_o(k_c r)$, $\rho = k\rho a$, k_c = wave number associated with the cylindrical wave, a = radius of cylinder, and $\omega_{\pm} = \omega_p \pm \omega_c$.

In this expression, Censor's small parameter ϵ has been replaced by $[P_c \left|H_1^{(1)}(k_c a)\right|]/(\rho_o \Omega a c_o)$, obtained by requiring the pressure and displacement at the surface of the cylinder to be consistent with Eq. (51).

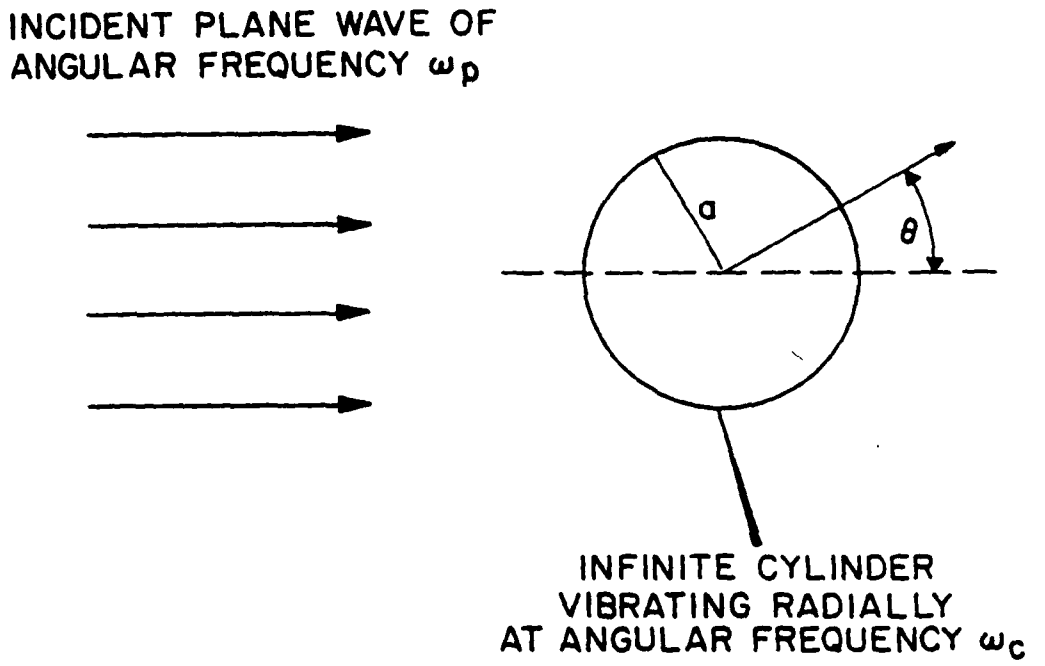

Fig. 4 - Geometry of plane wave scattering from a vibrating cylinder

2. Solution Using Second-Order Nonlinear Wave Equation

We must now solve the second-order nonlinear wave Eq. (48) using as P_1 the sum of: 1) solution of the linear wave equation

$$\Box^2 P_{(1)} = 0 \tag{105}$$

for the problem of linear rigid-body scattering from a cylinder plus 2) the linear solution for radiation from a cylindrical source. Thus $P_{(1)}$ may be represented as

$$P_{(1)} = P_{inc} + P_{scatt} + P_{rad} \tag{106}$$

with obvious meaning for the subscript notation. The expressions for the well-known linear-wave equation solutions may be found in any standard

acoustic text, such as Morse and Ingard [44]. They are

$$P_{inc} = P_o[J_o(\frac{\omega_p r}{c_o}) + 2 \sum_{m=1}^{\infty} i^m \cos m\theta J_m(\frac{\omega_p r}{c_o})]e^{-i\omega_p t}, \quad (107)$$

$$P_{scatt} = \sum_{m=0}^{\infty} A_m \cos(m\theta) H_m^{(1)}(\frac{\omega_p r}{c_o}) e^{-i\omega_p t}, \quad (108)$$

and

$$P_{rad} = A H_o^{(1)}(\frac{\omega_c r}{c_o}) e^{-i\omega_c t}, \quad (109)$$

where P_o = pressure amplitude of incident plane wave

A = pressure amplitude of radiated cylindrical wave

ω_p = angular frequency of incident plane wave

ω_c = angular frequency of cylindrical radiated wave.

J_m = m^{th}-order Bessel function of the first kind

$H_m^{(1)}$ = m^{th}-order Hankel function of the first kind

$$A_m = -(2 - \delta_{mo}) P_0 i^{m+1} e^{-i\gamma_m} \sin\gamma_m$$

$$\tan\gamma_o = [-J_1(\omega_p a/c_o)]/[N_1(\omega_p a/c_o)]$$

$$\tan\gamma_m = [J_{m-1}(\omega_p a/c_o) - J_{m+1}(\omega_1 a/c_o)]$$
$$[N_{m+1}(\omega_p q/c_o) - N_{m-1}(\omega_p a/c_o)]$$

N_m = m^{th}-order Neumann function

a = cylinder radius

c_o = linear sound speed.

The boundary condition appropriate for obtaining the linear rigid-body scattered solution is that the fluid particle velocity vanish at the surface of the cylinder.

Once again, in order to solve Eq. (48), we resort to the representations of $P_{(2)}$ and $\rho_o(\partial q/\partial t)$ provided by Eqs. (79) and (80). Also, as before, the surface integral of Eq. (83) does not contribute to the solution for the same reason given following that equation. Hence, the solution may still be represented by Eq. (84). Since the geometry of the current problem is cylindrical, Eq. (85) still provides the appropriate Green's function [contributions to the sum- and difference-frequency acoustic pressures from regions beyond the point of interest are again neglected, for the same reasons given following Eq. (85)].

As before, in order to have a representation of the solution, a representation of $B_n(r')$ must now be obtained. This is done by substituting the assumed forms [Eqs. (79) and (80)] into the second-order wave Eq. (48). Once again, we must carefully handle the complex quantities involved. We again use the theorem that $Re(z) = (z+z^*)/2$ to help obtain a representation for the first-order solution $P_{(1)}(r)$. This provides

$$P_1(\vec{r}) = AH_o^{(2)}\left(\frac{\omega_c r}{c_o}\right)e^{i\omega_c t} + \frac{1}{2}\left[P_o J_o\left(\frac{\omega_p r}{c_o}\right)\right.$$

$$+ \sum_{m=0}^{\infty} A_m^* \cos(m\theta) H_m^{(2)}\left(\frac{\omega_p r}{c_o}\right)$$

$$\left. + 2\sum_{m=1}^{\infty} P_o i^{-m}\cos(m\theta) J_m\left(\frac{\omega_p r}{c_o}\right)e^{i\omega_p t} + c.c.\right] \qquad (110)$$

We note that $P_{(1)}(r)$ is of the form

$$P_{(1)}(\vec{r}) = Z_1 e^{-i\omega_c t} + Z_1^* e^{i\omega_c t} + Z_2 e^{-i\omega_p t} + Z_2^* e^{i\omega_p t}, \tag{111}$$

where $Z_1 = \frac{A}{2} H_o^{(1)}(\frac{\omega_c r}{c_o})$ and

$$Z_2 = \frac{1}{2} P_o [J_o(\frac{\omega_p r}{c_o}) + \sum_{m=0}^{\infty} A_m \cos m\theta H_m^{(1)}(\frac{\omega_p r}{c_o})$$

$$+ \sum_{m=1}^{\infty} i^m \cos m\theta J_m(\frac{\omega_p r}{c_o})].$$

We must now determine which terms in $[P_{(1)}(r)]^2$ contribute to the sum- and difference-frequency pressures in the inhomogeneous simple source term $\partial q/\partial t$ of Eq. (48). These terms are [using Eq. (111)]:

$$P_{(1)+}^2 = 2Z_1 Z_2 e^{-i(\omega_p+\omega_c)t} + 2Z_1^* Z_2^* e^{i(\omega_p+\omega_c)t} \tag{112}$$

and

$$P_{(1)-}^2 = 2Z_1 Z_2^* e^{-i(\omega_p-\omega_c)t} + 2Z_1^* Z_2 e^{i(\omega_p-\omega_c)t}, \tag{113}$$

where $P_{(1)+}^2$ and $P_{(1)-}^2$ refer to contributions to the sum and difference frequencies, respectively. These expressions yield for the simple source term

$$(\rho_o \frac{\partial q}{\partial t})_+ = -\frac{(\omega_p+\omega_c)^2 A\Gamma}{2\rho_o c_o^4} [P_o H_o^{(1)}(\frac{\omega_c r}{c_o}) J_o(\frac{\omega_p r}{c_o})$$

$$+ \sum_{m=0}^{\infty} A_m \cos(m\theta) H_o^{(1)}(\frac{\omega_c r}{c_o}) H_m^{(1)}(\frac{\omega_p r}{c_o})$$

$$+ 2 \sum_{m=1}^{\infty} P_o i^m \cos m\theta H_o^{(1)}(\frac{\omega_c r}{c_o}) J_m(\frac{\omega_p r}{c_o}) e^{-i(\omega_p+\omega_c)t}] + \text{c.c.}$$

and

$$(\rho_o \frac{\partial q}{\partial t})_- = -\frac{(\omega_p-\omega_c)^2 A\Gamma}{2\rho_o c_o^4}\left[P_o H_o^{(1)}(\frac{\omega_c r}{c_o})J_o(\frac{\omega_p r}{c_o})\right.$$

$$+ \sum_{m=0}^{\infty} A_m^* \cos(m\Theta) H_o^{(1)}(\frac{\omega_c r}{c_o}) H_m^{(2)}(\frac{\omega_p r}{c_o})$$

$$\left. + 2\sum_{m=1}^{\infty} P_o i^{-m}\cos(m\theta) H_o^{(1)}(\frac{\omega_c r}{c_o}) J_m(\frac{\omega_p r}{c_o}) e^{-i(\omega_p-\omega_c)t}\right] + c.c. \qquad (114)$$

By the same argument as given for the case of cylindrical waves incident on a vibrating cylinder, the $B_n(r')$ are simply minus the coefficient of the negative time exponential in Eqs. (112) and (113). Two different solutions are obtained for the difference-frequency depending on whether $\omega_p > \omega_c$ or $\omega_c > \omega_p$, since each of these cases will give a different coefficient from the second of Eqs. (112) and (113). Since the procedures are similar in each of the three possible cases, we choose a particular one to represent the solution, namely the difference-frequency pressure when $\omega_p > \omega_c$ (this is chosen since it represents the case for which experiments were performed).

We may proceed to obtain the difference-frequency pressure $P_-(r)$ by substituting the expression obtained for $B_n(r')$ by the above-described method and the Green's function $g_n(r,r')$ of Eq. (85) into Eq. (84). The integrals on Θ' may again be performed using the theorem preceding Eq. (103).

This results in the following expression for the difference-frequency pressure:

$$P_{-}(\vec{r}) = \frac{-\pi i P_0(\omega_p-\omega_c)^2 A\Gamma}{2\rho_o c_o^4}\{H_o^{(1)}(k_d r)[\int_a^r dr' r' H_o^{(2)}(\frac{\omega_c r'}{c_o})J_o(\frac{\omega_p r'}{c_o})J_o(k_d r')$$

$$- \frac{J_o'(k_d a)}{H_o^{(1)\prime}(k_d a)} \int_a^r dr' r' H_o^{(2)}(\frac{\omega_c r'}{c_o})J_o(\frac{\omega_p r'}{c_o})H_o^{(1)}(k_d r')]$$

$$+ \sum_{\ell=0}^{\infty}(\frac{A_\ell}{P_0})\cos\ell\Theta H_\ell^{(1)}(k_d r)[\int_a^r dr' r' H_o^{(2)}(\frac{\omega_c r'}{c_o})H_\ell^{(1)}(\frac{\omega_p r'}{c_o})J_\ell(k_d r')$$

$$- \frac{J_\ell'(k_d a)}{H_\ell^{(1)\prime}(k_d a)} \int_a^r dr' r' H_o^{(2)}(\frac{\omega_c r'}{c_o})H_\ell^{(1)}(\frac{\omega_p r'}{c_o})H_\ell^{(1)}(k_d r')]$$

$$+ 2\sum_{\ell=1}^{\infty} i^\ell \cos(\ell\Theta)H_\ell^{(1)}(k_d r)[\int_a^r dr' r' H_o^{(2)}(\frac{\omega_c r'}{c_o})J_\ell(\frac{\omega_p r'}{c_o})J_\ell(k_d r')$$

$$- \frac{J_\ell'(k_d a)}{H_\ell^{(1)\prime}(k_d a)} \int_a^r dr' r' H_o^{(2)}(\frac{\omega_c r'}{c_o})J_\ell(\frac{\omega_p r'}{c_o})H_\ell^{(1)}(k_d r')]\}. \qquad (115)$$

Once again, the sum- and difference-frequency pressures can be stated in nondimensional terms. In this case the relevant parameters are $\tau = \omega_{\pm} t$, $\zeta = \omega_{\pm} r/c_o$, Θ, $\omega_{\pm} a/c_o$, and the frequency ratio.

At this point we undertake a calculation of the region of validity of Eq. (115). First we consider the smallest value of r for which Eq. (115) may reasonably be expected to be valid. There are several sources of error at radii close to the cylindrical surface. These are: 1) contributions due to the neglected D'Alembertian terms of Eq. (47), 2) contributions from the neglected Green's function integral between r and ∞, and 3) contributions due to the neglected Green's function surface integral. All of these are estimated in Section IV. B. From the computations in that section, it is

clear that an upper bound on this error is 10% at r = 3 cm (these errors decrease approximately as 1/r at distances beyond this radius). Hence r = 3 cm can be taken as a reasonable lower limit of validity.

Next we consider the largest value of r for which Eq. (115) is valid. As was done in the case of plane-wave scattering from a vibrating plane, we effect this estimate by comparing the energy densities of the secondary waves to that of the primary waves. A conservative estimate can be made by including only the cylindrically radiated wave and the rigid-body scattered waves in the estimate of the primary field's energy density. We choose to represent each of these waves respectively by the simple formulas $P_r = A_r/\sqrt{r}$ and $P_s = A_s/\sqrt{r}$. For the experiment described in Chapter III, the empirical coefficients have the approximate values $A_s = 5\times10^3$ Pa and $A_r = 1.36\times10^4$ Pa. Again, a conservative estimate of the primary energy density can be computed by using the plane-wave formula and adding the results. This results in an approximate primary energy density of $(4.66\times10^{-2}$J m)/r.

There are two distinct angular regions for the secondary waves: angles near 0° and angles far from 0°. At angles near 0°, the difference-frequency pressure grows approximately linearly. From the results of Chapter III, the formula $P_- = 300$ Pa/m r is seen to be approximately followed. Scaling for the sum-frequency case gives: $P_+ = 1300$ Pa/m r. Once again, we use the very conservative estimate that the pressures associated with the second harmonics follow the plane-wave Fubini-Ghiron formula (of course, the waves will actually grow much more slowly in this case). Using as a typical value the second-harmonic pressure formula obtained in the section on plane wave and scattering from a vibrating plane, we have $P_{2w} = 372$ Pa r (we will use this for the harmonics of each of the primaries). At a distance of 1 m from the cylindrical surface, the energy densities of the secondaries are less than 1% of the primaries. Hence, a reasonable region of validity of Eq. (115) may be taken to be r = 15 cm to r = 100 cm. (The discontinuity distance calculated in the section on plane-wave scattering from a vibrating plane can still be taken as a reasonable estimate. Since it was approximately 10 m, viscous terms may reasonably be said to play no significant role in the above estimate.)

In Eq. (115) the linear rigid-body scattering coefficients appear explicitly. In the Censor solution, given by Eq. (104), these do not appear because Censor chose to incorporate the expressions for the coefficients into

his solution. It is desirable to re-express his solution in a form in which these coefficients appear explicitly as they do in Eq. (115). This facilitates the calculation of the difference-frequency pressure in the case in which the surface is not rigid and the scattering coefficients A_m must be empirically determined. In terms of A_m, Censor's solution becomes:

$$P_-(\vec{r}) = \frac{-(\omega_-)}{2i} \frac{k_c P_c}{\rho_o \Omega^2 a} \left|H_1^{(1)}(k_c a)\right| \sum_{m=0}^{\infty} \cos m\theta$$

$$\times \left[\frac{P_0(a/c)J_m(k_p a)[i^m(2-\delta_{mo}) + A_m H_m^{(1)}(k_p a)}{H_m^{(1)\prime}(k_d a)}\right] H_m^{(1)}(k_d r). \qquad (116)$$

Three methods were developed to analyze the integrals in Eq. (115): 1) Numerical integration by the use of Gauss quadrature. 2) A new integration technique that enables the calculation of the integrals in terms of sums. 3) Expression of the integrals in closed form in terms of known, although rarely encountered associated Bessel functions for the case $k_c a \gg 1$.

Method 1 proved to be the most direct and efficient. Numerical results will be given in Section III. Methods 2 and 3 are discussed in the Appendix.

3. Connection with Previous Research

In 1962, Dean [20] solved the problem of two concentric cylindrical waves interacting nonlinearly. He obtained the following solution for the sum-frequency pressure in the farfield (for the case where $a \to 0$):

$$P_+ = \pi P_a P_b (2\rho_o c_o^2)^{-1} (\Gamma)(k_a k_b)^{1/2} k_+ a^2 e^{ik_+ r}, \qquad (117)$$

where k_a, k_b = wavenumbers of primaries, k_+ = sum-frequency wavenumber, P_a, P_b = constants that measure the acoustic pressure amplitudes of the cylindrical primaries, and Dean's $1-\Gamma$ has been replaced by Γ to be consistent with the notation used in this work. The constants P_a and P_b are related to the primary pressures through the relations

$$P_a(r) = P_a[H_0^{(1)}(k_a r)/H_1^{(1)}(k_a a)]$$

$$P_b(r) = P_b[H_0^{(1)}(k_b r)/H_1^{(1)}(k_b a).$$

The solution to the above problem can also be obtained using Eq. (115). In order to do so, the terms corresponding to the incident plane wave must be suppressed [these are all terms in Eq. (115) that are not multiplied by the scattering coefficients A_ℓ]. Furthermore, the scattering coefficients A_ℓ must be replaced with $\delta_{\ell o}$, the Kronecker delta. Lastly, the following identifications must be made between constants used in Dean's work and constants used in the present work:

$$P_0 = P_a/H_1^{(1)}(k_a a)$$

$$A = P_b/H_1^{(1)}(k_b a).$$

If the Hankel functions in Eq. (115) are all replaced by the first term of their asymptotic expansions, an elementary integral is obtained and Eq. (117) follows apart from an unimportant phase factor of $e^{i\pi/2}$.

III. NUMERICAL RESULTS

This chapter presents in graphical form the results of numerical calculations based on the analytical solutions of the nonlinear wave equation obtained in Chapter II. Censor gave only analytical expressions for his theory. In order to compare Censor's results with those of the nonlinear theory, his analytical expressions were evaluated numerically. The results of these evaluations are also presented graphically in this chapter.

The configuration selected for experimental investigation was the one in which a plane wave is normally incident on a vibrating cylindrical surface. Censor's solution [23] to this problem is given by Eqs. (5), (10), and (27) in his paper and by Eq. (104) of this report.

In order to illustrate Censor's solution (as well as the solution to the nonlinear theory), numerical values that were experimentally realizable were used to make example calculations. In these calculations, the plane-wave frequency was chosen to be 162 kHz, and the cylindrical-wave frequency was chosen to be 102 kHz (giving a difference-frequency of 60 kHz). The amplitude of the incident pressure wave was selected to be 1.0×10^5 Pa, and the cylindrical-wave amplitude coefficient (A) was selected to be 3.5×10^5 Pa.

The angular distribution of difference-frequency pressure at 15 cm from the symmetry axis of the cylinder obtained by numerically analyzing Censor's expressions is shown in Fig. 5. (The reasons for studying the difference-frequency case, as well as the reasons for selecting the particular experimental parameters indicated in Fig. 5 will be discussed in Chapter IV.) The maximum pressure at this radius occurs at 0° and is 0.9 Pa for the parameters given. (In Fig. 5, as well as all other polar plots, the dB scale is measured relative to the maximum pressure level at the radius of interest. The maximum pressure represented in a particular polar diagram is given in the information box associated with it and is referred to as "P_{MAX}".) As discussed in Chapter II, this pressure value is of the same order of magnitude as pseudosound.

In the figure captions for the difference-frequency pressure, the value of the quantity $\Delta_1 = (P_o P_c \Gamma)/(\rho_o c_o^2)$ is listed, since this factor may be used to obtain a nondimensional pressure. Here, P_c (the actual maximum cylindrical pressure amplitude) is used instead of the quantity A of Eq. (115), since the pressure represented by A is present at no point in the fluid. Similarly, the quantity $\Delta_2 = \omega_- a/c_o$ is also listed in the caption.

Also of interest in this problem is the variation of difference-frequency pressure with respect to distance from the cylinder symmetry axis at fixed angles. Figures 6, 7, and 8 present the results of Censor's theory at 0, 90, and 180°, respectively. These graphs can be interpreted in the following way: Censor's theory predicts the generation of difference-frequency waves (as well as sum-frequency waves) due to the presence of boundary conditions associated with the time-varying nature of the cylindrical surface. Hence, both the sum- and difference-frequency waves predicted by his theory are created solely at the surface of the scatterer. As the observation point is moved to increasingly greater distances from the boundary, these sum- and difference-frequency pressure waves must spread cylindrically (in a manner similar to the

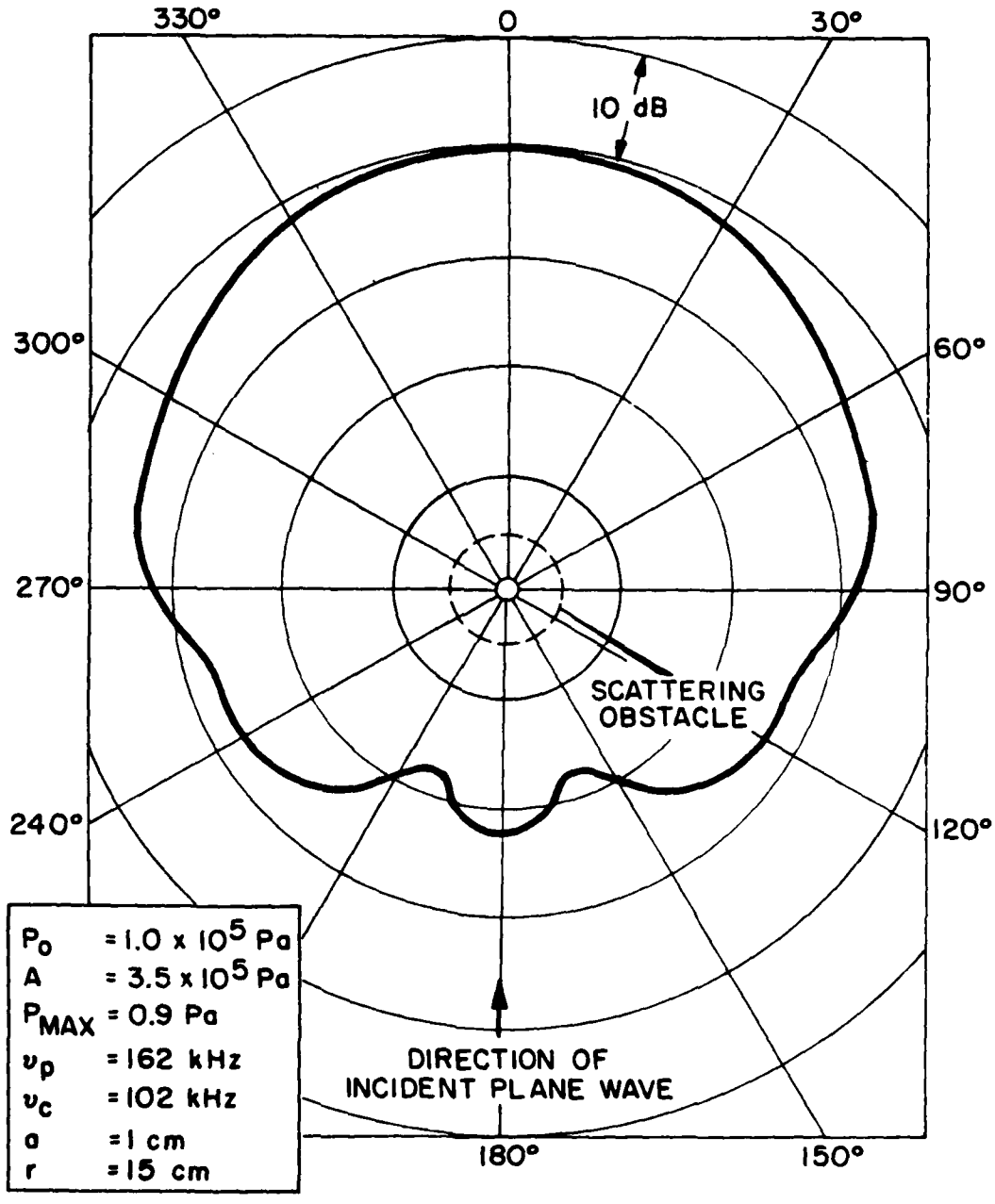

Fig. 5 - Typical angular distribution of Censor theory difference-frequency pressure

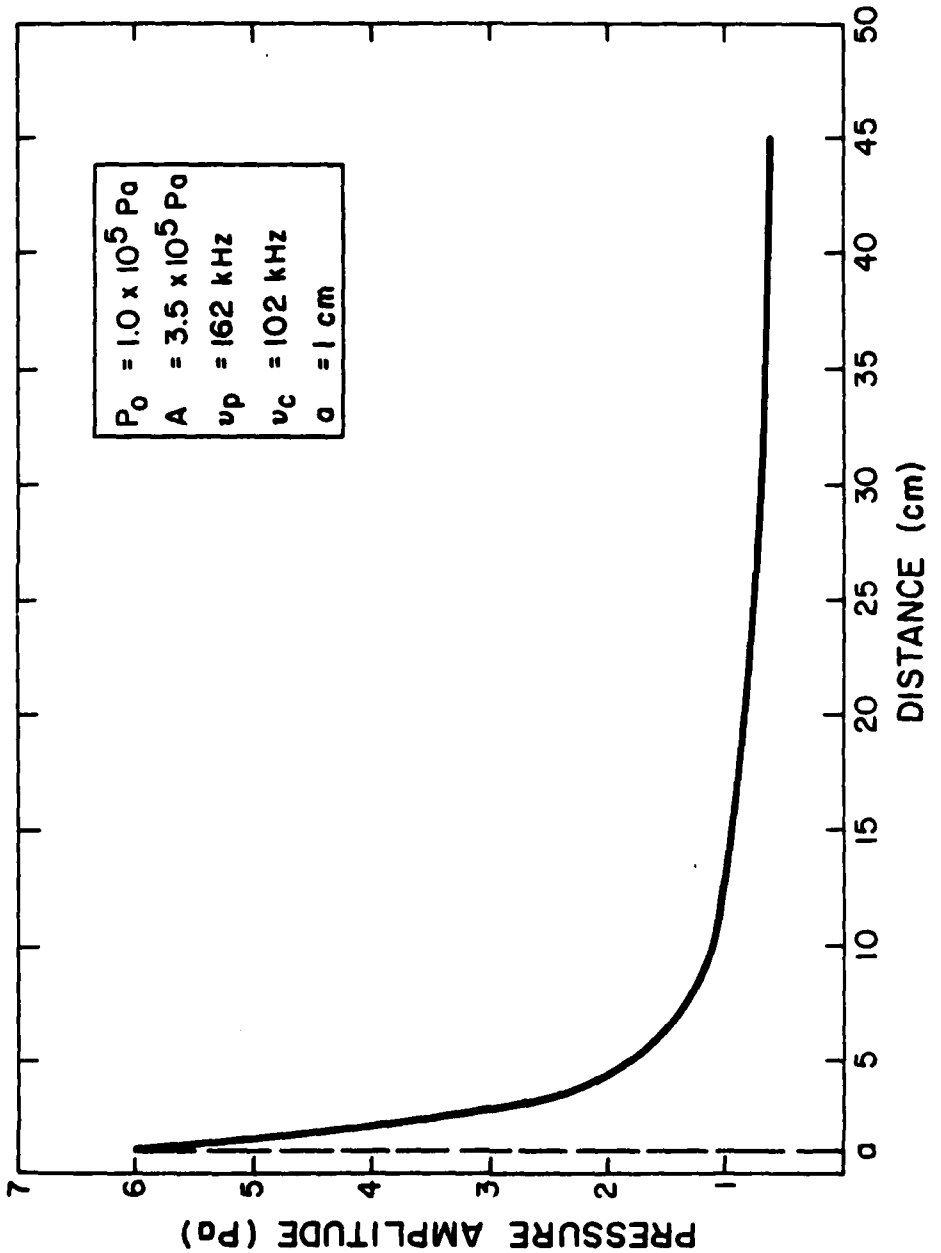

Fig. 6 - Censor theory difference-frequency pressure at 0 degrees

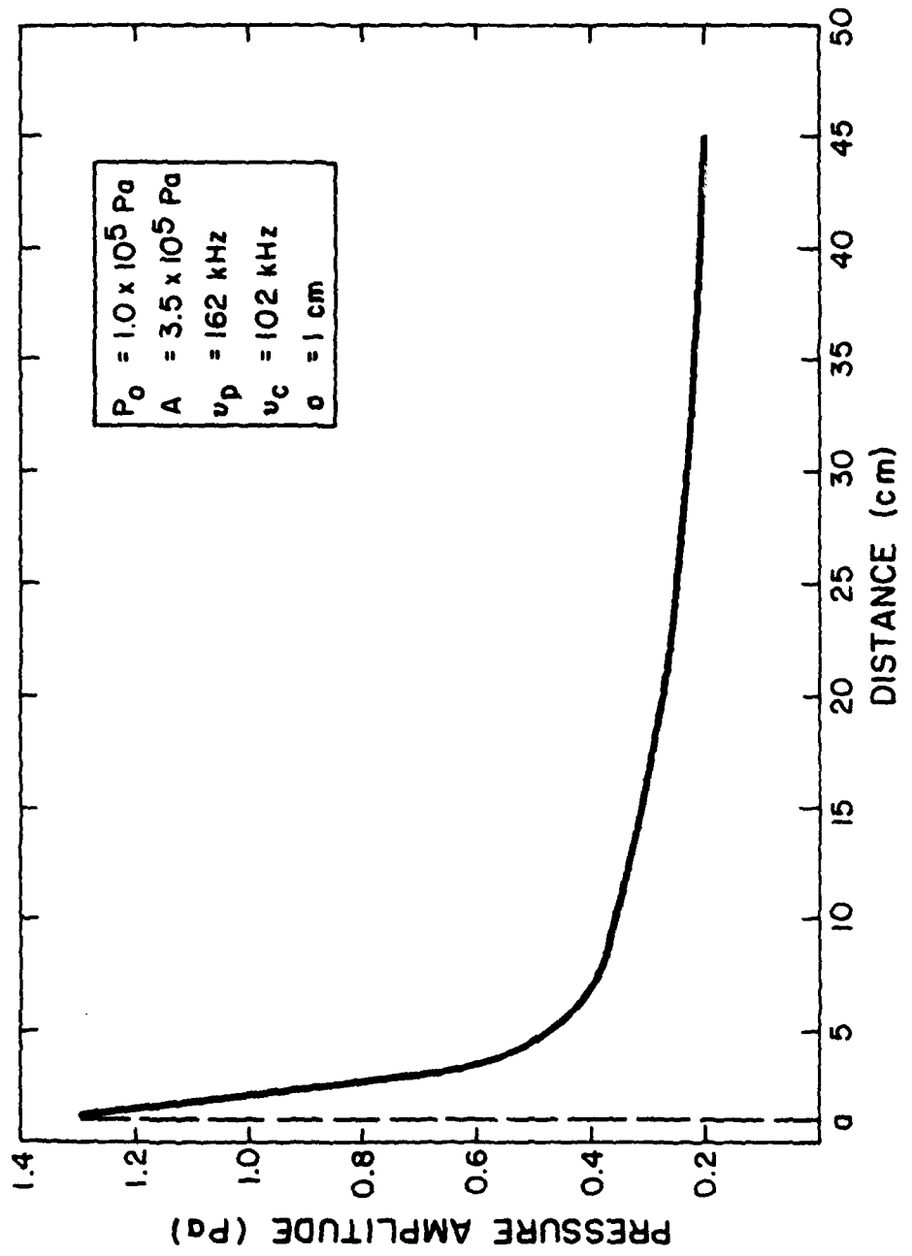

Fig. 7 - Censor theory difference-frequency pressure at 90 degrees

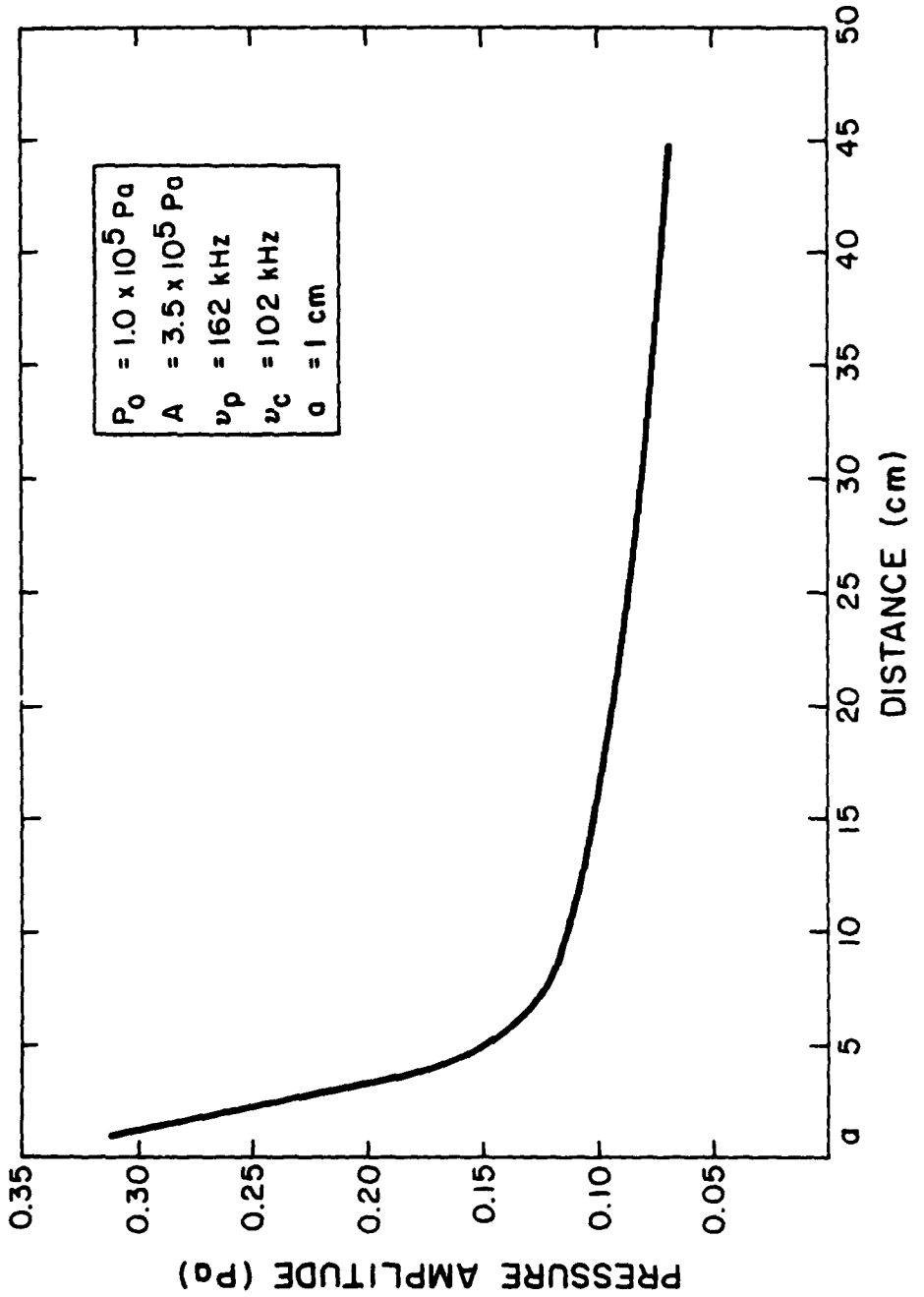

Fig. 8 - Censor theory difference-frequency pressure at 180 degrees

spreading of the first-order cylindrical field). Hence, it is expected that pressures associated with Censor's theory will (in the asymptotic limit) decrease in-versely as the square root of the radial distance from the symmetry axis. This does indeed prove to be the case for the pressures represented in Figs. 6 through 8.

The solution to the nonlinear wave equation for this problem is given by Eq. (115). Unlike Censor's theory, this equation involves complicated integrals over triple products of Bessel functions. A new technique of integration is presented in the Appendix for treating these integrals for the case in which the arguments of the Bessel functions corresponding to the radiated cylindrical wave as well as the arguments of the Bessel functions corresponding to either the incident plane wave or the difference-frequency wave are sufficiently large to be replaced by their asymptotic forms. Unfortunately, these conditions were not met for the case that was modeled experimentally; hence, these integrals had to be evaluated numerically. The numerical procedure chosen to analyze the integrals was the method of Gaussian Quadrature [32]. A 32-point quadrature was used. (Suitable abscissas and weighting factors are given in Ref. 45). To obtain good accuracy using the 32-point Gaussian Quadrature, the radial interval to be integrated (1 to 46 cm) had to be subdivided into ten equal sub-intervals. The full 32-point Gaussian Quadrature sum was used to obtain the integrals over each of these partial intervals. The integrals up to the final observation point were obtained by adding together the integrals over all subintervals below the observation point.

It is necessary at this point to justify that the subdivision scheme described above will indeed suffice to calculate the integrals of interest. First, it is essential to state the precision of the Gaussian Quadrature procedure. If m quadrature points are used, the integral of a polynomial of

degree 2m - 1 is represented exactly by this method [46]. Hence, it is reasonable to expect that if the integrand of interest contains not more than 2m-1 zeroes over the interval of integration, Gaussian Quadrature will provide a reliable numerical result.

In order to obtain a reasonable estimate of the number of zeroes occurring in the integrands of interest (over the partial intervals described above), it should be noted that the general behavior of the zeroes of the Bessel functions of the first two kinds can be surmised by a careful examination of tables listing their values [47]. It is clear from these tables that the spacing between these zeroes decreases for increasing arguments. Hence, since the greatest density of zeroes occurs for the greatest arguments, use of the asymptotic expansions of the functions will result in an upper bound on the number of zeroes that occur in any of the subintervals of interest. In the case of $J_\ell(kr)$, the location of the zeroes may be approximated by calculating the zeroes of the cosine term that occurs in the lowest order of this asymptotic expansion. These zeroes will occur at values of r that satisfy the relationship

$$kr - \frac{\pi}{2}\,\ell - \frac{\pi}{4} = (2n+1)\,\frac{\pi}{2},$$

where n,ℓ = integers.

Conversely, the above relationship may be used to obtain an upper bound on the number of zeroes occurring in a given r interval (for a given wavenumber k) by determining the greatest integer n that satisfies this relationship. The number of zeroes is then approximately equal to n+1 (since the first zero occurs at n = 0). It can also easily be seen from the expression above that the greatest number of zeroes occurs for $\ell = 0$.

Since the range of integration is taken from r = 1 cm to r = 46 cm, the total range of integration is 45 cm in length. Since the total interval is subdivided into 10 subintervals, the limits of integration over which the greatest values of the arguments of $J_0(kr)$ occur (and hence interval over which the greatest density of zeroes occurs) is from r = 41.5 cm to r = 46 cm. The above approximate expression may now be used to determine the number of zeroes of $J_0(kr)$ corresponding to each of the wavenumbers of interest (associated with the frequencies 162, 102, and 60 kHz) over this interval. Rounding all fractional values obtained in this way to the next greatest integer (to consider the worst case), the results of Table I are obtained.

Table I. Maximum Number of Zeroes of $J_0(kr)$ on the Interval r = 41.5 cm to r = 46 cm

Frequency	Maximum No. of Zeroes
162 kHz	11
102 kHz	8
60 kHz	7

The maximum number of zeroes of the integrand involving the product of the three $J_0(kr)$ functions herein considered is given by the sum of the number of zeroes for each of the individual functions. This gives 26 zeroes in the current example.

Since m = 32 Gaussian Quadrature points are used, 2m-1 = 63 zeroes would still result in an accurate value for this integral via this numerical method. Since the current example represents the worst case (in the sense that no other integrand of interest will have more than 26 zeroes over any of

the subintervals being considered), it may reasonably be expected that the Gaussian Quadrate numerical integration scheme chosen is adequate to perform all the required integrals.

The results of this numerical computation were checked in the high-frequency limit where the new technique of integration was appropriate. Excellent agreement was obtained between the Gaussian quadrature results and corresponding results using the series given for these integrals by Eq. (A21).

In addition to verifying the results of the numerical integration by comparison with numerical results obtained using Eq. (A21), another verification method was also available. A few of the ten subintervals were further subdivided and then evaluated using the 32-point quadrature over each of the smaller subintervals. The numerical results obtained by this further subdivision were always in good agreement with the results obtained with the original subdivision scheme, thus showing that the original subdivision was sufficient for evaluating the integrals. [It should be noted that this last method is applicable even for frequencies that are not large enough to allow the application of Eq. (A21) to the integrals of interest. This at least provides a check of consistency.]

The angular distribution of difference-frequency pressure obtained by analyzing Eq. (115) numerically (at 5, 10, and 15 cm from the scatterer's center) is presented in Figs. 9 through 11, respectively. (Figures 12 through 14 present radial plots of difference-frequency pressure at 0, 90, and 180°. These will be discussed shortly.) These graphs may be interpreted qualitatively in the following way: For angles near 0°, strong contributions to the difference-frequency pressure are obtained both from the "mixing' of the incident plane wave with the cylindrically radiated wave and from the "mixing" of the rigid-body scattered wave with the cylindrically radiated wave. Since the cylindrically radiated wave does not vary with angle, the variation of difference-frequency pressure with angle should be related primarily to the angular dependence of the sum of the incident plane-wave pressure and the rigid-body scattered pressure. Of course, since the nonlinearly generated field is expressed in terms of an integral from the cylindrical surface to the observation point, this field is not understandable simply in terms of the primary fields that happen to be located at the observation point. More illuminating in this respect is the evolution of the primary field as one

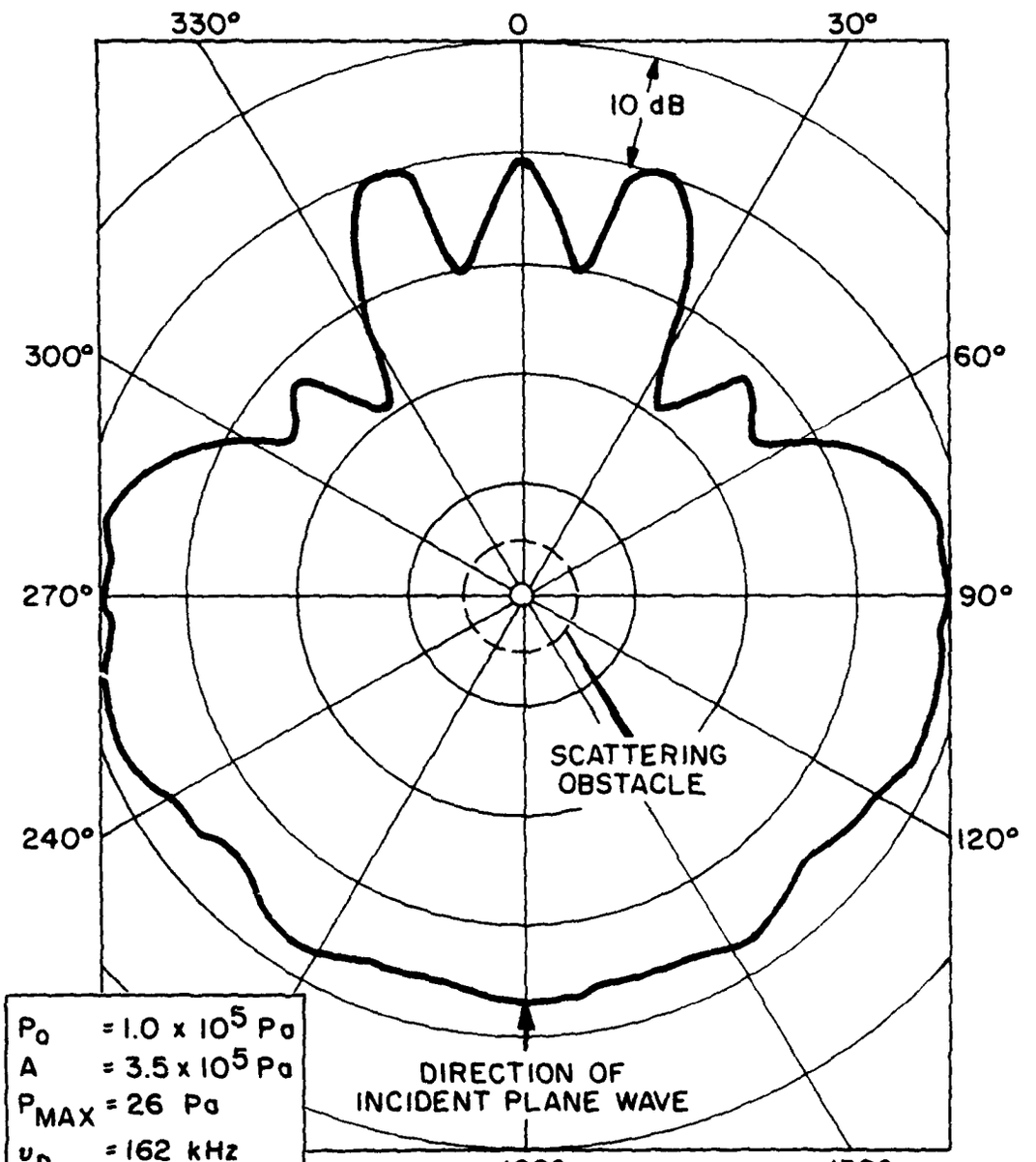

Fig. 9 - Angular distribution of nonlinear scattered field

Δ_1 = 1.56 Pa, Δ_2 = 2.51

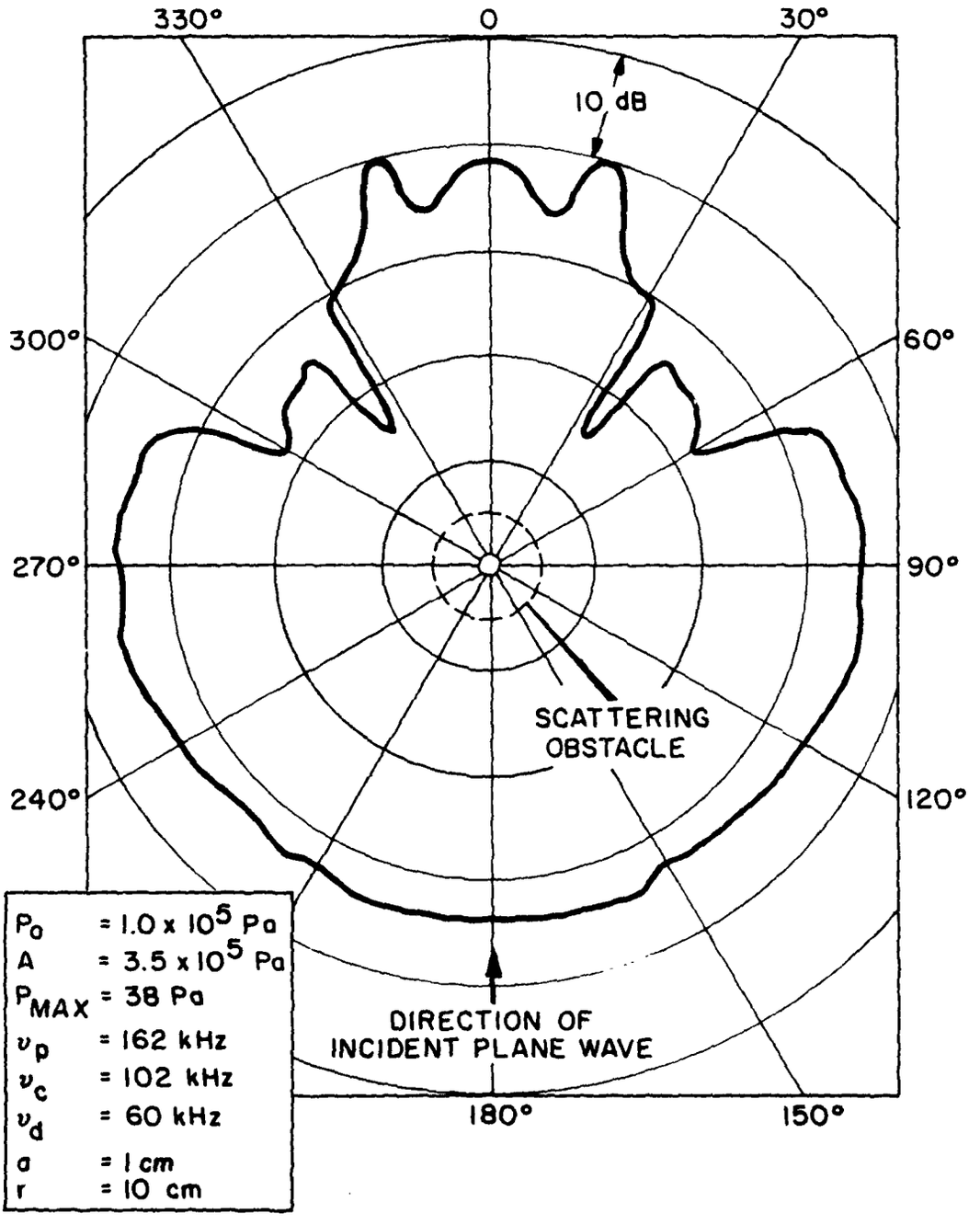

Fig. 10 - Angular distribution of nonlinear scattered field

$\Delta_1 = 1.56$ Pa, $\Delta_2 = 2.51$

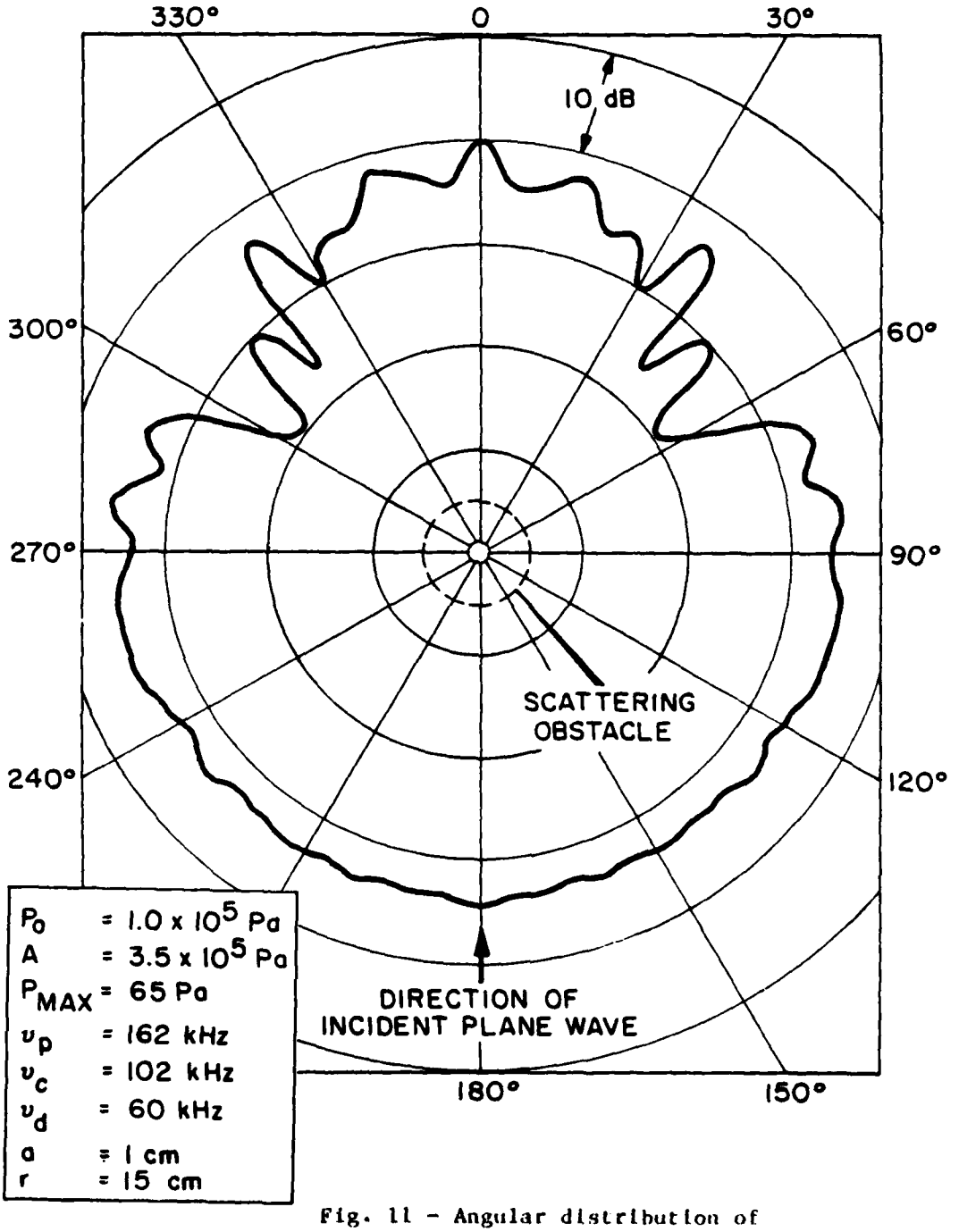

Fig. 11 – Angular distribution of nonlinear scattered field

Δ_1 = 1.56 Pa, Δ_2 = 2.51

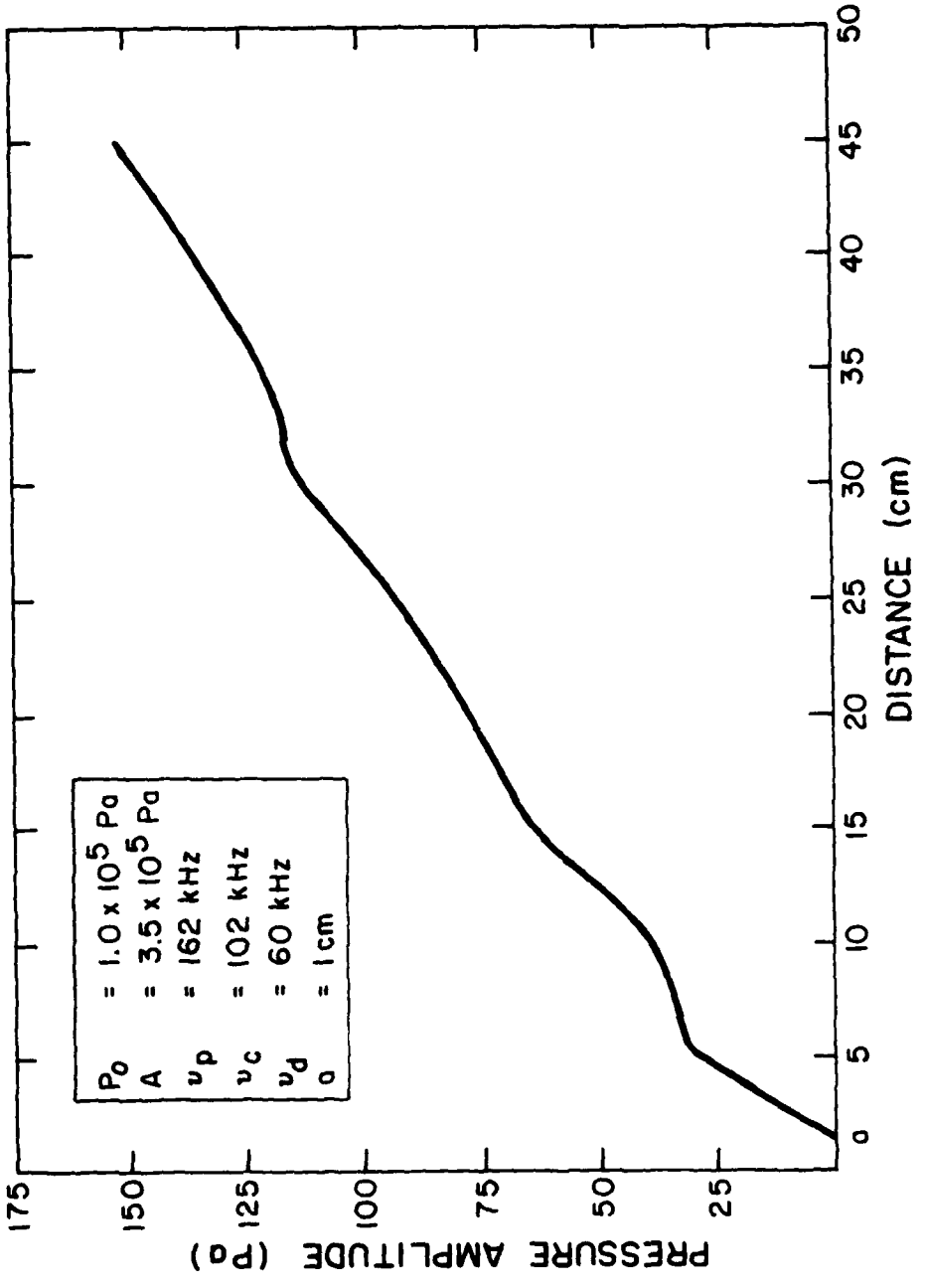

Fig. 12 - Difference-frequency pressure at 0 degrees

Δ_1 = 1.56 Pa, Δ_2 = 2.51

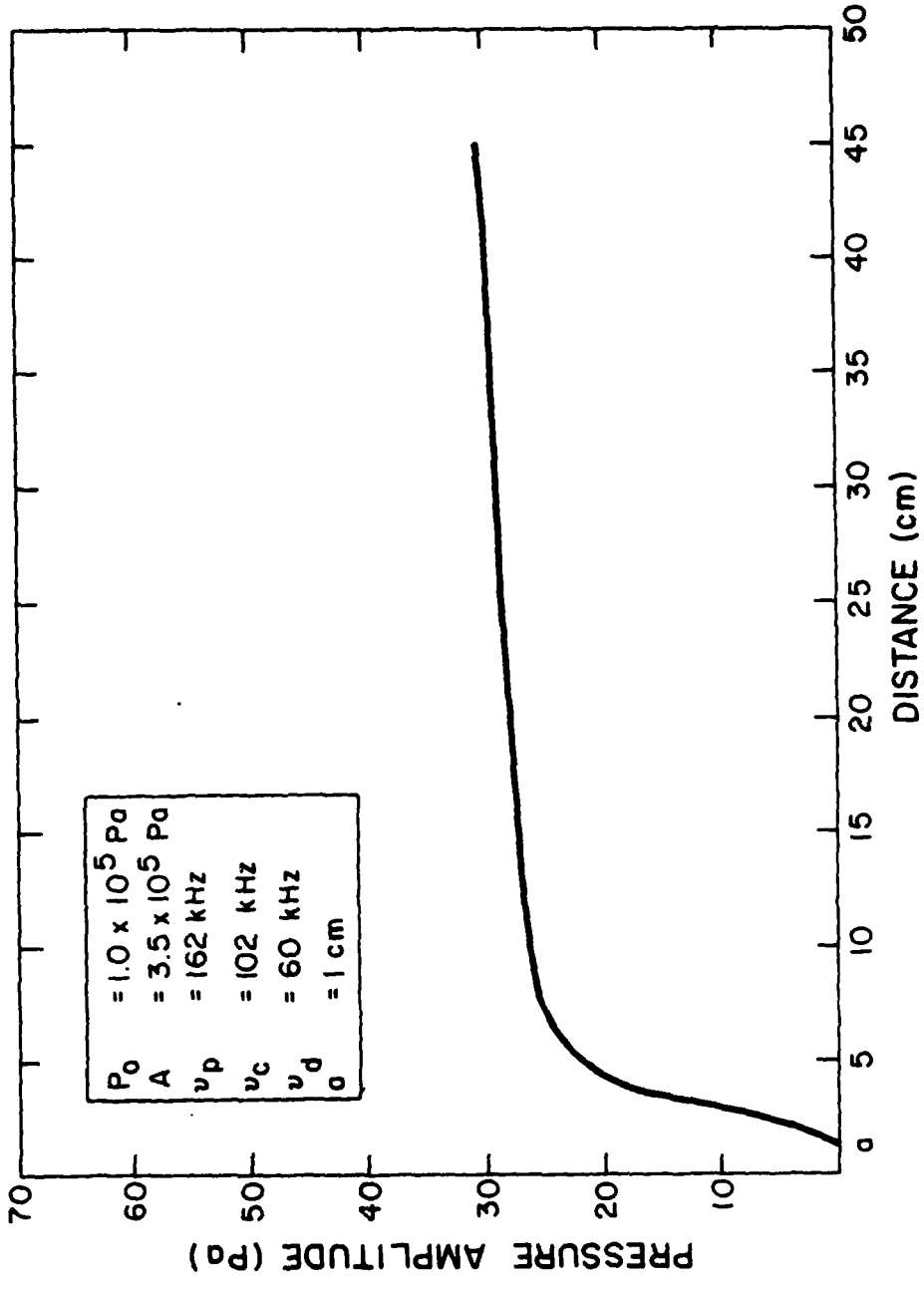

Fig. 13 - Difference-frequency pressure at 90 degrees

Δ_1 = 1.56 Pa, Δ_2 = 2.51

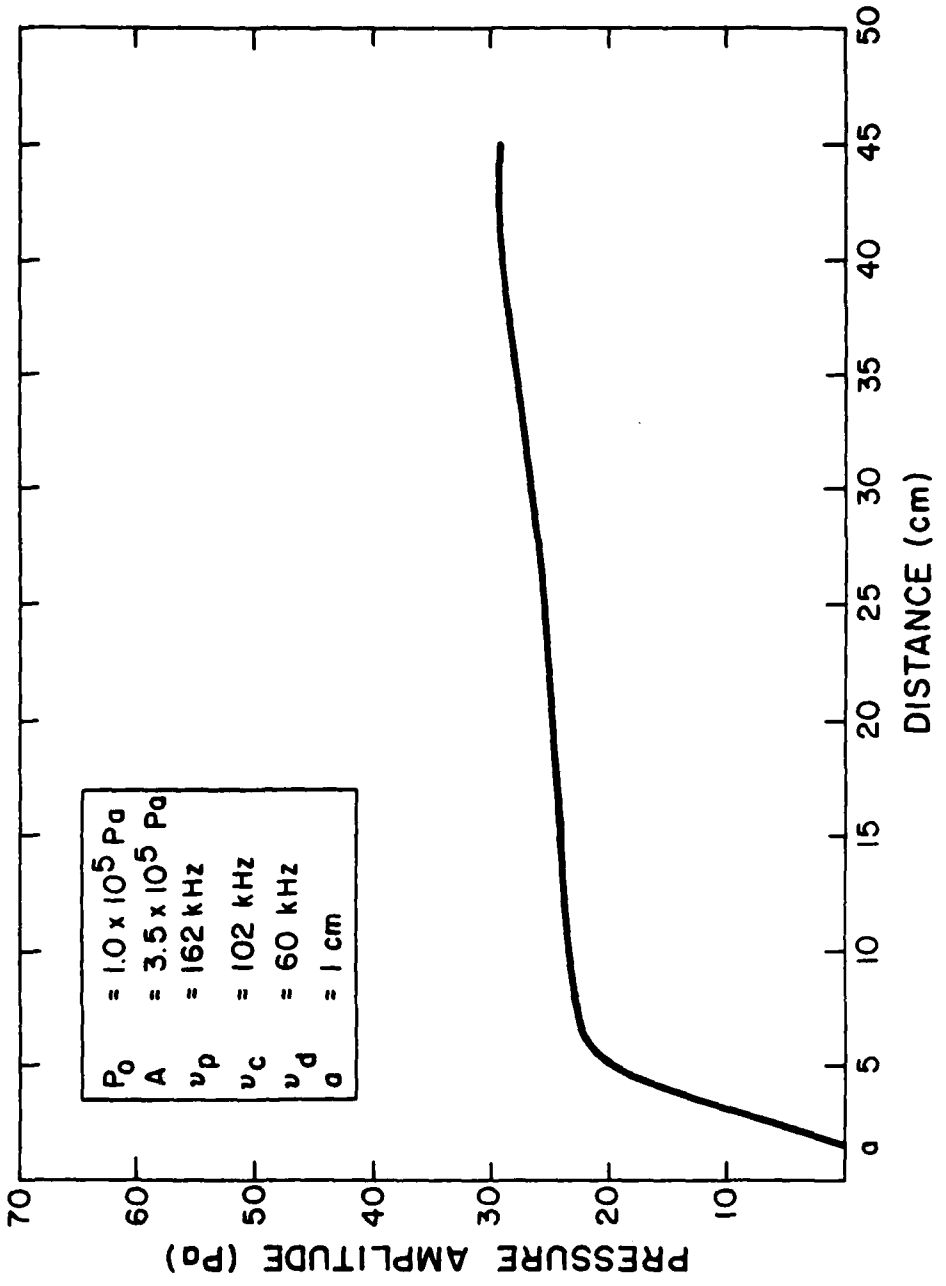

Fig. 14 - Difference-frequency pressure at 180 degrees

Δ_1 = 1.56 Pa, Δ_2 = 2.51

moves from the cylinder surface to the observation point. Figures 15 through 21 present the total pressure field of the linear rigid-body scattering problem (incident plane wave plus rigid-body scattered field) at 2-cm intervals. It is interesting to note that peaks evolve in this field at 0 and 15° that correspond closely to peaks in the nonlinear scattered field. At angles not equal (or close) to 0°, the incident plane-wave no longer contributes strongly to the nonlinear field (due to its unfavorable geometric relationship to the cylindrically radiated field).

Hence, for these angles, the angular dependence of the rigid-body scattered field alone is more appropriate in interpreting the angular dependence of the nonlinear field. The evolution of the rigid-body linearly scattered field at 2-cm increments is presented in Figs. 22 through 28. The most evident aspect of the nonlinear scattered field (between approximately 60 and 300°) is a pressure level nearly constant with angle. This corresponds well with the linear rigid-body scattering patterns with the exception of minima located at approximately 75, 135, 225, and 285° in these patterns. That these minima in the linear rigid-body scattered field do not contribute significantly to the nonlinear field may be qualitatively understood from the fact that these minima are not very wide in terms of angle. (The minima at 75 and 285° start with ~20 degrees of width and decrease to ~10 degrees of width. The minima at 135 and 225° remain at ~5 degrees of width up to the last radius of interest.) Also, in the case of the minima at 75 and 285°, the incident plane wave will still contribute something to the nonlinear field.

Even though correspondence between the primary fields and the nonlinear field is not exact, this is not a serious matter since the primary fields can be used only as a very rough guide to the behavior of the nonlinear fields. It must be remembered that the nonlinear field is calculated via volume

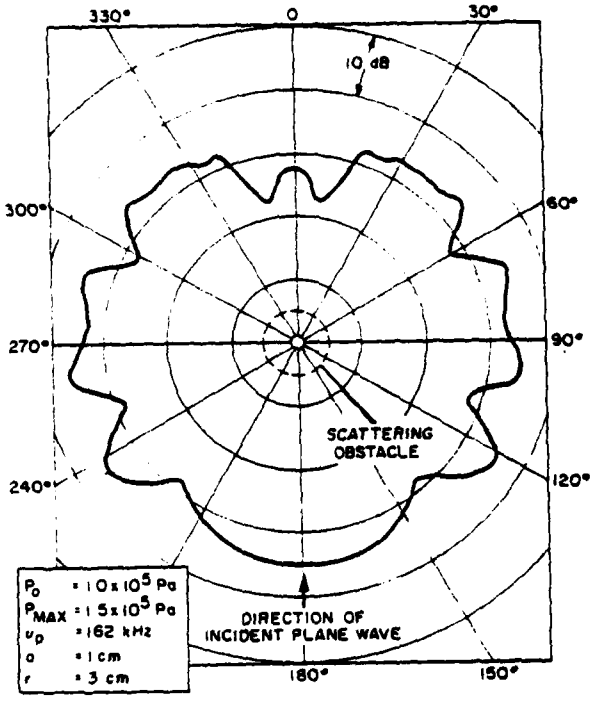

Fig. 15 - Total pressure of linear rigid-body scattering problem at 3 cm

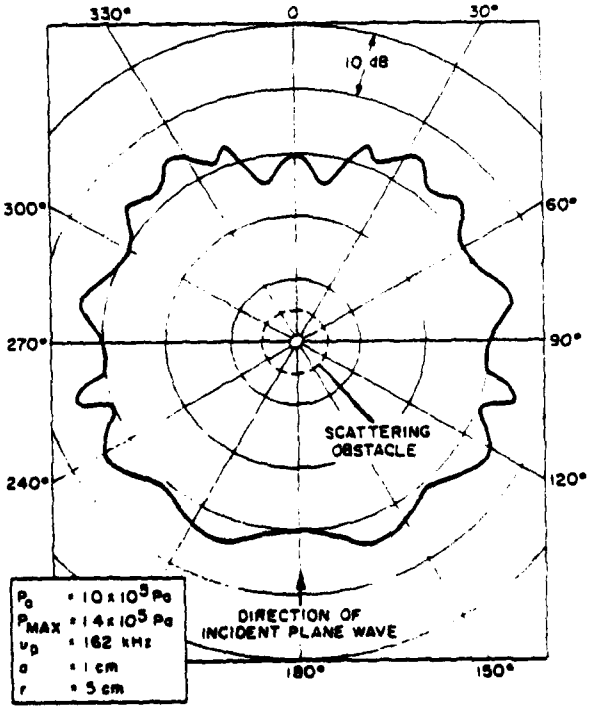

Fig. 16 - Total pressure of linear rigid-body scattering problem at 5 cm

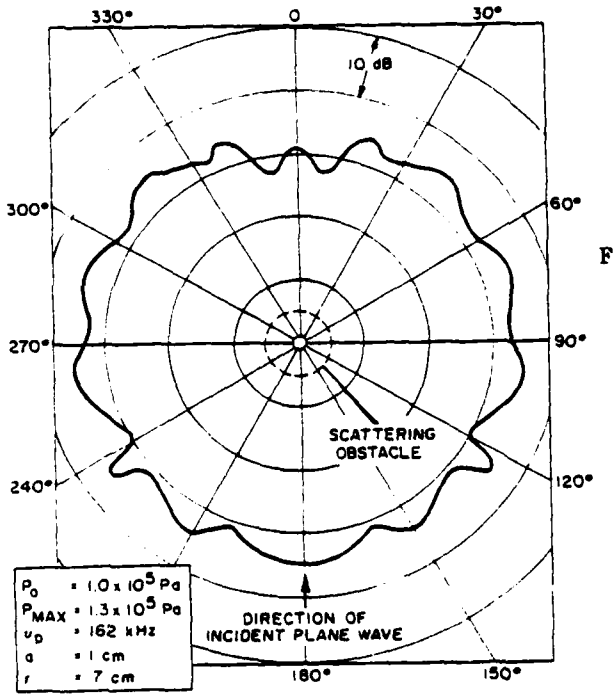

Fig. 17 - Total pressure of linear rigid-body scattering problem at 7 cm

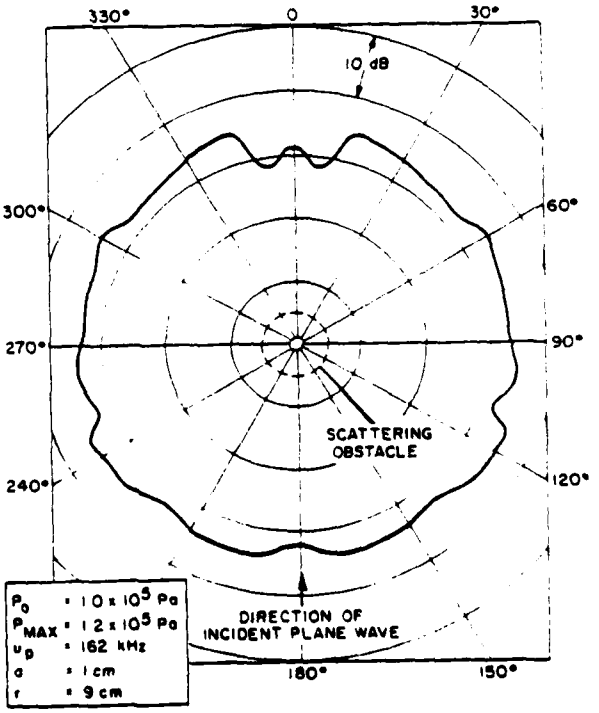

Fig. 18 - Total pressure of linear rigid-body scattering problem at 9 cm

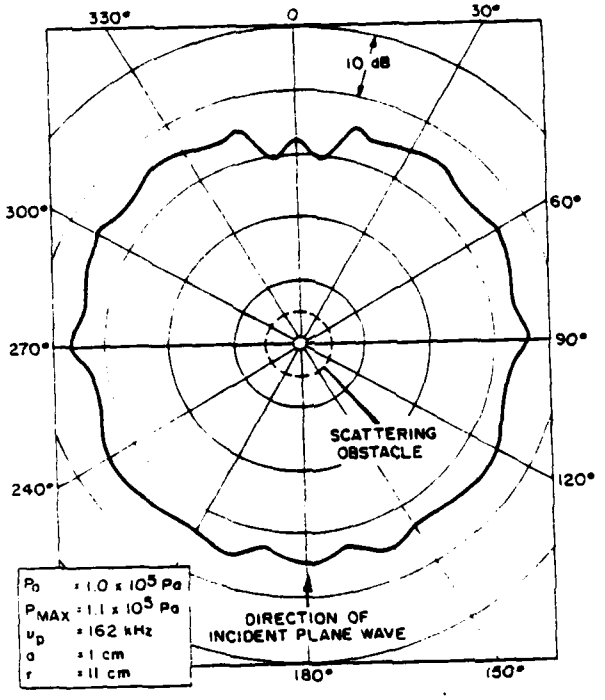

Fig. 19 - Total pressure of linear rigid-body scattering problem at 11 cm

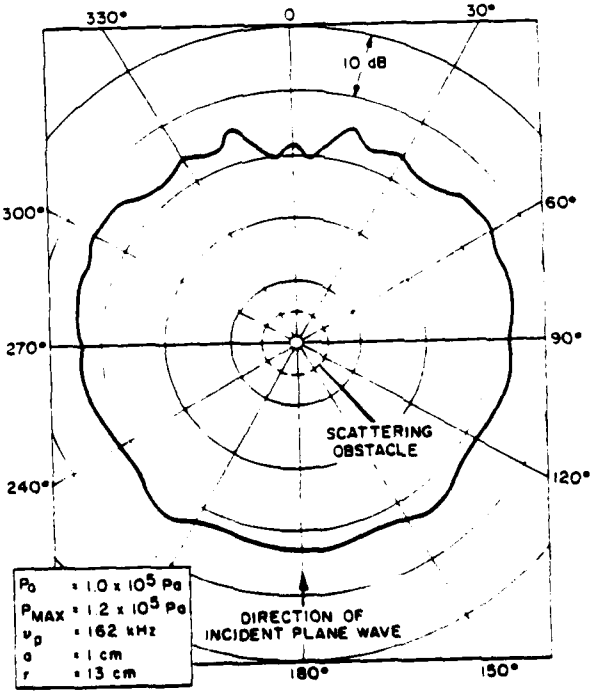

Fig. 20 - Total pressure of linear rigid-body scattering problem at 13 cm

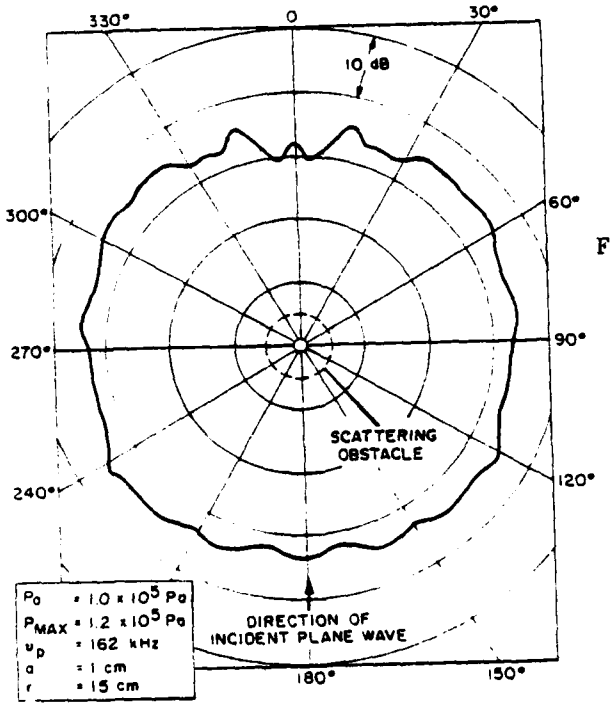

Fig. 21 - Total pressure of linear rigid-body scattering problem at 15 cm

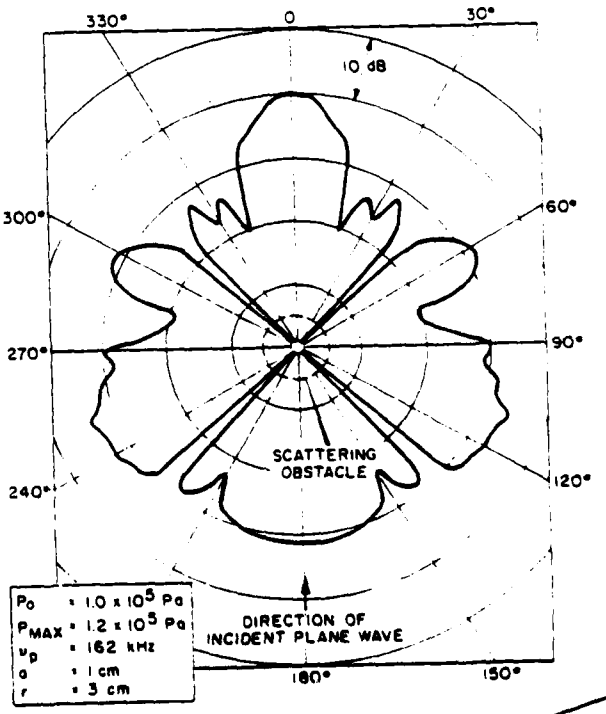

Fig. 22 - Angular distribution of linearly scattered field at 3 cm

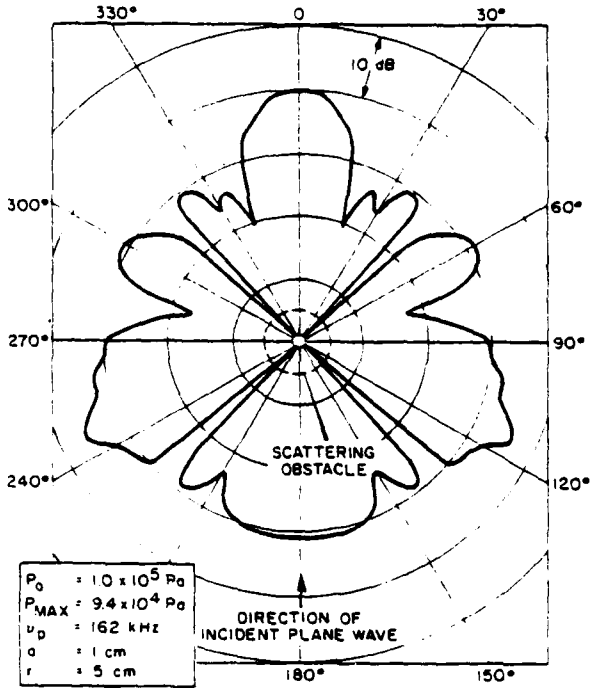

Fig. 23 - Angular distribution of linearly scattered field at 5 cm

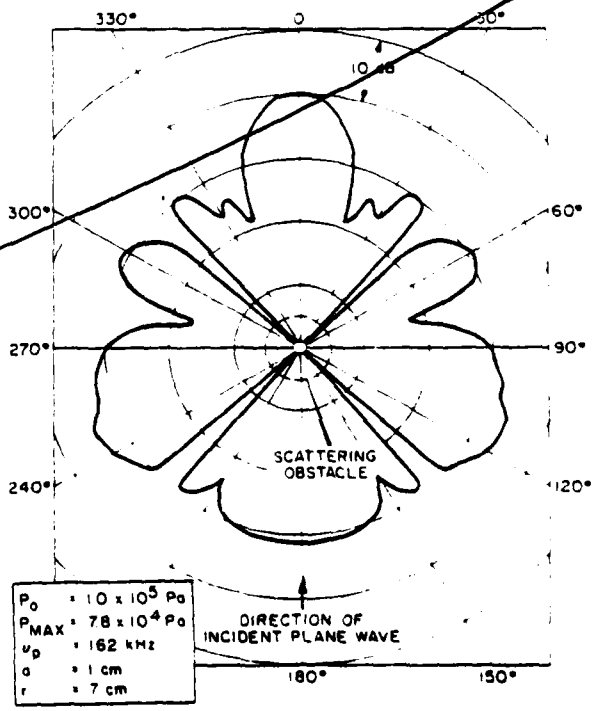

Fig. 24 - Angular distribution of linearly scattered field at 7 cm

AD-A129 282 NONLINEAR SCATTERING OF ACOUSTIC WAVES BY VIBRATING OBSTACLES(U) NAVAL RESEARCH LAB WASHINGTON DC J C PIQUETTE 01 JUN 83 NRL-MR-5077 2/2

UNCLASSIFIED F/G 20/1 NL

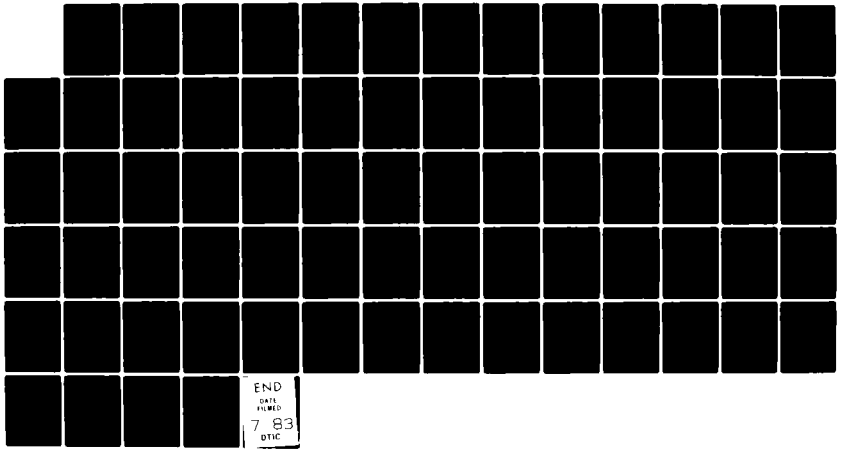

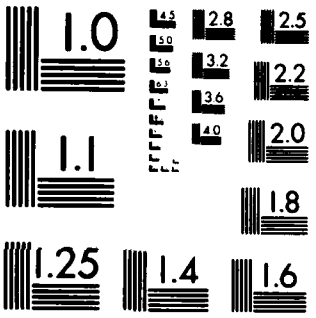

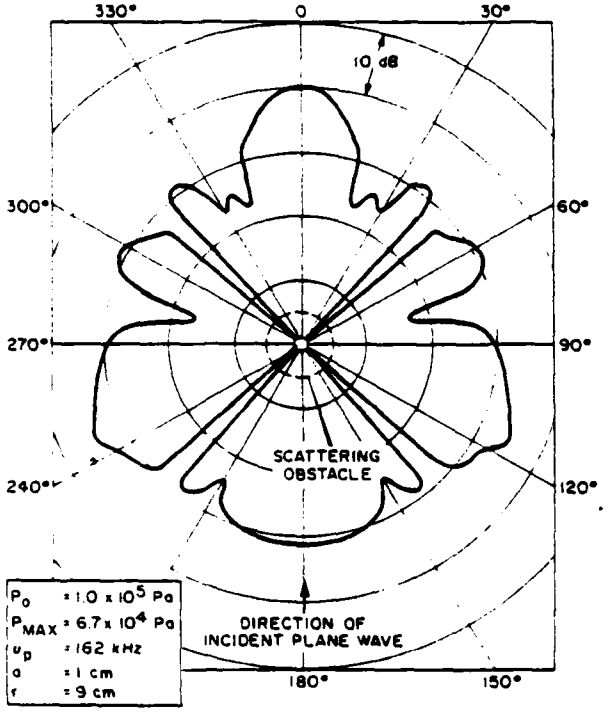

Fig. 25 - Angular distribution of linearly scattered field at 9 cm

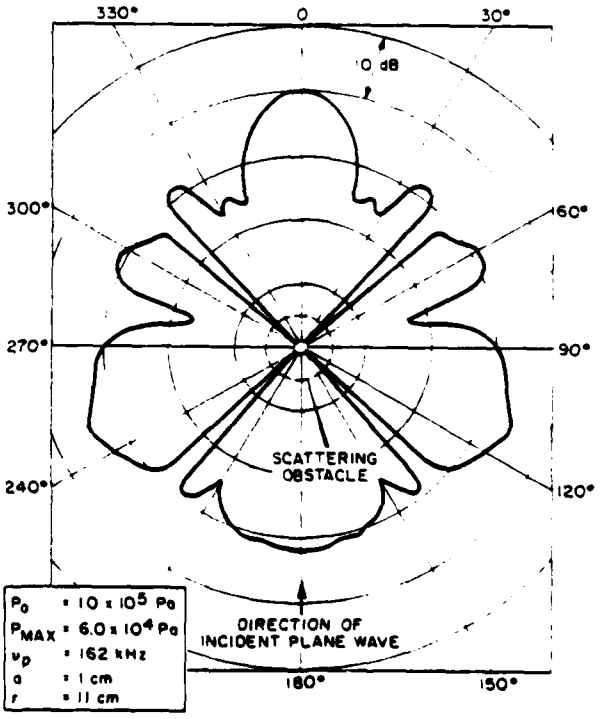

Fig. 26 - Angular distribution of linearly scattered field at 11 cm

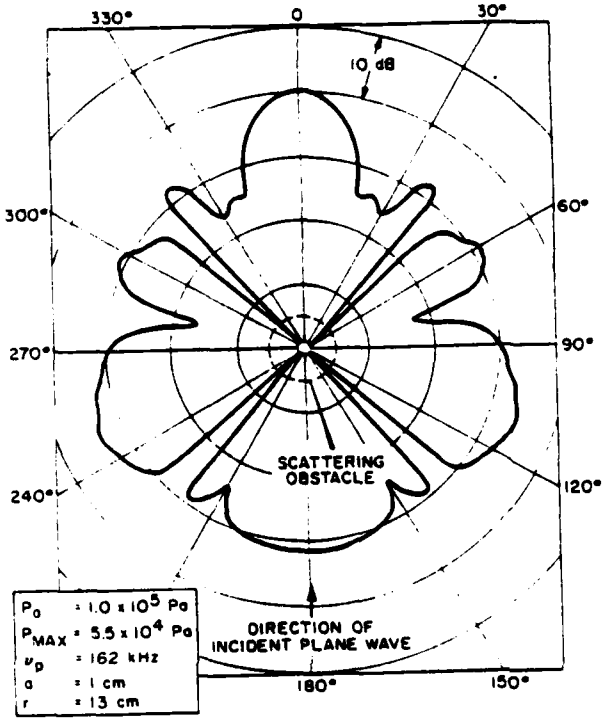

Fig. 27 - Angular distribution of linearly scattered field at 13 cm

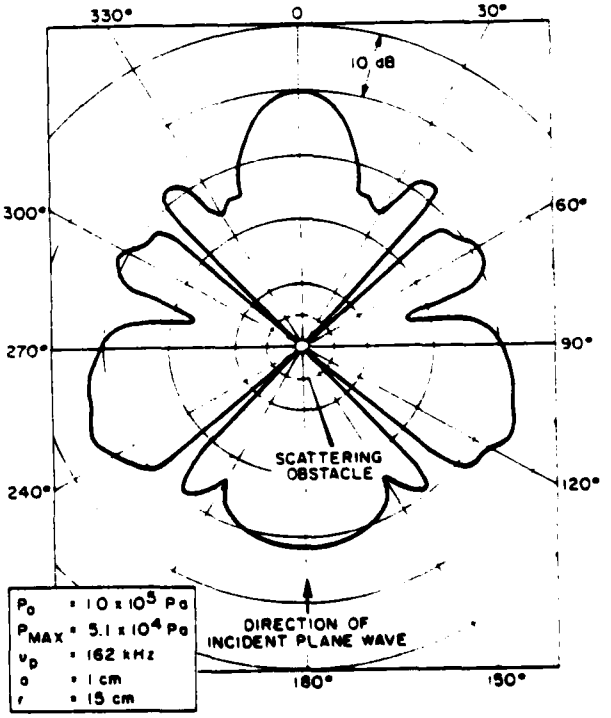

Fig. 28 - Angular distribution of linearly scattered field at 15 cm

integrals over the primary fields (not just integrals along the radius); hence, detailed variations in angle in the primary fields can easily disappear in the nonlinear field.

The angles between 15 and 60° and between 300 and 345° do not correspond closely to either of the two sets of patterns given in Figs. 15 through 21 or Figs. 22 through 28 (although some correspondence can still be seen between certain features). These angles may be regarded as a "transition region" through which the effects associated with mixing between the incident plane wave and cylindrically radiated wave diminish.

Behavior of the difference-frequency pressure at fixed angles and varying distance is illustrated in Figs. 12 through 14. Figure 12 gives the difference-frequency pressure at 0°; Figs. 13 and 14 give the difference-frequency pressures at 90 and 180°, respectively. It will be noted in Fig. 12 that the difference-frequency pressure in this direction increases approximately linearly with distance. This result is similar to the behavior of the parametric array [14] (in which a single piston source is driven at two different primary frequencies). It is understandable that the difference-frequency pressure at 0° in the current problem should behave approximately as a parametric array since the incident plane wave acts exactly as one of the primary waves does in the parametric array, and the radiated cylindrical wave approximates the behavior of the second primary (although it diminishes in amplitude).

At angles other than 0°, however, the geometrical relationship between the incident plane wave and cylindrically radiated wave is no longer favorable for the nonlinear generation of acoustic waves. Hence, at these angles, it is the mixing of the rigid-body scattered wave with the cylindrically radiated wave that is responsible for the production of the majority of the nonlinear field. Since the rigid-body scattered wave also spreads cylindrically, the interaction between these two waves is similar to the interaction of two concentric cylindrically radiated waves. This last problem was considered by Dean [20], who showed that in this case, unlike the parametric array, the nonlinearly generated waves approach a constant value as the observation point approaches the farfield. A similar behavior is apparent in the present problem from Figs. 13 and 14.

It is interesting at this point to attempt to establish an actual numerical connection between the asymptotic expression given for this case by Dean

(reproduced in Section III. G. 3 of this report) and the experimental parameters resulting in Figs. 13 and 14. We must, of course, rewrite the expression so it represents the difference-frequency case, and substitute the notation used for the pressure amplitudes used in this thesis. This results in

$$P_{-} \approx \frac{\pi P_0 A H_1^{(1)}(k_p a) H_1^{(1)}(k_c a)(\Gamma)(k_p k_c)^{1/2} k_d a^2}{2\rho_o c_o^2}.$$

We are now faced with the problem of choosing appropriate values for the pressure amplitudes P_0 and A, which are consistent with the present experimental parameters and which realistically represent the theoretical situation of concentric cylindrical waves. Clearly, one of these ought to be chosen as 3.5×10^5 Pa, the actual pressure-amplitude coefficient of the cylindrical source used in the experiment. The choice of the other pressure amplitude, however, is more subtle.

The scattered pressure plotted in Figs. 13 and 14 has been computed using Eq. (108). It is this equation that is used as a guide in selecting the second required pressure amplitude in the asymptotic calculation. We are representing our cylindrically radiated wave by an expression of the form $AH_o^{(1)}(kr)$. In analogy with this expression, we select the zeroth-order scattering coefficient as the required second pressure amplitude. The scattered pressure plotted in Figs. 13 and 14 actually results from a large number of terms in the series represented by Eq. (108). However, the geometrical collimation of the cylindrically radiated wave is clearly strongest with respect to the zeroth-order scattering term. Hence, we expect the majority of the difference-frequency pressure will be generated via the "mixing" of the cylindrically radiated wave with the zeroth-order partial wave of the scattered pressure field. We compute this coefficient using the expressions following Eq. (109) with 1.0×10^5 Pa as the incident plane-wave amplitude (corresponding to the actual experimental parameter). This results in a value of approximately 3×10^4 Pa for the zeroth-order coefficient. Using this as one of the required pressure amplitudes (with 3.5×10^5 Pa for the other pressure amplitude) in the asymptotic expression for the difference-frequency pressure, yields a value of approximately 41 Pa. In Figs. 13 and 14 the difference-frequency pressure has obtained a value of approximately 30 Pa at r = 45 cm

and is continuing to gradually increase. This is certainly a reasonable agreement and, hence, gives further verification that the computer routines are providing accurate calculations of the difference-frequency pressures.

IV. EXPERIMENT

A. Introduction

An experimental investigation was undertaken to confirm the theoretical predictions for the case in which a plane wave is normally incident on a cylindrical surface that deforms harmonically and uniformly in the radial direction. A discussion of the choice for the experiment including the principles upon which the experimental parameters were selected is given below in Section IV. B. Although the investigation was unsuccessful in confirming the theoretical predictions, it was nonetheless successful in identifying the several difficulties that arise in nearfield nonlinear experiments and resolving all but one of those identified. A discussion of these difficulties and the solutions that were achievable are given in Section IV. C.

In addition to these positive aspects, the experimental investigation also produced significant results in several other areas, primarily with regard to the selection and calibration of the sound sources and receivers used in the experiment. A description of these results is given in Sections IV. D, E, and F.

First, the selection and design of the sound sources is discussed in Section IV. D. Second, the selection and the first-order (linear) calibration of the sound sensors (hydrophones) is presented in Section IV. E. Lastly, Section IV. F describes the nonlinear calibration of these same (and a few additional) hydrophones both by a previously developed technique [48,49] and by a new method developed in this work.

B. Choice of the Experiment

Prior to describing the actual experiments performed, it is worth-while describing the principles upon which the experimental parameters were selected. Initial decisions were required as to which experimental geometry would be addressed, whether the sum-frequency component or the difference-

frequency component would be investigated and what particular primary frequencies would be suitable for measurement.

In this report, three geometries are considered theoretically. These are:

1. Plane wave normally incident on a uniformly vibrating infinite plane.

2. Plane wave normally incident on an infinitely long cylinder vibrating uniformly in the radial direction.

3. Cylindrical wave normally incident on an infinitely long cylinder vibrating uniformly in the radial direction.

Although Case 1 would be the most straightforward to implement experimentally, it is very similar to the standard case of two infinite plane waves propagating together in a fluid medium, which has been extensively studied previously [27,31,50-53] and, hence, is not of the greatest interest. In choosing between the final two cases, Case 2 appears to be the better one based on calculations that show a significantly greater amplitude of the difference-frequency component being generated than in Case 3. It will be appreciated that similar cases involving spherical geometry (which were not treated theoretically here) would give an even lower amplitude difference-frequency pressure since in these cases the energy is spreading into three dimensions whereas in the cylindrical case it spreads only into two dimensions.

In choosing between sum- and difference-frequency components, the difference-frequency component was selected for experimental measurement. The primary reason for this was that it avoids the difficulty of separating the sum-frequency component from harmonics of the primaries in the hydrophone received signal.

Having chosen the geometry of Case 2, appropriate frequencies must be selected. The cylinder is the source that provides the experimental limits in this regard. Since the cylinder must act as a high-amplitude sound source with vibration in the radial direction that is uniform along its axis, it should be operated near its lowest radial mode resonance, i.e., breathing mode. In addition to being nonuniform, higher modes of vibration

significantly limit this amplitude [54]. An additional requirement to obtain uniformity of vibration along the cylinder's axis is that a segmented, rather than a single piece, cylinder be used to avoid excitation of longitudinal (length) modes of vibration. Fabrication of such a cylinder is quite complicated. Fortunately, one was already available that had been used as a Navy standard. It has a breathing mode resonance frequency of 102 kHz. A cylinder with a resonance frequency much greater than this would be difficult to make and use since it would have an unacceptably small radius.

Assuming the cylinder to be operated at about 100 kHz, a suitable plane-wave frequency (and hence difference frequency) must be selected. There are two possibilities:

1. The plane-wave frequency is less than the cylindrical-wave frequency.

2. The plane-wave frequency is greater than the cylindrical-wave frequency.

Case 1 is preferable since the cylinder is more likely to behave as a rigid body scatterer of the plane wave in this case [3]. Unfortunately, certain practical considerations eliminate this case as a possibility. First, in order to maximize the ability to discriminate between the primary waves and the difference-frequency waves in the hydrophone received signal, the difference frequency must be less than either of the primary frequencies. (This allows all filters that the hydrophone's electrical output passes through to be operated in a low-pass mode thereby providing maximum discrimination.) Hence, the lowest possible plane-wave frequency is 50 kHz. This frequency is unacceptable, however, since it results in a difference frequency that is also 50 kHz. To avoid this, the plane-wave frequency must be chosen closer to the cylinder frequency. Unfortunately, the difference-frequency pressure generated nonlinearly in the water varies directly with the difference frequency. Hence, the closer the two frequencies become, the smaller the difference-frequency pressure becomes. The optimum frequency, which minimizes the "closeness" of the difference frequency to either primary frequency as well as giving a substantial value for the difference frequency is approximately 75 kHz. Unfortunately, the 25-kHz difference frequency associated with 100- and 75-kHz primaries is still quite small. Hence, a

plane-wave frequency less than the cylinder frequency appears to be a poor choice.

Selecting a plane-wave frequency greater than the cylinder frequency precludes the cylinder from behaving as a rigid body in scattering the plane wave [3]. However, it is possible to account for this by modeling the scattered field empirically. This is done by measuring the scattered pressure (both amplitude and phase) rather than assuming rigid-body scattering, and then calculating how the coefficients in the Hankel-function expansion of the rigid-body field must be modified in order to obtain the measured pressures. (No modification of the Green's function used in calculating the difference-frequency component is required since the cylinder can still properly be assumed rigid if the difference frequency is chosen to be below the cylinder resonance.) It remains now to select an appropriate plane-wave frequency above the cylinder frequency. Using the same reasoning as above, this results in a plane-wave frequency of about 150 kHz (in the experiment actually performed, the plane frequency used was 162 kHz).

At this point it should be recalled that in the discussion in Chapter II pertaining to Eq. (47), it was remarked that if the D'Alembertian terms on the right-hand side of this equation become significant relative to P_2, that the solution obtained by their neglect is questionable. It is essential, therefore, to estimate the value of these terms in the current measurement.

In order to facilitate this estimate, the actual fields in the current problem will be replaced by planar fields of the same frequencies as those of interest (this then calculates the worst case possible). Hence, the first-order fields will be represented as:

$$P_1 = P_0 e^{i(k_p x - \omega_p t)} + P_s e^{i(k_p x - \omega_p t)} + A e^{i(k_c x - \omega_c t)}.$$

In this equation P_0, A, k_c, ω_c, k_p, ω_p have the same meaning as in Chapter II. The symbol P_s stands for the maximum amplitude of the scattered pressure field. Equation (46) can be used to relate the velocity potential to the pressure. This relationship may be taken to be:

$$P = -i\omega\rho_o\phi$$

where sinusoidal time dependence has been assumed. A complex quantity Z_1, which is related to the first-order velocity potential ϕ, therefore, may be defined as:

$$Z_1 = \frac{A}{\omega_o \rho_o} e^{i(k_c x - \omega_c t)} + \frac{P_0}{\omega_\rho \rho_o} e^{i(k_p x - \omega_p t)} + \frac{P_s}{\omega_\rho \rho_o} e^{i(k_p x - \omega_\rho t)}.$$

The quantity ϕ_1 is then the real part of Z_1, or

$$\phi_1 = (Z_1 + Z_1^*)/2.$$

Also of interest in analyzing the D'Alembertian terms of Eq. (47) are the gradient and the time derivative of ϕ_1. Complex quantities Z_2 and Z_3 may be defined, then, as

$$Z_2 = \nabla Z_1 = \frac{ik_c A}{\omega_c \rho_o} e^{i(k_c x - \omega_c t)} + \frac{ik_p P_0}{\omega_\rho \rho_o} e^{i(k_p x - \omega_p t)} + i \frac{k_p P_s}{\omega_\rho \rho_o} e^{i(k_p x - \omega_p t)}$$

$$Z_3 = \frac{\partial Z_1}{\partial t} = \frac{-iA}{\rho_o} e^{i(k_c x - \omega_c t)} - \frac{iP_0}{\rho_o} e^{i(k_p x - \omega_\rho t)} - i \frac{P_s}{\rho_o} e^{i(k_p x - \omega_p t)}.$$

[Note that in the definition of Z_2 the vector nature of the gradient has been suppressed since it will have no effect. This is due to the fact that plane waves are being considered, and it is actually Z_2^2 that is of interest in analyzing the D'Alembertian terms of Eq. (47).] The quantities $[\nabla\phi_{(1)}]^2$ and $\partial\phi_{(1)}/\partial t$ may now be calculated from Z_2 and Z_3 as

$$[\vec{\nabla}\phi_{(1)}]^2 = (\mathrm{Re}Z_2)^2 = (Z_2+Z_2^*)^2/4$$

$$(\frac{\partial\phi_{(1)}}{\partial t})^2 = (\mathrm{Re}Z_3)^2 = (Z_3+Z_3^*)^2/4.$$

The quantities of interest in calculating the D'Alembertian terms need only be calculated insofar as the difference frequency is affected. These contributions to the difference frequency can be denoted by the subscript [-], and can be related to Z_1, Z_2, and Z_3 in the following way:

$$[\frac{\partial^2\phi_{(1)}}{\partial t^2}^2]_- = \frac{1}{2}\frac{\partial^2}{\partial t^2}(Z_1Z_1^*)_-$$

$$[|\vec{\nabla}\phi_{(1)}|^2]_- + \frac{1}{2}(Z_2Z_2^*)_-$$

$$[(\frac{\partial\phi_{(1)}}{\partial t})^2]_- = \frac{1}{2}(Z_3Z_3^*)_-.$$

Using the given equations for Z_1, Z_2, and Z_3 these expressions may be analyzed retaining only contributions to the difference frequency. Furthermore, since calculation of the worst case is of interest, the exponentials will be dropped and only the amplitudes will be retained. This procedure gives:

$$[\frac{\partial^2\phi_{(1)}}{\partial t^2}^2]_- = \frac{A(P_0+P_s)(\omega_p-\omega_c)^2}{\rho_o^2\omega_p\omega_c}$$

$$[|\nabla\phi_{(1)}|^2]_- = A(P_0+P_s)/\rho_o^2c_o^2$$

$$[(\frac{\partial\phi_{(1)}}{\partial t})^2]_- = \frac{A(P_0+P_s)}{\rho_o^2}.$$

Now, these expressions may be combined with the fact that

$$\Box^2\left[\frac{1}{2}\rho_o^{-1}c_o^{2}\Delta\rho^2 - \frac{1}{2}\rho_o u^2 - \frac{1}{2}\rho_o c_o^{-2}\frac{\partial^2}{\partial t^2}(\phi^2)\right]$$

$$= \Box^2\left[\frac{1}{2}\rho_o c_o^{-2}\left(\frac{\partial\phi_{(1)}}{\partial t}\right)^2 - \frac{1}{2}\rho_o\left|\vec{\nabla}\phi_{(1)}\right|^2\right.$$

$$\left. - \frac{1}{2}\rho_o c_o^{-2}\frac{\partial^2}{\partial t^2}(\phi_{(1)}^{2})\right]$$

to analyze the D'Alembertian terms of Eq. (47). This results in

$$\left[\frac{1}{2}\rho_o c_o^{-2}\left(\frac{\partial\phi_{(1)}}{\partial t}\right)^2 - \frac{1}{2}\rho_o\left|\vec{\nabla}\phi_{(1)}\right|^2 - \frac{1}{2}\rho_o c_o^{-2}\frac{\partial^2}{\partial t^2}\phi_{(1)}^{2}\right]$$

$$= -A(P_0 P_s)(\omega_c-\omega_p)^2/(2\rho_o c_o^{2}\omega_c\omega_p).$$

In order to use this expression to estimate the D'Alembertian terms, the experimental values of ω_p and ω_c may be used directly. However, it would not be reasonable to directly substitute the value for A, since this pressure occurs nowhere in the fluid surrounding the scatterer. It is more reasonable to use the value of the amplitude of the pressure of the cylindrically radiated wave analyzed at the cylinder's surface. This is approximately 1.35×10^5 Pa. For the expression (P_0+P_s) it is reasonable to use the maximum value of the total pressure field associated with the first-order rigid-body scattering problem. The value of this quantity is approximately 1.7×10^5 Pa. Using these values, the above expression for the terms under the D'Alembertian operator gives a magnitude of 1.1 Pa*. This is less than 5% of the values predicted for the difference-frequency pressure in all directions at distances

- - - - - - - - - - -

*It is interesting to compare this value with that obtained for pseudosound in Section IV. F. (0.1 Pa). We note that the D'Alembertian terms are of the same general magnitude as pseudosound.

greater than approximately 10 cm from the cylinder's center (compare with Figs. 12-14). Hence, these terms are sufficiently small so as to not severely affect the theoretical treatment at all distances greater than a few centimeters from the surface of the cylinder.

Of course, at shorter distances, this value becomes a more significant fraction of the second-order pressure. Hence, the solutions represented by Eq. (15) are not likely to be accurate at distances where the predicted pressure amplitude is small (say of the order of pseudosound).

One more consideration is of interest in demonstrating the fact that the influence of the D'Alembertian terms on the solution is quite small. If, in solving Eq. (47), the D'Alembertian terms are not grouped with the second-order pressure, they must be included as a part of the virtual source term in the Green's function solution represented by Eq. (84). In this case, the virtual source term will include quantities of the form $\Box^2 Z^2$, which vanishes identically for Z = plane wave. Hence, any nonvanishing contributions must arise from the nonplanar geometry of the actual primaries, and such effects may reasonably be expected to be small.

Another consideration of some concern is the effect that the D'Alembertian terms might have on the neglected surface integral of Eq. (83). This is very difficult to estimate accurately, owing to the complicated form of the Green's function and the first-order fields involved. An extremely simple estimate that may give some indication of the order of magnitude of the error may be obtained by inserting for the D'Alembertian terms in this surface integral the constant value of 1.1 Pa obtained above, multiplied by the difference-frequency wavenumber, k_d (since it is the gradient of the source terms which appears in this surface integral). We replace the Green's function by its asymptotic form, but simply analyze its value on the cylindrical surface [see Eq. (7.3.17) of Reference 29]. Lastly, the surface integral itself reduces to simply 2π times the cylindrical radius. Hence, the D'Alembertian terms result in

$$(2\pi a)(k_d)(1.1 \text{ Pa})\left[\frac{1}{4}\sqrt{2/\pi k_d a}\right] \approx 2.2 \text{ Pa}$$

of influence on the surface integral. This too may be regarded as sufficiently small to neglect, provided the second-order pressure solution is

not expected to be accurate at distances extremely close to the cylindrical surface (where, once again, "close" refers to distances at which the second-order pressure approaches the value of pseudosound).

At this point we can also put the discussion of the neglect of the Green's function integral between r and ∞ discussed in Chapter II on a somewhat firmer mathematical ground for this particular case by the following semi-quantitative argument: The integral of concern represents an integration over a product of the virtual source term and the Green's function. We may symbolically represent the major contributions to this integral by the following two associated integrals

$$I_1 = \left(\frac{k_d^2 \Gamma}{\rho_o c_o^2}\right) \int_0^{2\pi} d\Theta' \int_r^{\infty} dr' r' P_p(\vec{r}') P_c(\vec{r}') G(\vec{r},\vec{r}')$$

$$I_2 = \left(\frac{k_d^2 \Gamma}{\rho_o c_o^2}\right) \int_0^{2\pi} d\Theta' \int_r^{\infty} dr' r' P_s(\vec{r}') P_c(\vec{r}') G(\vec{r},\vec{r}'),$$

where the coefficient arises from the formulation of the simple source, P_p represents the incident plane wave, P_c represents the radiated cylindrical wave, P_s represents the rigid-body scattered waves, and $G(\vec{r},\vec{r}')$ represents the Green's function. We consider I_1 first.

We represent $P_p(\vec{r}')$ as $P_0 e^{ik_p r' \cos\Theta'}$ and $P_c(\vec{r}')$ (neglecting an unimportant phase factor) as $A\sqrt{2/\pi k_c r'}\, e^{-ik_c r'}$ (we have used the asymptotic form of the Hankel function since $k_c r \geq 4.18$ cm^{-1}r, for which the asymptotic form is reasonably accurate). For the Green's function we use

$$G(\vec{r},\vec{r}') = \frac{i}{4} H_0^{(1)}(k_d w),$$

where $w^2 = (x-x')^2 + (y-y')^2$. This is the infinite-space Green's function. We will discuss the errors in using this instead of the proper Green's function following the present estimates. This error will prove to be insubstantial.

It is clear that $G(\vec{r},\vec{r}')$ has a singularity at $r = r'$. Hence, we will break the integral I_1 into two parts: $I_1 = \int_r^{r+\epsilon} + \int_{r+\epsilon}^{\infty}$, where ϵ is infinitesimal.

We now note that in I_1, both an integral Θ' and r' are required. We consider the angular integral first. It should be noted that only the functions P_p and G have a Θ' dependence. Hence, we consider the associated integral

$$I_{\Theta'} = \frac{i}{4} \int_0^{2\pi} d\Theta' e^{ik_p r' \cos\Theta'} H_0^{(1)}(k_d w).$$

There is a singularity in this integral at $\Theta' = 0$ (since w vanishes at this value of Θ'). Hence, we choose to resolve $I_{\Theta'}$ as follows: $I_{\Theta'} = \int_{\delta}^{2\pi-\delta} + \int_{-\delta}^{\delta}$, where δ is an infinitesimal angle. In the integral between $-\delta$ and δ, it is reasonable to replace the factor $e^{ik_p r' \cos\Theta'}$ by $e^{ik_p r'}$, since Θ' has infinitesimal values over the entire range of integration. We also note that $H_0^{(1)}(k_d w)$ may be resolved into functions of r and r' alone (see Ref. 43, p. 979, Eq. 8.531.2). Hence, this integral becomes

$$\int_{-\delta}^{\delta} = \frac{i}{4} e^{ik_p r'} \int_{-\delta}^{\delta} d\Theta' [J_o(k_d r) H_0^{(1)}(k_d r')$$

$$+ 2 \sum_{m=1}^{\infty} J_m(k_d r) H_m^{(1)}(k_d r') \cos(m\Theta')].$$

The integrals are elementary and give

$$\int_{-\delta}^{\delta} = \frac{i}{4} e^{ik_p r'} [J_o(k_d r) H_o^{(1)}(k_d r')(2\delta)$$

$$+ 4 \sum_{m=1}^{\infty} j_m(k_d r) H_m^{(1)}(k_d r') \sin(k_d \delta)].$$

Both terms in the brackets vanish in the limit $\delta \to 0$. Therefore, $\lim_{\delta \to 0} \int_{-\delta}^{\delta} = 0$. This demonstrates the singularity at $\Theta' = 0$ in $I_{\Theta'}$ is

inconsequential. We consider next the integral $\int_{\delta}^{2\pi-\delta}$. Since the singularity has been removed, no error should result (for purpose of the current estimate) if the function $H_o^{(1)}(k_d w)$ is treated casually. We note that w may be rewritten as $w = (r^2 + r'^2 - 2rr'\cos\Theta')^{1/2}$. This quantity varies from 0 to 2r' as Θ' varies from 0 to 2π. We choose to replace w by r' (which is, in a certain sense, an average value). Thus, $I_{\Theta'}$ becomes simply

$$I_{\Theta'} = \frac{i}{4} H_o^{(1)}(k_d r') \int_{\delta}^{2\pi-\delta} d\Theta' e^{ik_p r'\cos\Theta'}.$$

We note that this integral can be performed in the limit $\delta \to 0$. This result is (see Ref. 43, p. 482, Eq. 3.915.2)

$$\int_0^{2\pi} d\Theta' e^{ik_p r'\cos\Theta'} = \pi[J_o(k_p r') + J_o(-k_p r')].$$

We choose to replace the Bessel functions by their asymptotic limits. This gives

$$I_{\Theta'} = \frac{i}{4} H_o^{(1)}(k_d r') \sqrt{2\pi/k_d r'} \left[\cos\left(k_d r' - \frac{\pi}{4}\right) + i\cos\left(k_d r' + \frac{\pi}{4}\right)\right].$$

This can now be used to give the following expression for the r' integral in the region between r' = r and r' = r+ε

$$\int_r^{r+\varepsilon} = \frac{k_d^2 \Gamma A P_0}{\rho_o c_o^2} \frac{i}{4} \int_r^{r+\varepsilon} dr' r' H_o^{(1)}(k_c r) H_o^{(1)}(k_d r')$$

$$\times \frac{2\pi}{k_d r'} \left[\cos\left(k_d r' - \frac{\pi}{4}\right) + i\cos\left(k_d r' + \frac{\pi}{4}\right)\right].$$

Each cosine term can be resolved into exponentials. If we also replace the Hankel functions with asymptotic forms discussed above, the integral $\int_r^{r=\varepsilon}$ will become a sum of integrals of the general form $\int_r^{r=\varepsilon} dr' \frac{e^{ikr'}}{\sqrt{r'}}$,

where k represents various combinations of the relevant wavenumbers. We can relate each of these integrals to a Fresnel integral (see Ref. 32, p. 300),

$$C_1(x) = \frac{1}{\sqrt{2\pi}} \int_0^x \frac{\cos t}{\sqrt{t}}\, dt,$$

since $\int_r^{r=\varepsilon} = \int_r^0 + \int_0^{r=\varepsilon}$. Using the asymptotic expression for $C_1(x)$ (Ref. 32, pp 300 and 302) we can easily show that $\int_0^x \frac{\cos t}{\sqrt{t}}\, dt \approx \frac{\sqrt{\pi}}{2} + \frac{1}{x}$. Hence, the integrals $\int_r^{r=\varepsilon}$ are proportional to the quantity $\frac{1}{r+\varepsilon} - \frac{1}{r}$, which clearly vanishes in the limit $\varepsilon \to 0$.

In order to conclude the analysis of I_1, we next consider the r' integral $\int_{r+\varepsilon}^{\infty}$. It is clear that the same analysis used on the θ' integral during the discussion of the integral $\int_r^{r+\varepsilon}$ is still appropriate. In this case, however, the result of integration on r' will not vanish, and hence we must treat the sum $\cos(k_d r' - \frac{\pi}{4}) + i\cos(k_d r' + \frac{\pi}{4})$ somewhat more carefully. We note that the absolute maximum value that the magnitude of this sum can have is $\sqrt{2}$. In order to estimate the r' integral $\int_{r+\varepsilon}^{\infty}$ we replace this sum by this numerical quantity (this will furnish a conservative estimate of the upper bound for this integral). Again replacing the Hankel functions by their asymptotic expressions results in:

$$\int_{r+\varepsilon}^{\infty} = \frac{k_d^2 \Gamma A P_0}{\rho_o c_o^2} \frac{i}{4} \sqrt{2/\pi k_c}\, \sqrt{2/\pi k_d}\, \sqrt{2\pi/k_d}\, \sqrt{2} \int_{r=\varepsilon}^{\infty} dr' \frac{e^{ik_p r}}{\sqrt{r'}}.$$

The integral on r' can now be analyzed by again using the asymptotic form of a Fresnel integral. If we now let $\varepsilon \to 0$, the final result for I_1 is

$$|I_1| \approx \left(\frac{k_d \Gamma A P_0 \sqrt{2}}{\rho_o c_o^2 \sqrt{\pi k_c} k_p^{3/2}} \right) \frac{1}{r} .$$

Hence, $|I_1|$ falls off even more quickly than would be expected on the basis of cylindrical spreading. This is consistent with the argument of the negligibility of the Green's function integral between r and ∞ presented in Chapter II, which was based on phase cancellation arguments. Using the present experimental values, we get $|I_1| \approx 3.37/r$, where the answer will be in Pa if r is in cm. Hence, at a propagation distance of just 10 cm, the contribution of I_1 is 0.337 Pa. This is very small when compared with the numerical values presented in Chapter III, which were approximately 38 Pa at $\Theta = 0°$ and 25 Pa at $\Theta = 90°$ at this radius.

We next consider I_2. The easiest way to handle $P_r(\vec{r}')$ in this integrand is to determine empirical coefficients α and β for the series representation of the field up to the dipole term. This representation is

$$P_p(\vec{r}') = \frac{(\alpha + \beta \cos\Theta) e^{ik_p r}}{\sqrt{k_p r}} .$$

Using the numerical values presented in Chapter III for the linearly scattered field at r = 15 cm, these constants become: $\alpha = 3.4 \times 10^5$ Pa, $\beta = 1.56 \times 10^5$ Pa (where values at $\Theta = 0°$ and $\Theta = 90°$ have been used to analyze the constants). The singularity at $\Theta' = 0$ in I_2 can be shown to be inconsequential via the same technique as used for I_1. Hence, we can proceed to analyze the angular integral without regard for this singularity. As before, we resolve $H_o^{(1)}(k_d w)$ into a sum over Bessel functions of the individual radii. Thus, the angular integral involved in I_2 becomes:

$$\int d\Theta' = \frac{i}{4} \int_0^{2\pi} d\Theta' \, \frac{(\alpha + \beta \cos\Theta')}{\sqrt{k_p r'}} e^{ik_p r'} \left[J_o(k_d r) H_o^{(1)}(k_d r') + 2 \sum_{m=1}^{\infty} J_m(k_d r) H_m^{(1)}(k_d r') \cos m\Theta' \right].$$

The angular integrals are again simple and result in

$$\int d\theta' = \frac{(\pi i)e^{ik_p r'}}{2\sqrt{k_p r'}} [\alpha J_o(k_d r) H_o^{(1)}(k_d r') + \beta J_1(k_d r) H_1^{(1)}(k_d r')].$$

If we replace the Bessel functions in this expression by their asymptotic forms (as well as the remaining Hankel functions in I_2), and choose to neglect phase factors (which can only reduce the value of the integral of interest), we obtain the further estimate for I_2

$$I_2 \approx \frac{(\alpha+\beta)e^{ik_d r} 2k_d \Gamma i A}{\sqrt{k_p k_c}\, \rho_o c_o^2 \sqrt{r}} \int_r^\infty dr' \frac{e^{ik_p r'}}{\sqrt{r'}}.$$

We again compute the r' integral with the aid of the asymptotic form of a Fresnel integral, giving

$$|I_2| \approx \left[\frac{(\alpha+\beta)2k_d \Gamma A}{\sqrt{k_c}\rho_o c_o^2 k_p^2}\right] \frac{1}{r^{3/2}}.$$

Again we note the falloff is greater than that based on cylindrical spreading, due once again to phase cancellations. Using the present experimental values, we obtain $|I_2| \approx 1.68/r^{3/2}$, where again the answer is in Pa if r is in cm. This gives just 5.3×10^{-2} Pa at a propagation distance of just 10 cm. Hence, we once again note the negligibility of these integrals relative to the numerical values presented in Chapter III, thus reinforcing their neglect during the computation.

We consider lastly the consequences of using the infinite space Green's function instead of the correct rigid-body Green's function for the purposes of this estimate. We note that the effect (in the case of a rigid plane) of the boundary term is essentially a doubling of the pressure associated with the free-space Green's function. (This can be understood from the fact that a simple image source behind the plane is all that is required to satisfy the

boundary condition.) This case may reasonably be regarded as an upper limit to the potential scattered pressure level in any other scattering geometry. Since both contributions discussed above are well under 1 Pa at r = 10 cm, it is resonable to assume that even including the surface terms in the Green's function would no more than double the result. Since this still gives less than 1 Pa, no great harm is done via use of the free-space Green's function in making the above estimates.

Even with the choices made following the careful procedure detailed above, several difficulties arise in a nearfield nonlinear scattering experiment that have not been encountered in previously published experiments. These difficulties will be described next.

C. Difficulties in the Present Experiment not Encountered in Previous Research

In investigating the nonlinear scattering of acoustic waves by vibrating obstacles, several fundamental experimental difficulties arise. Previous experiments involving two high-amplitude primaries interacting (i.e., mixing) nonlinearily in a fluid medium could be designed to avoid these difficulties. The present experiment could not be designed to avoid them. The most important of these difficulties are:

1. Inadvertent direct radiation of the sources at the difference frequency.

Since the sources are finite in extent, measurements must be made in the extreme nearfield* of the sources in order to approximate an infinite plane wave and infinitely long cylinder. Hence, direct radiation of the sources at the difference frequency will tend to be a greater source of error when the measuring hydrophone is near the sources.

- - - - - - - - - - -

*In acoustics the term farfield (nearfield) is a relative term that describes observation points at distances large (small) compared with the dimensions of the source and the wavelengths involved. In the case of a piston source, the farfield (nearfield) is defined to be distances greater (lesser) than the distance to the last maximum in the on-axis diffraction pattern. This last maximum is located approximately at a distance equal to the square of the piston radius divided by the wavelength. The farfield (nearfield) is frequently referred to as the region in which Fraunhofer (Fresnel) diffraction effects occur.

2. Electrical filtering problems due to experimental constraints.

The difference frequency was only about one half the lowest primary frequency. In addition, the pulse lengths had to be less than about 10 cycles at the difference frequency to avoid interfering reflections from neighboring surfaces. Hence, the usual passive methods employed for electrical filtering in previous farfield, nonlinear measurements were inappropriate.

3. Difference-frequency voltage generated nonlinearly in the hydrophone's sensitive element.

This effect, due to nonlinear mixing of the primaries in the hydrophone, provided larger difference-frequency voltages than those produced by the difference-frequency pressure generated by nonlinearities of the fluid medium. The effect was observed for a wide range of available hydrophones.

Previous experimental investigations [27,31,50-53] have not had to contend with the limitations enumerated above because:

(a) Circular piston sources were used in these investigations enabling virtually any choice of frequency. Then the difference frequency was chosen very much lower than the average primary frequency (high downshift ratio).

(b) Previously measurements were carried out in the acoustic farfield of the sources (or at least not in the extreme nearfield).

Recently, measurements were made in the nearfield of circular and rectangular piston* sources [55,56]. In one case [55], the average frequency of the primaries was so high (1.435 MHz) that the primaries were absorption limited. This means that the primaries were strongly attenuated (mostly by viscous absorption) by the water through which they propagated prior to reaching the hydrophone (the acoustic absorption coefficient varies approximately as the square of the frequency [57]). In the second case [56],

- - - - - - - - - - -

*In acoustics the term "piston" refers to a planar surface, all points of which are moving at the same velocity. The cross-section of a piston is generally circular or rectangular.

although the hydrophone was not in the farfield, it was not in the extreme nearfield either. (In the current sense, the "extreme nearfield" is defined in the case of a piston source as being within the Rayleigh length of the piston face. The Rayleigh length is the square of the radius of the piston face divided by the wavelength.) The closest measurement made in this case was at a hydrophone position 2.72 times the Rayleigh length from the piston face. Hence, neither of these studies had to face the difficulties inherent in a nonlinear scattering experiment.

Fortunately, the first difficulty listed above (direct radiation at the difference frequency) was fairly straightforward to eliminate. By adding an appropriate pulse-shaping network to the electromagnetic driving pulses (prior to amplification), 95% of the directly radiated difference-frequency component was eliminated. Prior to the addition of this network, the directly radiated difference-frequency component was comparable in magnitude to that generated nonlinearly by the fluid medium. Thus, after the addition of the network, the direct radiation became a small component of the total difference-frequency pressure field.

The second difficulty noted above (the problem of electrical filtering) was also resolved by the selection of extremely linear state-of-the-art active electrical filters. There are two reasons why previous nonlinear measurements were not faced with this problem. First, earlier measurements were made at least moderately far from the sources and did not involve the possibility of unwanted single or multiple reflections. Hence, long pulse lengths could be used without interfering reflections being received and a passive filter could be used. Since passive filters are generally far more linear than active filters, nonlinear generation in these filters did not present a problem. In addition, highly effective low-pass filters can be designed passively--even more effective than active filters due to lower internal noise--when one can tolerate the attendant long turn-on transients. Secondly, since very large downshift ratios were used (typically 50 thru 100), the filters did not have to be able to separate a very small amplitude difference-frequency component from the electrically large amplitude primaries that were very close in frequency to it.

In order to assure that no appreciable difference-frequency component was being generated nonlinearly in the active filters chosen in this work, a

mixing amplifier was used to electrically add two electrical signals of the same frequencies as those of the two primaries used in the experiment. The voltage amplitudes of these electrical signals were chosen to be comparable to the voltage amplitudes arising from the hydrophone's linear response to the primary pressures.

No difference-frequency component could be measured under these conditions except for that associated with the noise floor of the receiver devices. This noise floor corresponds to 27 Pa, which is half the theoretically predicted difference frequency in the forward direction at just 6 cm from the center of the cylinder. The nonlinear signal continues to grow approximately linearly in this direction from this point. Although it is clear that this noise level is large enough to prevent precise definitive measurements of the difference-frequency component close to the cylinder, it is small enough to demonstrate that filter nonlinearity was not the source of the difference frequency measured (which was typically about 10 times the theoretical value).

Unfortunately, the third difficulty (nonlinearity of the hydrophone) could not be eliminated. At the time the experiment described here was started, no one even suspected that hydrophones were nonlinear to a measurable degree. Well after the start of the present experiment, however, a study of hydrophone nonlinearity was performed jointly by scientists at the Naval Undersea Systems Center and the Underwater Sound Reference Detachment of the Naval Research Labortory. The results of this study became available in preliminary form [48,49]. Initially it was hoped that the results (measured in the nearfield at a high downshift ratio for a piston source driven at two frequencies) could be extrapolated to the case of a nonlinear nearfield scattering measurement. This did not prove to be the case. In fact, when the hydrophones' nonlinear responses were measured by a more appropriate technique (different than that used in Refs. 48 and 49), they proved to be too nonlinear to make a correct measurement of the theoretically predicted difference frequency generated in a nonlinear scattering experiment. Hence, the nonlinearity of the hydrophones proved to be the limiting factor for this experiment prohibiting valid measurements from being carried out. A description of nonlinearity measurements performed on the hydrophones considered for use in this experiment is provided in Section IV. F. The new

method developed in this work for measuring hydrophone nonlinearity and results obtained using the method will also be presented in that section.

D. Selection and Design of Sound Sources

The initial factor in choosing the sound sources or transducer elements was the availability of a suitable cylindrical transducer. Having such a device produced commercially would have been time consuming as well as costly. Fortunately, standard Navy cylindrical transducers (Type TR-127/WQM) were readily available that proved to be adequate for the experiment.

The TR-127/WQM transducer is constructed of eight cylindrical rings (O.D. = 2 cm; I.D. = 0.938 cm; length = 1.905 cm) made of Type 1 Ceramic [PZT-4, MIL STANDARD 1376 (ships)] mounted coaxially to create a line 15.24-cm long. As used by the Navy, the active elements are contained in an oil-filled, butyl-rubber boot or covering. This boot was removed for the present experiment in order to avoid any interfering effects that may have been caused by these materials. Unfortunately, the exposed ceramic became deteriorated by the chlorine used to prevent algae growth in the test pool. To avoid this, a second cylinder was coated with Krylon, a commercially available clear plastic spray coating. No further deterioration was noted.

This transducer was determined to have a breathing mode resonance frequency at 102 kHz. When driven at a signal level of 200-V amplitude, the cylinder produces an acoustic pressure in the water that corresponds to a value of 3.5 atmospheres for the constant A in the asymptotic expression for the cylinder field:

$$P_c = AH_o^{(1)}(k_c r) \sim \frac{A}{\pi}\sqrt{\lambda/r}.$$

This corresponds to a pressure at the outer surface of the cylinder ($r = a = 1$ cm) of 1.35 atm.

Once the frequency of the cylinder was chosen, this constrained the design of the piston plane-wave source for essentially three resons:

1. In order to most effectively filter the primary-wave components from the hydrophone electrical response, it was necessary that the difference frequency $\nu_- = \nu_p - \nu_c$ be significantly less than both the plane-wave frequency (ν_p) and the cylindrical-wave frequency (ν_c). (This enables the use of low-pass filtering.)

2. The piston source had to be capable of producing an approximately planar wave over a reasonable propagation distance. The greatest distance from a uniformly vibrating piston source where the wave may be considered to be approximately planar is at the position of the last maximum value of the on-axis piston pressure. This position occurs at $X = a^2/\lambda$ where a = piston radius [58]. Since X varies inversely as λ, a small wavelength and hence a high frequency is desirable for this purpose.

3. As can be seen from an analysis of the expression for the difference-frequency pressure [Eq. (115)], the amplitude of the difference-frequency wave varies approximately as the difference frequency. Hence, as the difference frequency becomes smaller, the amplitude of the difference-frequency pressure wave becomes more difficult to measure.

A value of $\nu_p \sim 1.5\ \nu_c$ tends to satisfy simultaneously all three of the above requirements. This results, for the chosen cylinder frequency, in a value of ν_p of approximately 150 kHz.

It turned out that two cylindrical disks of PZT-4 were commercially available with a thickness of 1.27 cm and a radius a of 6.35 cm. If one of the disks is mounted so it is air backed, the sound pressure produced on the side opposite from the air-backed side is nearly doubled (since acoustic radiation into water is far more efficient than into air). When the disk is operated at its fundamental thickness-mode resonance, the wavelength in the ceramic λ_m is equal to twice the thickness t of the ceramic. To calculate the corresponding resonance frequency of such a disk, it is necessary to know the longitudinal sound speed V_3^D in the material in the thickness direction; i.e., the Z axis. This is given for piezoelectric materials by [59]

$$V_3^D = \sqrt{C_{33}^D/\rho}$$

where C_{33}^D is the elastic stiffness at constant electric displacement, measured along the z axis, and ρ is the mass density of the ceramic. To evaluate this expression as well as several others given below, the following values of certain constants [59] for PZT-4 will be needed:

$\varepsilon_{33}^S/\varepsilon_o = 635$; relative dielectric constant, clamped;

$C_{33}^D = 15.9 \times 10^{10}/m^2$;

$\rho = 7.5 \times 10^3$ kg/m^3;

$e_{33} = 15.1$ C/m^2; piezoelectric stress constant.

Using these values in the above equation for V_3^D gives $V_3^D = 4.6\times10^3$ m/sec. This results in a resonance frequency of about 181 kHz for the disk (which is close to the desired value). Since clamping the ceramic in place was expected to lower this frequency, the available ceramic was deemed adequate. (The measured resonance frequency turned out to be 162 kHz.)

At a frequency of 162 kHz, the maximum distance from the piston face within which the waves could reasonably be expected to be planar is equal to $a^2/\lambda \sim 37$ cm. This distance was considered large enough to allow an experimental test of the theory. However, it still remained to be seen whether the piston could provide an acoustic wave with sufficient pressure amplitude (at least 10^5 N/m^2) at a reasonable operating power and voltage.

The peak acoustic pressure P produced in the nearfield of an air-backed piston at its fundamental thickness-mode resonance is given approximately by [60]

$$P = \frac{2e_{33}V}{t},$$

where V is the amplitude of the sinusoidal voltage applied across the two faces of the piston. For a peak pressure of 3×10^5 N/m^2, this expression gives a required applied voltage amplitude of 126 V.

To calculate the acoustic power radiated by the piston, the following equivalent circuit [53] (at resonance) is useful:

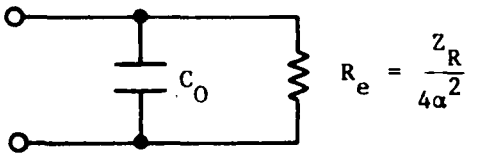

where the acoustic radiation impedance $Z_R = \rho_0 cS$ (c = sound speed in water, S = piston face area), the transformation factor $\alpha = e_{33}S/t$, and $C_0 = \varepsilon_0 \varepsilon_{33}^S S/t$, the usual equation for the capacitance of a disk. Using these expressions gives $R_e = 20.8$ ohm. The input electrical impedance of the above equivalent circuit is $Z = (20.5 + 2.43j)$ ohm; i.e., the impedance is primarily real (resistive).

The average acoustic power radiated W by the disk at an applied voltage amplitude of 126 V is given by [60]:

$$W = 2\alpha^2 V^2 / Z_R \approx \frac{V^2}{2R_e} = 382 \text{ W}.$$

The corresponding average electrical power into the piston is $(384 - 5.70\times10^{-3}j)$W.

A power amplifier capable of producing the above power (in a pulsed mode) and voltage was available. Therefore, the available ceramic disks were deemed appropriate to the experiment.

Unfortunately, these disks suffered the same damage as the cylinder when placed in chlorinated water. In addition, they suffered minor pitting due to the high electric field existing at the points of contact of the electrical conductors. One of them was repaired by filling the damaged areas with a conducting epoxy and by also epoxying on two thin stainless-steel circular plates of the same radius as the ceramic disks, one each to the front and rear surfaces (to prevent anomalously high electric fields at the points of electrical contact). Although this procedure worked well in remedying the above problems, the characteristic impedance of the disk-ceramic combination

was significantly different than the ceramic alone. Fortunately, the available high-power amplifier was capable of driving the disk to a high enough voltage (360-V amplitude) to produce an acoustic pressure amplitude of 3.16×10^5 N/m^2.

E. Calibration of Selected Hydrophones to Determine First-Order (Linear) Sensitivity

From a rather broad range of available hydrophones, three were ultimately selected for first-order calibration based on their inobtrusiveness to the sound field, as well as the expectation that their nonlinearity would be small (this latter aspect will be discussed in detail in the next section). These three hydrophones were all fabricated at the USRD. They shall be here referred to as: 1) small spherical hydrophone, 2) F42D hydrophone, 3) lead metaniobate hydrophone. A brief description of each follows.

1. Small Spherical Hydrophone.

This hydrophone was made of a 0.38-cm-O.D., 0.159-cm-I.D., PZT-4 spherical shell in a small rubber boot. Although the linear sensitivity was expected to be relatively small for this hydrophone, due to its relatively small size, it was believed this would be compensated for by a very low hydrophone nonlinearity. Also, the small size of the hydrophone assured that it would be especially inobtrusive to the measured sound field.

2. F42D Hydrophone.

The F42D is a standard hydrophone available for use by customers of the USRD. Its active element is PZT-4 ceramic, configured in a spherical shell design with an O.D. of 1.28 cm and an I.D. of 1.08 cm. The spherical shell is encapsulated in polyurethane. Although somewhat larger than the small spherical hydrophone, it is not unacceptably so. Its larger size gives a corresponding increase in first-order sensitivity, easing analysis of the received signals.

3. Lead Metaniobate Hydrophone.

This hydrophone's active element, as its name implies, is made of lead

metaniobate fashioned into a cylindrical shape and encapsulated in a transparent rubber boot. Being of single-piece design, it was believed the nonlinearity of this hydrophone would be exceptionally low (since glue joints and other bonds can be contributing factors to this nonlinearity). Additionally, being of approximately the same diameter as the F42D hydrophone, it also was expected to have a higher first-order sensitivity than the small spherical hydrophone, as well as being sufficiently inobtrusive acoustically.

The first-order (linear) sensitivity of a hydrophone in V/μPa is defined as the ratio of the voltage developed across the open-circuited hydrophone terminals when a plane wave is incident on the hydrophone to the acoustic pressure of the plane wave. The sensitivity is a complex quantity; it contains both an amplitude and a phase angle. The phase angle is not required for the present work. The sensitivity is also a function of frequency. It must be separately determined for each frequency component that is to be measured. It can also depend on the direction of the incoming plane wave, especially at higher frequencies. For low frequencies, however, it is often uniform over all 4π steadians. The method chosen for first-order calibration was one recently developed at the USRD [61]. Although phase calibration was not required for this experiment, this procedure also gave the magnitude of the first-order sensitivity, was simple to implement, and the rigging and necessary equipment were readily available.

Since the frequencies of interest were already established by the selection of the cylinder and piston at 102, 162, and 60 kHz (difference frequency), these hydrophones had to be calibrated only at these frequencies. Table II gives the results of this calibration.

F. Determination of Hydrophone Nonlinearity

1. General Considerations.

In two recent reports [48,49] it is noted that the response of ceramic hydrophone elements is not strictly linear but may be more accurately represented by the parabolic relationship

$$e = mP + \eta P^2 \tag{118}$$

where e = voltage produced by the hydrophone in pressure field P

P = pressure wave incident on the hydrophone

m = first-order (linear) response of the hydrophone (in V/μPa)

n = second-order (nonlinear) response of the hydrophone [in $V/(\mu Pa)^2$].

They define the first-order sensitivity (M) in dB re 1 V/μPa as

$$M = 20 \log(m) \tag{119}$$

and the second-order sensitivity in dB re 1 $V/(\mu Pa)^2$ as

$$k = 20 \log(n). \tag{120}$$

Table II. Hydrophone Linear Sensitivities

HYDROPHONE	FREQUENCY (kHz)	SENSITIVITY (V/μPa)	SENSITIVITY (dB re 1 V/μPa)
SMALL SPHERE	162	1.45×10^{-12}	-236.8
	102	1.55×10^{-12}	-236.2
	60	1.33×10^{-12}	-237.5
F42D	162	4.35×10^{-11}	-207.2
	102	2.48×10^{-11}	-212.1
	60	2.91×10^{-11}	-210.7
LEAD METANIOBATE	162	1.54×10^{-11}	-216.2
	102	2.20×10^{-11}	-213.2
	60	5.80×10^{-12}	-224.7

The unit dB refers to a decibel, which in this case is 20 times the logarithm to the base 10 of the sensitivity divided by the reference sensitivity of 1 V/μPa.

In the treatment given in the Moffett-Blue and Moffett-Henriquez reports for incident waves containing two primary components, the primary pressure waves are assumed to be of equal amplitude. Since this was clearly not to be the case in the present experiment, the theory is generalized here for the case of unequal primary pressure fields.

Let the total pressure wave at the hydrophone due to primary waves of angular frequencies ω_1, ω_2 and amplitudes P_1, P_2 be represented as

$$P = P_1\cos(\omega_1 t) + P_2\cos(\omega_2 t). \tag{121}$$

The contribution to the quadratic term in Eq. (118) due to difference-frequency components may be calculated by squaring Eq. (121) and suitably identifying terms. By use of the trigonometric identity $\cos\theta + \cos\phi = 2[\cos(\theta-\phi)/2][\cos(\theta+\phi)/2]$, P^2 may be readily put into the form

$$P^2 = (P_1^2/2)[1 + \cos(2\omega_1 t)] + (P_2^2/2)[1 + \cos(2\omega_2 t)]$$

$$+ P_1P_2[\cos(\omega_1+\omega_2)t + \cos(\omega_1-\omega_2)t]. \tag{122}$$

According to Eq. (118) the contribution to the voltage produced by the hydrophone due to its self nonlinearity is ηP^2. The contribution to this voltage at the difference frequency may be readily seen in Eq. (122) to be $\eta P_1 P_2$ since this is the coefficient of the difference-frequency term. This indicates that the pressure amplitudes for each of the two primary waves must be measured in addition to the voltage produced at the difference frequency due to the hydrophone nonlinearity. Only then can the nonlinear response η of the hydrophone be determined.

In the experimental portion of the Moffett-Blue and Moffett-Henriquez research, the two primary frequencies were chosen close together to produce a large downshift ratio (the downshift ratio is the quotient of the average value of the primary frequencies to the difference frequency). This avoids several sources of error in the nonlinear measurement (to be described in detail later on). Unfor-tunately, for the frequencies of interest in the

current nonlinear scattering measurement, the downshift ratio is only about 2.2, com-pared with more usual values of 50 to 100. In order to circumvent difficulties associated with this unusually small downshift ratio, an approximate approach to the measurement of η and K was adopted.

The following quantities are useful in describing the approach taken:

K_{162}, η_{162}: The hydrophone second-order sensitivity at 162 kHz and the second-order response at a 2-kHz difference frequency in the presence of primaries at 161 and 163 kHz.

K_{102}, η_{102}: The hydrophone second-order sensitivity at 102 kHz and the second-order response at a 2-kHz difference frequency in the presence of primaries at 101 and 103 kHz.

K_{60}, η_{60} the hydrophone second-order sensitivity at 60 kHz and the second-order response at a 60-kHz difference frequency in the presence of primaries at 102 and 162 kHz.

It was initially assumed that K_{60} would be approximately the average of K_{102} and K_{162}; i.e.,

$$K_{60} = \frac{K_{102} + K_{162}}{2}, \tag{123}$$

or equivalently that

$$\eta_{60} = \sqrt{\eta_{102}\eta_{162}} \ . \tag{124}$$

Equations (123) and (124) are reasonable since the nonlinear effect is quadratic. Measurement of η_{102} and η_{162} would not prove as difficult as directly measuring η_{60}, because each of these has a reasonably large downshift ratio (51 and 81, respectively). K_{102} and K_{162} are directly calculable from η_{102} and η_{162} by the relationship $K = 20 \log|\eta|$, and Eqs. (123) and (124) can be used to obtain K_{60}.

There are essentially three sources of error in the nonlinear calibration of a hydrophone, all of which are minimized by the selection of a large downshift ratio. Each of these will now be considered in detail.

a. Generation of difference frequency by nonlinear interaction of the primaries in the water - The entire basis for the present scattering experiment is the fact that when sound waves of two different frequencies are simultaneously present in water, a difference-frequency component is generated. The problem in a nonlinear hydrophone calibration is to minimize this so that only the difference-frequency components generated by a hydrophone's self nonlinearity are present in the hydrophone electrical output. This can be done in two ways. First, it is known that the difference-frequency component generated in the water tends to grow with distance from the source. Therefore, to minimize the effect, the hydrophone should be placed as close as practicable to the source. The problem of calculating the difference-frequency pressure generated in the extreme nearfield of a piston source is not trivial. However, the source levels can be estimated from data presented by Moffett and Mellen [62]. Use of this data indicated that the levels generated for the selected downshift ratios would be on the same level as pseudosound (see Section F. 1. c below), if the hydrophone is placed 5-10 cm from the source. Hence, this source of error can be made negligibly small.

b. Direct radiation at the difference frequency by the piston source - Since any amplifier will be nonlinear to some extent, it can be expected that when time-varying signals are applied to the amplifier input at two different frequencies that a voltage will appear at the output at the difference frequency. This will in turn be applied across the piston source and will be directly radiated into the water. This must be calculated beforehand, therefore, to determine if it can have a serious effect on the received voltage at the difference frequency.

In order to do so, we first note that the equation for the normal surface velocity of an air-backed piston face in contact with a fluid medium (chosen to be water) is given by [63]

$$u = \frac{2\alpha V}{Z_e - jC_{33}^D S/(\omega t)} \tag{125}$$

where V = voltage applied across the piston

S = surface area of the piston face = πa^2

ω = angular frequency of the applied voltage

t = piston thickness

Z_e = acoustic radiation impedance

and where α and C_{33}^D have the same meaning as in Section D of this chapter. The expression for the acoustic radiation impedance of a piston face is given by [64]:

$$Ze = S\rho_o c(\Theta_o - i\chi_o)$$

$$\Theta_o \to \begin{cases} \frac{1}{2} k^2 a^2 & ka \to 0 \\ 1 & ka \to \infty \end{cases}$$

$$\chi_o \to \begin{cases} 8ka/(3\pi) & ka \to 0 \\ 2/(\pi ka) & ka \to \infty \end{cases} \qquad (126)$$

where ρ_o is the water density.

It is clear from Eq. (126) that the impedance becomes very small relative to $S\rho_o C$ as $ka \to 0$.

Since in Eq. (125) this impedance is combined with another term $(-jC_{33}^D S/\omega t)$, which is much larger, the impedance term is negligible. Equating it to zero in Eq. (125) we obtain

$$u = 2\alpha\omega t\, jV/(C_{33}^D S). \qquad (127)$$

Equation (127) can be combined with the expression for the pressure radiated a distance r by a periodic simple source [65]

$$P = \frac{-jk\rho c}{4\pi r} S_\omega e^{ik(r-ct)} \qquad (128)$$

where the volume velocity S_ω of the source is equal to uS in the present case. This produces the radiated pressure per unit applied voltage

$$\frac{P}{V} = \frac{k\rho c e_{33}^{D} S_{\omega}}{2\pi c_{33}^{D} r} , \qquad (129)$$

where α has been replaced by the expression given for it in Section IV. D. Using a frequency of 2 kHz (as would be present in measuring η_{102} or η_{162}), and a distance of 1 cm, Eq. (129) yields a value of 3.02 Pa/V. The measured amplifier output voltage at the difference frequency was at most 6 V. This gives a maximum radiated pressure of about 18.1 Pa. To determine what effect this would have on the measurement, the first-order sensitivities (Table II) must be used to calculate the voltages produced at the difference frequency by this pressure. They are

Small Sphere: 2.40×10^{-5} V
F42D: 5.30×10^{-4} V
Lead Metaniobate: 1.05×10^{-4} V.

These voltages are comparable to the measured voltages at the difference frequency. Although this indicates that a directly radiated difference-frequency component is to a certain extent significant, it nonetheless does not invalidate the nonlinearity calibrations but rather sets a bound below which the nonlinearity of the hydrophones in question cannot be accurately determined. This is sufficient for the purpose of this experiment.

c. Pseudosound - In any acoustical measurement, a hydrophone's motion is uncertain by an amount of the same order as the difference between Lagrangian and Eulerian coordinates (since the hydrophone cannot be completely free to move with the fluid nor can it be completely rigidly held in a fixed position). Hence, there is an uncertainty in the meaning of the value of the measured acoustic pressure that corresponds to the difference between the Lagrangian and Eulerian frames of reference. This is presently a fundamental experimental limitation in that it cannot be fully eliminated using present-day technology (although it can be reduced by using a massive receiver well below its lowest mechanical resonance). The difference in acoustic pressure between a Lagrangian and

Eulerian frame of reference is known as pseudosound. An estimate can be made of the level of pseudosound by expanding any Lagrangian quantity $q^L(a,t)$ in terms of the appropriate Eulerian quantity $q^E(x,t)$ as [66]

$$q^L(a,t) = q^E(x,t)\Big|_{x=a+\xi(a,t)}$$

$$= q^E(x,t)\Big|_{x=a} + \frac{\partial q^E(x,t)}{\partial x}\Big|_{x=a}\xi(x,t) + \ldots \quad . \tag{130}$$

For definitions of a, x, ξ see Section II. B. Using Eq. (130) to expand the pressure gives

$$P^L(a,t) = P^E(x,t)\Big|_{x=a} + \frac{\partial P^E}{\partial x}(x,t)\Big|_{x=o}\xi(x,t). \tag{131}$$

To obtain an upper bound for pseudosound, the pressure present may be represented as plane waves as follows

$$P^E(x,t) = P_1{}^E(x,t) + P_2{}^E(x,t)$$

$$\mathrm{Re}[P_{10}e^{i(k_1x-\omega_1t)} + P_{20}e^{i(k_2x-\omega_2t)}], \tag{132}$$

where P_{10},P_{20} are real constants. Equation (132) may be combined wit Eq. (51) to obtain the following expression for $\xi(x,t)$ in terms of pressure

$$\xi(x,t) = \xi_1(x,t) + \xi_2(x,t)$$

$$= \mathrm{Re}\left[\frac{ik_1}{\rho_o\omega_1^2}P_1{}^E(x,t) + \frac{ik_2}{\rho_o\omega_2^2}P_2{}^E(x,t)\right]. \tag{133}$$

Equation (132) may also be used to express $[\partial P^E(x,t)]/\partial x$ as

$$\frac{\partial P^E(x,t)}{\partial x} = \mathrm{Re}[ik_1P^E(x,t) + ik_2P_2{}^E(x,t)]. \tag{134}$$

Hence, pseudosound (the difference between the Lagrangian and Eulerian expression for the pressure) may be written

$$P^L - P^E = \mathrm{Re}[ik_1 P_1{}^E(x,t) + ik_2 P_2{}^E(x,t)]$$

$$\times \mathrm{Re}[i(\frac{k_1 P_1{}^E(x,t)}{\rho_o \omega_1{}^2} + \frac{k_2 P_2{}^E(x,t)}{\rho_o \omega_2{}^2})]. \qquad (135)$$

At this point, it is helpful to make a few definitions:

$$Z_1 \equiv ik_1 P_1$$

$$Z_2 \equiv ik_2 P_2$$

$$a_1 \equiv 1/(\rho_0 \omega_1{}^2)$$

$$a_2 \equiv 1/(\rho_0 \omega_2{}^2).$$

Equation (135) may now be expressed as

$$P^L - P^E = \mathrm{Re}(Z_1+Z_2)\mathrm{Re}(a_1 Z_1 + a_2 Z_2)$$

$$= \frac{1}{4}(Z_1 + Z_1{}^* + Z_2 + Z_2{}^*)(a_1 Z_1 + a_1 Z_1{}^* + a_2 Z_2 + a_2 Z_2{}^*). \qquad (136)$$

Contributions to the difference frequency can arise only from the cross-terms; therefore, pseudosound at the difference frequency is given by

$$(P^L - P^E)_{diff} = \frac{1}{4}(a_2 Z_1 Z_2{}^* + a_2 Z_1{}^* Z_2 + a_1 Z_2 Z_1{}^* + a_1 Z_2{}^* Z_1) \qquad (137)$$

or

$$(P^L - P^E)_{diff} = \frac{k_1 k_2}{2\rho_o}\left(\frac{1}{\omega_1{}^2} + \frac{1}{\omega_2{}^2}\right) P_{10} P_{20}. \qquad (138)$$

Using the experimental values involved in the nonlinear calibration in Eq. (141) yields less than 0.1 Pa in both measurements. Hence, pseudosound is a rather negligible source of error in this measurement.

2. Measurement Setup and Results.

Figure 29 is a schematic representation of the measurement configuration used in the nonlinear calibration. Table III gives the results. The quantities η_{60} and K_{60} are the values obtained using Eqs. (123) and (124).

The results shown in Table III can be misleading. Apparently the small spherical hydrophone is less nonlinear than the F42D hydrophone (due to its smaller value of η_{60}). However, η_{60} cannot be considered independently of the first-order sensitivity m. An important quantity in determining the desirability of a hydrophone for use in a nonlinear experiment is the apparent pressure present at the hydrophone at the difference frequency that corresponds to the electrical signal produced by the nonlinearity of the hydrophone. Let the ratio of this quantity to the product of the primary pressures be called the "nonlinearity" and be given the symbol D. The apparent pressure (in Pa) may be calculated from the product of the primaries in terms of the first- and second-order sensitivities as

$$P_{app} = \frac{10^6 \eta P_1 P_2}{m} . \tag{139}$$

Therefore, the quantity D (measured in units of apparent Pa per squared Pa of primary) may be calculated from

$$D = 10^6 \eta / m. \tag{140}$$

[The factors of 10^6 in Eqs. (139) and (140) above are required to render consistent the units chosen.] Using the data in Tables II and III in Eq. (140) gives for the small spherical hydrophone and the F42D hydrophone the following results:

$$D_{\substack{\text{Small} \\ \text{Sphere}}} = 4.74 \times 10^{-8} \ \frac{\text{Pa(app)}}{\text{Pa}^2\text{(primary)}} \tag{141}$$

$$D_{F42D} = 5.43 \times 10^{-9} \ \frac{\text{Pa(app)}}{\text{Pa}^2\text{(primary)}}. \tag{142}$$

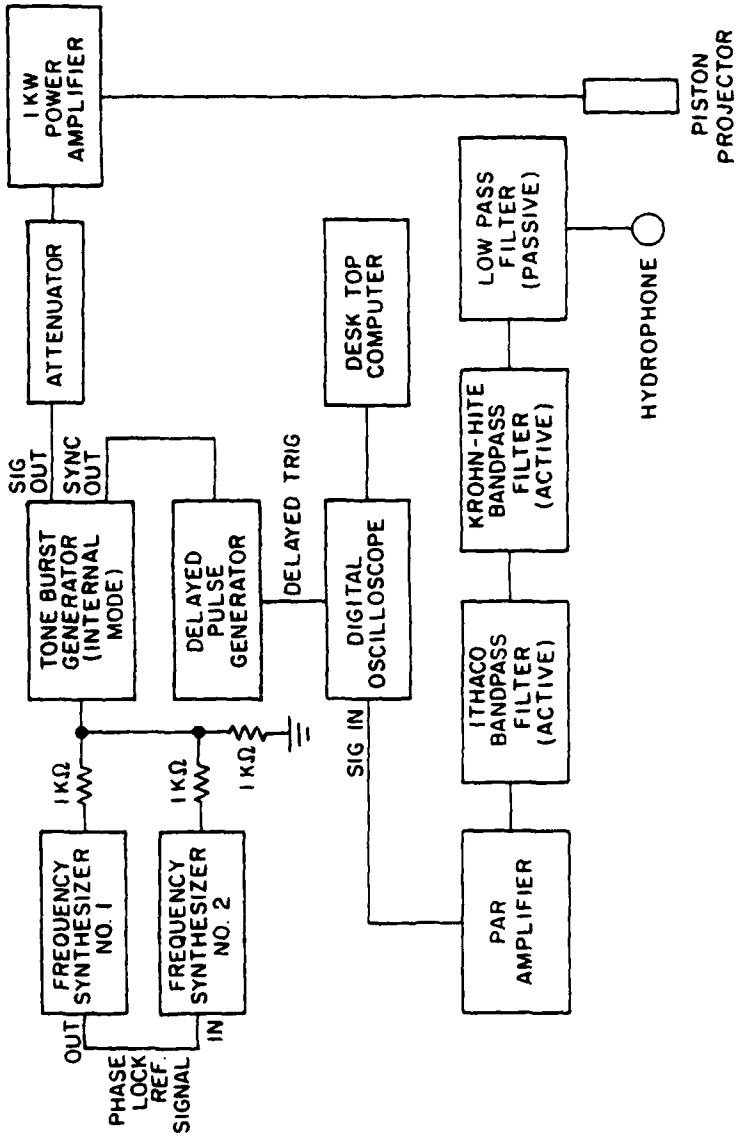

Fig. 29 - Measurement configuration for nonlinear hydrophone calibration via the Moffett-Blue method

Table III. Nonlinear Calibration of Hydrophones by Moffett-Blue and Moffett-Henriquez Approaches*

HYDROPHONE	$\eta_{102}[V/(\mu Pa)^2]$	$\eta_{162}[V/(\mu Pa)^2]$	$\eta_{60}[V/(\mu Pa)^2]$	K_{60}[dB re 1 $V/(\mu Pa)^2$]
Small Sphere	$<1.90\times10^{-26}$**	1.96×10^{-25}	6.31×10^{-26}	-504
F42D	1.52×10^{-25}	1.62×10^{-25}	1.58×10^{-25}	-496
Lead Metaniobate	$<3.8\times10^{-25}$**	$<1.1\times10^{-26}$**	6.31×10^{-26}	-504***

*Given values accurate to within 13% as determined by reproducibility of data.

**Values were too small to measure. Upper bounds determined by measured system errors.

***Results varied by as much as 14 dB from run to run. This is a possible indication of loose material in a hydrophone, as proposed by Moffett-Blue.

Although η_{60} for the F42D hydrophone is about 2.5 times greater than that for the small spherical hydrophone, it is not the more nonlinear of the two. Results in Eqs. (141) and (142) show that the small spherical hydrophone is more than 8.7 times more nonlinear than the F42D hydrophone.

Although the value of D for the F42D hydrophone is apparently sufficiently low to perform the nonlinear scattering measurements, preliminary results gave anomalously large values for the difference frequency. This indicated that the values of D obtained by the above method are not applicable to this experiment for two possible reasons:

a. The value of D obtained by the Moffett-Blue and Moffet-Henriquez approaches at high downshift ratio may not apply to low downshift ratio (indicating the hydrophone nonlinearity is extremely sensitive to downshift ratio).

b. The hydrophone nonlinearity is a function of the angle at which the primaries intersect at the hydrophone (in the Moffett-Blue and Moffett-Henriquez approaches, this is always exactly 0°; but in a nearfield scattering experiment, a wide continuum of angles is simultaneously present).

In order to determine whether either or both of the above possibilities were present during the experiment, a new approach to determine hydrophone nonlinearity (which more closely approximated the experiment of interest) was attempted. The geometry of this measurement is shown in Fig. 30, and a schematic representation of the measurement configuration is presented in Fig. 31.

In this measurement, the hydrophone of interest is placed at a distance X from the center of the active surfaces of the piston and the cylinder. Acoustic pulses are sent from each source that are of sufficient lengths to overlap at the position of the hydrophone at the moment of measurement (i.e., of length just greater than X). This ensures that no difference frequency will be generated by the fluid medium, since the waves will not have had time to overlap in the fluid. (Hence, all measured difference frequency will be generated in the hydrophone itself.) The piston and cylinder were driven at the same frequencies as were to be used in the nonlinear scattering

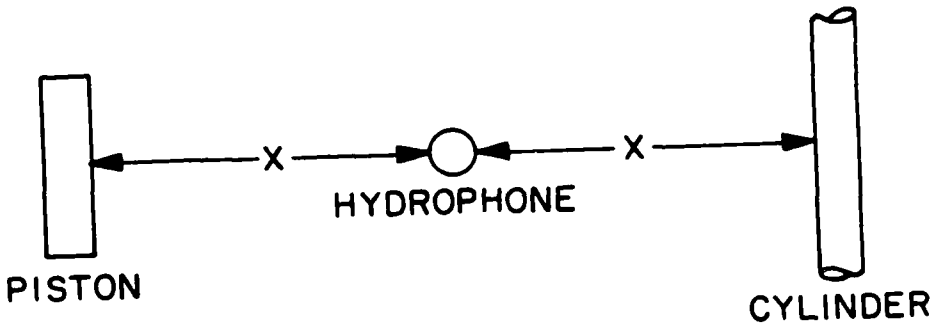

Fig. 30 - Geometry of new method of nonlinear hydrophone calibration

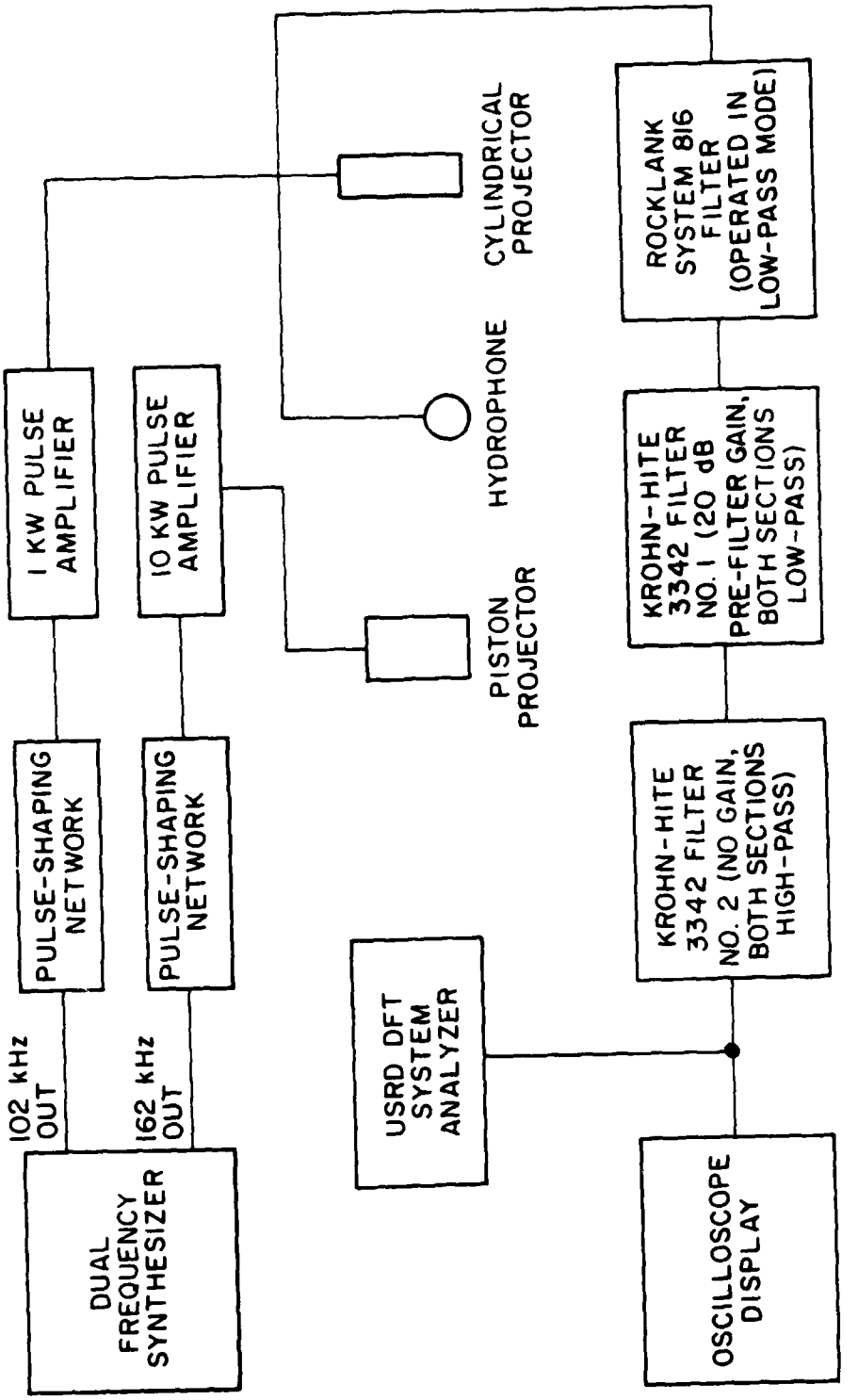

Fig. 31 - Measurement configuration for new method of nonlinear hydrophone calibration

experiment, 162 and 102 kHz, respectively. The product of the pressure levels of the primaries was also similar to that in the nonlinar scattering experiment, specifically 10^{10} Pa^2. The values of D obtained using this method on the same hydrophones tested using the Moffett-Blue and Moffett-Henriquez approaches are presented in Table IV.

Table IV. Values of D Obtained from Second Hydrophone Nonlinearity Calibration Method

Hydrophone	D $\frac{Pa(apparent)}{(Pa^2)\ (primary)}$
Small Sphere	2.47×10^{-7}
F42D	6.51×10^{-8}
Lead Metaniobate	5.34×10^{-8}

(Values accurate to within 7% as determined by reproducibility of experimental data)

It can be seen from Table IV that the results were considerably greater in all cases than the values obtained by the Moffett-Blue and Moffett-Henriquez methods. In an attempt to find a suitable hydrophone, several others were tested. The results are given in Table V.

Table V. Values of D for Some Additional Hydrophones

Hydrophone	D $\frac{Pa(apparent)}{(Pa^2)\ (primary)}$
F42C50	4.81×10^{-8}
F42D36	5.92×10^{-8}
F42D14	7.40×10^{-8}

(Values accurate to within 7% as determined by reproducibility of experimental data)

Since the product of the pressure values of the primaries in the nonlinear scattering experiment everywhere gave values of order 10^{10} Pa^2 and since typical pressures expected theoretically at the difference-frequency component were of the order of 100 Pa, it was clear that no hydrophone available was sufficiently linear to perform the experiment.

G. Suggestions for Future Measurements

As we have seen, it is the hydrophone self-nonlinearity that precludes a successful measurement of the difference-frequency pressure generated in the water when a plane-wave scatters from a vibrating cylinder. Until such time as a sufficiently linear hydrophone is available, it would appear that confirmation of the theory is not possible. However, if a method can be found for increasing the difference-frequency pressure generated in the water while maintaining the product amplitude of the primary waves approximately constant, it may be possible to make the difference-frequency voltage generated by the hydrophone self-nonlinearity a small part of the total difference-frequency signal. It will be recalled that during the discussion regarding the choice of the experiment, it was remarked that having the difference frequency lower than either primary frequency was highly desirable because it greatly simplified the necessary electrical filtering (as well as avoiding harmonics of the primaries). Unfortunately, due to the severe constraints on the

possible frequency of the cylindrical source (recall that 100 kHz was judged to be about the maximum possible), the difference-frequency choice was also severely constrained. The 60-kHz difference frequency chosen was about the greatest possible that also allowed electrical filtering to distinguish it from the primaries, and yet it resulted in a pressure-amplitude too small to measure once the hydrophone nonlinearity was discovered. However, it may be possible to choose a difference frequency above the cylinder frequency and yet sufficiently removed from the higher cylinder harmonics, such that their disturbing influence on the measurement becomes acceptably small. For example, if we retain a 100-kHz cylinder frequency but allow a 1-MHz plane frequency, the difference frequency of 900 kHz represents the ninth harmonic of the cylinder. For a cylinder pressure-amplitude of 10^5 Pa, the ninth harmonic is approximately 6 Pa (in the plane-wave case). However, since the difference frequency in this case scales approximately as the square root of the primary frequencies and directly as the difference frequency (see the expression for the farfield limit given in Chapter II), the difference-frequency pressure should be approximately 37.5 times greater than in the case experimentally studied here. This gives (for directions away from the forward-scattering direction) a difference-frequency pressure of about 900 Pa. Of course, even this suggested measurement is not without great difficulties. The worst of these are: 1) The 900-kHz difference frequency is only about 1 dB below the 1-MHz planar primary frequency, resulting in even greater electrical filtering difficulties. 2) Once again the plane-wave frequency is above the resonance frequency of the cylinder. Hence, the cylinder will not act as a rigid body, and the primary field will again have to be determined empirically. This is far more difficult to do in this case, however, since the wavelength of the scattered primary field (~ 0.15 cm) is becoming small compared with any currently available hydrophone. Hence, accurate phase measurements needed to determine the scattering coefficients would be very difficult to perform.

Another possibility is to operate the cylinder at a higher frequency (using a higher harmonic or a different vibrational mode). Although the radiated pressure amplitude of the cylindrical wave will be substantially lower, if a significant increase in difference-frequency pressure is possible due to frequency scaling, then a more favorable overall experimental condition might result. For example, if the cylinder can be operated at a frequency of

1 MHz, and the plane-wave frequency is chosen to be 1.5 MHz, the 25-Pa difference-frequency pressure computed for the present research would scale to over 2000 Pa. Hence, even if the pressure amplitude of the radiated cylindrical wave is two orders of magnitude less than that at its 102-kHz resonance, the difference-frequency pressure will remain comparable to that predicted with the parameters chosen for the experimental measurement attempted here. This would result in approximately two orders of magnitude of improvement in the ratio of the nonlinear fluid signal to the hydrophone's self-nonlinearity signal. On the other hand, 20 Pa is still not a very large signal and may remain below the noise floor of the receiving equipment (although measurement at angles near $\Theta = 0°$ might nonetheless be possible since the difference-frequency pressure at these favorable angles may be of sufficient amplitude to measure). Of course, if no cylinder resonance frequency can be found that generates a cylindrical primary pressure amplitude greater than an amplitude three orders of magnitude less than that produced by the 102-kHz frequency used, it is doubtful even at $\Theta = 0°$ that a sufficient propagation distance exists to simultaneously yield difference-frequency pressure amplitude large enough to measure and also satisfy the constraints of the theory in regard to the region of validity.

Thus, we see that there is no obvious or straightforward way to improve the experimental measurement. However, it may nonetheless be possible to in some manner take advantage of the direct scaling of the difference-frequency pressure with the difference frequency to avoid the significant interference of the difference-frequency signal associated with hydrophone self nonlinearity.

V. CONCLUSIONS

The objectives of this research were threefold: 1) To re-derive the simple-source formulation of the second-order nonlinear wave equation for arbitrary primary fields. 2) To investigate theoretically the solutions of this equation for three cases involving the scattering of acoustic waves by vibrating obstacles. 3) To subject the case of plane-wave scattering by a vibrating cylindrical obstacle to an experimental analysis. The first two of these objectives were successfully achieved, but accomplishment of the third

objective was inhibited by hydrophone nonlinearities that were larger than were previously thought to exist.

In deriving the simple-source formulation of the second-order nonlinear wave equation, care was taken to avoid using perturbation analysis until the final step. While the acuracy of a solution obtained via a perturbative approach becomes questionable when second-order fields become comparable to first-order fields, this is not so for analyses based on the inherent physical dependence of the acoustic variables on Mach number. Since the derivation of the simple-source formulation of the second-order nonlinear wave equation presented here was based on the inherent dependence of the variables on the Mach number (in all but the final step), the validity of all second-order equations up to this point are not restricted when the second-order quantities become comparable to the first-order quantities. Also, since third-order acoustic quantities are never significant in water and since no restriction was placed on the geometry of the fields, this equation may be viewed as being valid in a very general sense.

The problem of nonlinear scattering of acoustic waves by vibrating obstacles was solved via a perturbation solution of the simple source formulation of the second-order nonlinear wave equation for: 1) plane-wave scattering by a vibrating plane, 2) cylindrical-wave scattering by a vibrating cylinder, and 3) plane-wave scattering by a vibrating cylinder. Since the solutions were obtained via a perturbation method, they are restricted to situations in which the second-order fields remain small relative to the first-order fields. This means the solutions are restricted to the nearfield of the scattering obstacles. It was further demonstrated that the solutions to this problem obtained via the Censor approach for the sum- and difference-frequency pressures are of the order of pseudosound. Since the solutions of the second-order nonlinear wave equation for the sum- and difference-frequency pressures tend to grow with increasing distance from the scatterer's surface, they overhelm the effect predicted by Censor within a fraction of a wavelength of propagation distance (as was conjectured by Rogers [24]). Graphical results were presented in the case of plane-wave scattering from a vibrating cylinder for both Censor's theory and the nonlinear theory.

Although a successful comparison of theory and experiment was not achieved, several significant observations were made. No previous

experimenters had performed measurements of nonlinearly generated difference-frequency acoustic signals in the extreme nearfield of the sources. Several potential sources of error in such measurements were identified. They included: 1) direct radiation of difference-frequency pressure by the sources, 2) electrical filtering problems due to experimental constraints, and 3) difference-frequency voltage generated nonlinearly in the hydrophone. Although solutions to the first two difficulties were found, the third difficulty proved to be unresolvable. However, several significant measurements of hydrophone nonlinearity were made via a new technique. This new technique represents a significant advance over the technique of Moffett-Blue and Moffett-Henriquez. As of the writing of this thesis, a positive effect of the new nonlinearity measurement presented herein has been a significant expansion of the effort to develop a linear hydrophone at the USRD.

It is hoped that this work has firmly established the rather general validity of the simple-source formulation of the second-order nonlinear wave equation. Similarly, it is hoped that the new technique of hydrophone nonlinearity calibration developed during the course of this work will form the basis for a standard method of second-order hydrophone calibration.

DEDICATION

This report, based on the author's Ph.D. thesis, is dedicated to Charles Pine for his unequalled enthusiasm for Physics.

ACKNOWLEDGMENTS

I would like to thank those whose efforts (directly or indirectly) contributed substantially to the production of this report and the thesis on which it is based. My wife, Marice, deserves special recognition for her understanding and support while being married to a graduate student for over ten years. I am indebted to Dolores Pieper who transformed my virtually illegible drafts into this beautiful manuscript. I also would like to extend thanks to all of the many research and support personnel at the Underwater Sound Reference Detachment of the Naval Research Laboratory who provided assistance during my research. Finally, I extend my deepest gratitude to A. L. Van Buren who, through his patient guidance and invaluable technical discussions, has transformed me from a student of physics into a physicist.

REFERENCES

1. Lord Rayleigh, The Theory of Sound, Dover Publications, 1945, Vol. II, (spherical case, p. 272, cylindrical case, p. 309).

2. P.M. Morse, Vibration and Sound, McGraw Hill, 1948, p. 346.

3. J.J. Faran, "Sound scattering by solid cylinders and spheres," J. Acoust. Soc. Am. 23, p. 405 (1951).

4. L.D. Hampton and C.M. McKinney, "Experimental study of the scattering of acoustic energy from solid metal spheres in water," J. Acoust. Soc. Am. 33, p. 664 (1961).

5. R.T. Beyer, Nonlinear Acoustics, Naval Ship Systems Command, 1974, p. 1.

6. S. Earnshaw, Phil. Trans. Roy. Soc. (London), 150, p. 133 (1860).

7. E. Fubini-Ghiron, "Anomalies in the Propagation of Acoustic Waves of Finite Amplitude," an undated translation by the Ultrasonics Group, Dept. of Physics, Michigan State University of Fubini-Ghiron's original paper in Alta-Frequenze 4, p. 530 (1935).

8. W. Kech and R.T. Beyer, Phys. Fluids 3, p. 346 (1960).

9. W.D. Hayes, Fundamentals of Gas Dynamics, edited by H.W. Emmons, Princeton University Press, 1958, Chap. D.

10. J. Burgers, Advanc. App. Mech. I, p. 171 (1948).

11. D.T. Blackstock, "Approximate Equations Governing Finite-Amplitude Sound in Thermoviscous Fluids," AFOSR-5223 Suppl. Tech. Report (May 1963).

12. D.T. Blackstock, "Thermoviscous attenuation of plane, periodic, finite-amplitude soundwaves," J. Acoust. Soc. Am. 36, 1964, p. 534.

13. D.T. Blackstock, "On plane, spherical, and cylindrical sound waves in lossless fluids," J. Acoust. Soc. of Am. 36, p. 217 (1964).

14. D.H. Trivett and A.L. Van Buren, "Propagation of plane, cylindrical, and spherical finite amplitude waves," J. Acoust. Soc. Am. 69, 1981, pp 943-949.

15. C. Eckart, "Vortices and Streams Caused by Sound Waves," Phys. Rev. 73, pp. 68-76 (1948).

16. P.J. Westervelt, "Scattering of sound by sound," J. Acoust. Soc. Am. 29, p. 199 (1957).

17. P.J. Westervelt, "Parametric acoustic array," J. Acoust. Soc. Am. 35 (4), pp. 535-537 (1963).

18. M.J. Lighthill, Proc. Roy. Soc. (London), A211, p. 564 (1952).

19. J.L.S. Bellin and R.T. Beyer, "Experimental investigation of an end-fire array," J. Acoust. Soc. Am. 34, p. 1051 (1962)

20. L.W. Dean, "Interactions between sound waves," J. Acoust. Soc. Am. 34, p. 1039 (1962).

21. V.R. Lauvstad, "Nonlinear Interaction of Two Monochromatic Sound Waves," Acustica 16, p. 191 (1966)

22. L.W. Dean and S.B. Friedlander, S.B. Quart. Progr. Report No. 75, p. 39 (1964).

23. D. Censor, "Scattering by Time-Varying Obstacles," J. Sound & Vib. 25 (1), pp. 101-110 (1972).

24. P.H. Rogers, "Comments on 'Scattering by Time-Varying Obstacles'," J. Sound & Vib. 28 (4), pp. 764-68 (1973).

25. Reference 17, Eq. (7).

26. P.J. Westervelt, "Scattering of sound by sound," J. Acoust. Soc. Am. 29, p. 934 (1957).

27. J.J. Truchard, "A Theoretical and Experimental Investigation of the Parametric Acoustic Receiving Array," Applied Research Laboratories, The University of Texas at Austin, Report No. ARL-TR-74-17 (1974).

28. A.L. Van Buren, P.H. Rogers, & J.C. Piquette, "Some Comments on the Interaction of Sound With Sound," presentation at 98th Mtg. of Acoust. Soc. Am., Nov 1979.

29. P.M. Morse & K.U. Ingard, Theoretical Acoustics, McGraw-Hill, 1968, p. 310.

30. Reference 5, p. 109.

31. B.J. Smith, "An Experimental Study of a Parametric End-Fire Array," J. Sound & Vib. 14, pp. 7-21 (1971).

32. See, for example, Abramowitz & Stegun, Handbook of Mathematical Functions, Dover, 1972, p. 887.

33. D.E. Gray (coordinating editor), AIP Handbook, Third Edition, McGraw-Hill, 1972 (Section 3C by Hunt).

34. L.E. Kinsler and A.R. Frey, Fundamentals of Acoustics, John Wiley and Sons (1962) p. 235.

35. A.L. Van Buren and M.A. Breazeale, "Reflection of finite-amplitude ultrasonic waves II. Propagation," J. Acoust. Soc. Am. 44, p. 1021 (1968).

36. A.B. Coppens, R.T. Beyer, M.B. Seidin, J. Donahue, F. Guipin, R.H. Hodson, and C. townsend, "Parameter of nonlinearity in fluids," J. Acoust. Soc. Am. 38, p. 797 (1965).

37. F.V. Hunt, "Notes on the exact equations governing the propagation of sound in fluids," J. Acoust. Soc. Am. 27, p. 1019 (1955).

38. A.L. Van Buren, "The Effect of Third Order Terms in the Equation of State," Dept. of Physics, University of Tennessee, Ultrasonics Lab. Memo. #10, Jan 1968.

39. P.M. Morse & K.U. Ingard, Handbuch der Physik Vol. Xl/1, Springer-Verlag, 1961, pp 26-27.

40. D.T. Blackstock, "Approximate Equations Governing Finite Amplitude Sound in Thermoviscous Fluids," General Dynamics Corp. Tech. Report No. GD-1463-52, 1963, p. 17.

41. Reference 29, p. 283.

42. Reference 29, p. 366, Eq. 7.3.18.

43. Gradshteyn and Ryzhik, Table of Integrals, Series and Products, Academic Press, 1965, p. 979, Eq. 8.53.1.2.

44. Reference 29, p. 401.

45. A.H. Stroud & D. Secrest, Gaussian Quadrature Formulas, Prentice-Hill, Inc., Englewood Cliffs, N.J., 1966.

46. F.B. Hildebrand, Introduction to Numerical Analysis, McGraw-Hill, 1956, p. 319.

47. Reference 32, pp. 411-412.

48. M.B. Moffett and J E. Blue, "Hydrophone Nonlinearity Measurements," Naval Underwater Systems Center Tech. Memo. No. 801150, Sep. 1980.

49. M.B. Moffett and T.A. Henriquez, "Hydrophone Nonlinearity Measurements," J. Acoust. Soc. Am. 72, pp 1-6 (1982).

50. J.L.S. Bellin & R.T. Beyer, "Experimental investigation of an end-fire array," J. Acoust. Soc. Am. 34, p. 1051 (1962).

51. H. Hoback, "Experimental Investigation of an Acoustical End Fired Array," J. Sound & Vib. 6, p. 460 (1967).

52. T.G. Muir & J.E. Blue, "Experiments on the acoustic modulation of large amplitude waves," J. Acoust. Soc. Am. 46, p. 227 (1969).

53. T.G. Muir & J.G. Willette, "Parametric acoustic transmitting arrays," J. Acoust. Soc. Am. 52, p. 1481 (1972).

54. J.E. Manning and G. Mardanik, "Radiation properties of cylindrical shells," J. Acoust. Soc. Am. 36, p. 1691 (1964).

55. A.I. Eller, "Application of the USRD type E8 transducer as an acoustic parametric source," J. Acoust. Soc. Am. 56, p. 1735 (1975).

56. M.B. Moffett & R.H. Mellen, "Nearfield characteristics of parametric acoustic sources," J. Acoust. Soc. Am. 69, p. 404 (1981).

57. L.E. Kinsler & A.R. Frey, Fundamentals of Acoustics, John Wiley & Sons, 1962, p. 226, Eq. 9.17a.

58. Reference 5, p. 44.

59. W.P. Mason (editor) Physical Acoustics, Part IA, Section 3 (D.A. Berlincourt, D.R. Curran, & H. Juffe), Academic Press, 1964, p. 230.

60. T.F. Hueter & R.H. Bolt, Sonics, John Wiley & Sons, 1965, p. 97.

61. L.D. Luker & A.L. Van Buren, "Phase calibration of hydrophones," J. Acoust. Soc. Am. 70, p. 516, 1981.

62. Reference 56, p. 406, Fig. 1.

63. This equation can be readily derived from Eqs. 4.18, 4.19, and 4.21 in Reference 57, pp 94-95, noting that Z_e is not equal to $\rho_o c$ as is assumed there.

64. Reference 29, p. 384, Eq. 7.4.31.

65. Reference 29, p. 311, Eq. 7.1.5.

66. Reference 5, p. 93, Eq. 3.4.

67. N.J. Sonine, Math. Ann., XVI, 1880, pp 1-80.

68. G.N. Watson, A Treatise on the Theory of Bessel Functions, Cambridge U. Press, London, 1966, pp 132-134.

69. Y.L. Luke, Integrals of Bessel Functions, McGraw-Hill, N.Y., 1962.

70. B.A. Peavy, "Indefinite integrals involving Bessel functions," J. of Research, National Bureau of Standards, B, V. 71B (1967), pp 485-490.

71. E.W. Ng, "Recursive Formula for the computation of certain integrals or Bessel functions," J. Math. Phys. 46 (1967), pp 223-224.

72. F.W. Cotton, "A Study of the Linear stability problem for viscous incompressible fluids in circular geometries by means of a matrix-Eigenvalue approach", Ph.D. thesis, Stevens Institute of Technology, 1977.

73. Y.L. Luke, "An associated Bessel function," J. Math. Phys. 31, pp 131-138 (1952).

74. N.W. McLachlan and A.L. Meyers, "Integrals involving Bessel and Strove functions," Philos. Mag. 21, pp 437-448 (1936).

75. See e.g., G.M. Murphy, Ordinary Differential Equations and Their Solutions, D. Van Nostrand, Princeton, N.J. (1960).

APPENDIX

A NEW TECHNIQUE FOR EVALUATING A GENERAL CLASS OF INDEFINITE INTEGRALS

1. The Technique.

We consider integrals of the form

$$I = \int dx f(x) \prod_{i=1}^{m} R_{\mu_i}^{(i)}(x) \ , \tag{A1}$$

where $R_{\mu_i}^{(i)}(x)$ is the i^{th} type of special function of order μ_i obeying the following set of recurrence relations:

$$R_{\mu+1}^{(i)}(x) = a_\mu(x)R_\mu^{(i)}(x) + b_\mu(x)R_{\mu-1}^{(i)}(x), \tag{A2a}$$

$$DR_\mu^{(i)}(x) = c_\mu(x)R_\mu^{(i)}(x) + d_\mu(x)R_{\mu-1}^{(i)}(x). \tag{A2b}$$

Integrals of the form (A1) are considered by several other authors [67-74] when the functions $R_{\mu_i}^{(i)}(x)$ are Bessel functions. In relations A2, a_μ, b_μ, c_μ, and d_μ are known functions corresponding to $R_\mu^{(i)}$. The symbol D represents d/dx. The function f(x) and the product $\pi R_\mu^{(i)}$ are both assumed bounded and continuous (or with at most a finite number of discontinuities) over an interval $[x_1,x_2]$, insuring that the integral I exists in the same interval.

Recurrence relations [Eq. (A2)] may be combined to show that the functions $R_\mu^{(i)}$ satisfy the differential equation

$$D^2R_\mu^{(i)} + \left[\frac{a_{\mu-1}d_{\mu-1}}{b_{\mu-1}} - c_\mu - c_{\mu-1} - \frac{1}{d_\mu}(Dd_\mu)\right] DR_\mu^{(i)}$$

$$+ \left[c_\mu c_{\mu-1} - Dc_\mu + \frac{c_\mu}{d_\mu} Dd_\mu \right.$$

$$\left. - \frac{d_{\mu-1}}{b_{\mu-1}}(d_\mu + c_\mu a_{\mu-1})\right] R_\mu^{(i)} = 0. \qquad \text{(A3)}$$

Equation (A3) is a special case of the Sturm-Liouville differential equation

$$D[\rho(x)D\psi(x)] + [S(x) + \gamma r(x)]\,\psi(x) = 0\ , \qquad \text{(A4)}$$

where $r(x) = 0$

$$\rho(x) = \exp\left\{\int dx\left[\frac{a_{\mu-1}d_{\mu-1}}{b_{\mu-1}} - c_\mu - c_{\mu-1} - \frac{1}{d_\mu} Dd_\mu\right]\right\}$$

$$S(x) = \rho(x)\left[c_\mu c_{\mu-1} - Dc_\mu + \frac{c_\mu}{d_\mu} Dd_\mu - \frac{d_{\mu-1}}{b_{\mu-1}}(d_\mu + c_\mu a_{\mu-1})\right]$$

$$\psi(x) = R_\mu^{(i)}(x)\ .$$

If either Eq. (A2a) or (A2b) is a two-term recurrence relation (i.e., if b_μ or d_μ is equal to zero for all μ), then the above expressions are undefined and $R_\mu^{(i)}$ does not satisfy the Sturm-Liouville differential equation. In this case $R_\mu^{(i)}$ satisfies instead a first-order differential equation and is in the form of an exponential. This may be readily seen by letting $d_\mu = 0$ in Eq. (A2b), in which case

$$R_\mu^{(i)}(x) = \exp[\int dx c_\mu]\ . \qquad \text{(A5)}$$

On the other hand, if $b_\mu = 0$, we obtain from Eq. (A2a): $R_\mu^{(i)} = a_{\mu-1}R_{\mu-1}^{(i)}$, which when combined with Eq. (A2b) yields

$$R_{\mu}^{(i)}(x) = \exp\left\{\int dx[c_{\mu} + (d_{\mu}/a_{\mu-1})]\right\}. \qquad (A6)$$

An extensive search of the literature indicated that functions satisfying the recurrence relations [Eq. (A2)] have not previously been named. For the purposes of this Appendix we shall refer to them as birecurrent functions. Most of the special functions of physics fall into this category (including all Bessel functions, Legendre functions, Hermite polynomials, etc.). We exclude the special cases given in Eqs. (A5) and (A6) from this category, preferring to call them exponential terms instead.

At this point it will be noted that the assumed form [Eq. (A1)] may be applied to the integrals occurring in Eq. (115) with the following identifications made

$$f(x) \rightarrow r'$$

$$R_{\mu_i}^{(i)} \rightarrow Z_{\ell}^{(m)}(k_n r'),$$

where $Z_{\ell}^{(m)}(k_n r')$ is the ℓ^{th} order Bessel function of the m^{th} kind. For $m = 1$, Z_{ℓ} may be taken to be J_{ℓ}, the Bessel function of the first kind. For $m = 2$, Z_{ℓ} may be taken to be either $H_{\ell}^{(1)}$ or $H_{\ell}^{(2)}$, the Hankel functions of the first and second kinds, respectively. The quantity k_n is taken to be any of the appropriate wavenumbers occurring in Eq. (115). Hence, the technique herein described could potentially be applied directly to the integrals occurring in this equation (as will be noted later, this turns out to be somewhat impractical).

The integration technique presented in this Appendix involves a generalization of the method (described by Watson [68]) used by Sonine [67] to evaluate certain indefinite integrals of Bessel functions. The integral to be evaluated in Sonine's method is replaced by a differential equation. A particular solution of the differential equation is then sufficient to express the result of integration. In the present work we generalize the method to include all functions obeying the relations [Eq. (A2)]. In addition we

describe an approach for obtaining and solving the appropriate differential equations.

2. The Details.

We assume the integral [Eq. (A1)] may be expressed in the form,

$$I = \sum_{p_1=0}^{1} \sum_{p_2=0}^{1} \cdots \sum_{p_m=0}^{1} A_{p_1,p_2,\cdots,p_m}(x) \prod_{i=1}^{m} R^{(i)}_{\mu_i+p_i}, \tag{A7}$$

where the 2^m coefficients $A_{p_1,p_2,\cdots,p_m}(x)$ are functions to be determined. For convenience, we will represent the multiple summation and the coefficients in Eq. (A7) by the shorthand notations $\sum_{\{p\}}$ and A_p, respectively. In order to determine the functions A_p, we differentiate Eq. (A7), substitute for DI the integrand from Eq. (A1), and obtain

$$f(x) \prod_{i=1}^{m} R^{(i)}_{\mu_i} = \sum_{\{p\}} \left[A_p D \prod_{i=1}^{m} R^{(i)}_{\mu_i+p_i} + (DA_p) \prod_{i=1}^{m} R^{(i)}_{\mu_i+p_i} \right]. \tag{A8}$$

Due to the recurrence relations [Eq. (A2)], it is always possible to express the first sum on the right-hand side of Eq. (A8) in the form

$$\sum_{\{p\}} A_p \sum_{q_1=0}^{1} \sum_{q_2=0}^{1} \cdots \sum_{q_m=0}^{1} B_{qp} \prod_{i=1}^{1} R^{(i)}_{\mu_i+q_i},$$

or

$$\sum_{\{p\}} \sum_{\{q\}} B_{pq} A_q \prod_{i=1}^{m} R^{(i)}_{\mu_i+p_i}, \tag{A9}$$

where the 2^{2m} coefficients $B_{pq} \equiv B_{p_1,p_2,\cdots,p_m q_1,q_2,\cdots,q_m}(x)$ are known functions resulting from repeated applications of the relations [Eq. (A2)] and the regrouping of terms in the form $\prod_{i=1}^{m} R^{(i)}_{\mu_i+p_i}$.

Using Eq. (A9) we can rewrite Eq. (A8) to obtain

$$f(x) \prod_{i=1}^{m} R_{\mu_i}^{(i)} = \sum_{\{p\}} \left[DA_p + \sum_{\{q\}} B_{pq} A_q \right] \prod_{i=1}^{m} R_{\mu_i + p_i}^{(i)} . \tag{A10}$$

We can now obtain a coupled set of differential equations for the functions A_p by imposing the sufficient condition that the coefficients of like special functions on each side of Eq. (A10) be equal. Doing this, we obtain the following coupled set of linear inhomogeneous differential equations of first order

$$f(x) \prod_{j=1}^{m} \delta_{0,p} = DA_p + \sum_{\{q\}} B_{pq} A_q , \tag{A11}$$

where δ is the Kronecker delta.

In solving the set [Eq. (A11)] of 2^m equations in the 2^m unknown functions A_p, one normally proceeds by differentiation and algebraic manipulation to uncouple a particular function from the remainder. This results in a differential equation of order 2^{m+1}. A particular solution of this uncoupled equation involves a particular choice of 2^{m+1} constants. Since this is exactly the number of arbitrary constants that the original set [Eq. (A11)] involves, one must be careful not to introduce any further arbitrary constants. In this case we obtain the remaining functions by expressing them in terms of derivatives of the initial function that has been calculated, rather than in terms of integrals of it. Regardless of the method used in obtaining a particular solution of Eq. (A11), one must avoid introducing more than 2^{m+1} arbitrary constants. Otherwise, the solution so obtained will neither satisfy Eq. (A11) nor provide, via Eq. (A7), a proper representation of the integral Eq. (A1).

When the integrand of Eq. (A1) contains more than one birecurrent function, it may be desirable to move one (or possibly more) of the birecurrent functions out of the product term and treat it as part of f(x). Each birecurrent function appearing in the product term doubles the number of unknown coefficient functions A_p and, hence, doubles the number of coupled differential equations to be solved. Thus, we halve the number of

differential equations each time we move a birecurrent function out of the product term and group it with f(x). However, each function so grouped will appear in the inhomogeneous term of the final set of differential equations. Conversely, none of the birecurrent functions grouped in the product term will appear explicitly in the final set of differential equations.

Any particular solution of Eq. (A11) will give a set of functions A_p that can be used in Eq. (A7) to express the result of the integration. We can see this if we differentiate the expression that results by substitution of this particular set into Eq. (A7). The resulting Eq. (A8) is obviously satisfied since the A_p are a <u>particular</u> solution. The fact that only a particular, rather than a general, solution is required is a powerful aspect of the technique.

The coupled set [Eq. (A11)] is a standard form of linear inhomogeneous differential equations of first order that may be solved by well-known methods. A particular solution of Eq. (A11) is easier to obtain than one may suspect since each equation contains exactly one term involving the derivative of a particular function A_p and the derivative of each of the functions A_p appears in only one equation.

The technique described above is equally applicable, with slight modifications, when one or more of the birecurrent functions in the product term of Eq. (A1) is replaced by an exponential term of the form Eq. (A5) or (A6). Because the exponential terms satisfy two-term recurrence relations, we do not have to include p = 1 terms for them in Eq. (A7). This reduces the number of unknown coefficients A_p and the resulting coupled differential equations by a factor of 2. Moving the exponential term from the product term into f(x) does not change the number of differential equations to be solved.

3. <u>An Example</u>.

To illustrate the technique, we obtain the result to the following well-known integral: $I = \int dx x \sin\mu x$. In this case, $f(x) = x$ and $R_\mu(x) = \sin\mu x$.

The simplest way to apply the technique to this problem is to consider $\sin\mu x$ as the imaginary part of the exponential $R_\mu(x) = \exp(i\mu x)$ and assume that $I = A(x)\exp(i\mu x)$. Only one term, and hence only one unknown coefficient A(x), is required in I in this case because differentiation of the exponential

does not produce new functions (i.e., recurrence relation [Eq. (A2b)] reduces to a 2-term equation relating DR_μ to R_μ).

We shall use instead a somewhat more complicated approach that requires two unknown coefficients in order to illustrate several important aspects of the technique. This approach is based on the fact that the set of two functions $\sin\mu x$ and $\cos\mu x$ is closed under differentiation so that it is convenient to choose $R_\mu = \sin\mu x$ and $R_{\mu+1} = \cos\mu x$. We now proceed to obtain the integral following a step-by-step procedure:

a. We assume I may be expressed in the form

$$I = A_0(x)\sin\mu x + A_1(x)\cos\mu x \ . \tag{A12}$$

b. Differentiation produces $DI = \mu A_0(x)\cos\mu x + [DA_0(x)]\sin\mu x - \mu A_1(x)\sin\mu x + [DA_1(x)]\cos\mu x$.

c. Equating DI to the integrand $x\sin\mu x$ and separately equating coefficients of $\sin\mu x$ and $\cos\mu x$, we obtain the following differential equations

$$DA_0 - \mu A_1 = x, \tag{A13a}$$

$$\mu A_0 + DA_1 = 0. \tag{A13b}$$

d. We now uncouple A_0 and A_1 by substituting into Eq. (A13a) the expression for A_0 obtained from Eq. (A13b). This gives

$$D^2A_1 + \mu^2A_1 = -\mu x. \tag{A14}$$

e. A particular solution of Eq. (A14) is

$$A_1(x) = -x/\mu. \tag{A15}$$

Substitution of Eq. (A15) into Eq. (A13b) yields

$$A_0(x) = 1/\mu^2. \tag{A16}$$

f. Substitution of Eq. (A15) and Eq. (A16) into Eq. (A12) gives the result $\int dx x \sin\mu x = (\sin\mu x - \mu x \cos\mu x)/\mu^2$.

In order to investigate the consequences of using a different particular solution than the one chosen, we first obtain the general solution of Eq. (A14). It is

$$A_1(x) = C_1 \sin\mu x + C_2 \cos\mu x - x/\mu, \tag{A17}$$

where C_1 and C_2 are arbitrary constants. Substitution of Eq. (A17) into Eq. (A13b) yields

$$A_0(x) = -C_1 \cos\mu x + C_2 \sin\mu x + 1/\mu^2. \tag{A18}$$

Substitution of these general solutions for A_0 and A_1 into Eq. (A12) produces the following expression for the desired integral:

$$\int dx x \sin\mu x = (\sin\mu x - \mu x \cos\mu x)/\mu^2 + C_2 \, . \tag{A19}$$

Equation (A19) involves only a single arbitrary constant to which the indefinite integral under consideration is entitled. Since the completely general solution to Eq. (A14) was used in obtaining Eq. (A19), it is clear that any particular solution to Eq. (A14) would have sufficed, with only the constant C_2 in Eq. (A19) being affected by a different choice.

4. A Second Example.

Although the first example provides a succinct illustration of the present integration technique, an integration-by-parts approach would certainly have been more straightforward.

Another example is presented that is less susceptible to standard techniques and is more relevant to the nonlinear scattering problem at hand.

We note again that the integrals contained in Eq. (115) may all be put into the form Eq. (A1). Unfortunately, if this were done directly, it would result in a set of eight coupled first-order differential equations.

Uncoupling of this equation has not, as yet, proved to be a tractable problem. However, if the Zeroth-order Hankel function (which occurs in all of the integrals) and one of the other of the two remaining Bessel functions are replaced by their asymptotic forms (for large argument as compared to order), the following general type of integral is obtained

$$I = \int dr r^{\mu} Z_{\nu}(r) \exp(ir), \tag{A20}$$

where $Z_{\nu}(r)$ is an arbitrary Bessel function of one of the first three kinds of real argument r, and the range of integration is restricted to r>0. For generality, both the order ν and the exponent μ are chosen to be complex.

To begin the technique, we assume that I may be written as

$$I = A_0(r) Z_{\nu}(r) + A_1(r) Z_{\nu+1}(r) \ . \tag{A21}$$

Differentiating Eq. (A21), expressing the resulting Bessel function derivatives in terms of Z_{ν} and $Z_{\nu+1}$ by use of the appropriate recurrence relations, equating the result to the integrand of Eq. (A20), and imposing the sufficient condition that coefficients of like-order Bessel functions be equal, we obtain the following coupled set of differential equations

$$A_0 - DA_1 + [(\nu + 1)/r]A_1 = 0,$$

$$DA_0 + (\nu/r)A_0 + A_1 = r^{\mu} \exp(ir). \tag{A22}$$

These equations may be uncoupled to yield

$$D^2 A_1 - (1/r)DA_1 + [1 + (1 - \nu^2)/r^2]A_1 = r^{\mu} \exp(ir). \tag{A23}$$

We now define a function $\rho(r)$ such that

$$A_1(r) = r\rho(r). \tag{A24}$$

Substitution into Eq. (A23) yields

$$r^2D^2\rho + rD\rho + [r^2 - \nu^2]\rho = r^{\mu+1}\exp(ir). \tag{A25}$$

One particular solution to Eq. (A25) is an associated Bessel function as defined by Luke [69], namely, $\rho(r) = i^{\mu+1}H_{\mu,\nu}(-ir)$, so that

$$A_1(r) = i^{\mu+1}rH_{\mu,\nu}(-ir). \tag{A26}$$

Use of the known properties of the associated Bessel functions results in

$$A_0(r) = i^{\mu+1}r\,[(\mu - \nu)(\mu - \nu - 1)H_{\mu-1,\nu+1}(-ir) + (-ir)^{\mu}\exp(ir)]/(2\mu + 1), \tag{A27}$$

when the expression for A_1 given by Eq. (A26) is substituted into the first of the Eqs. (A22). We thus have

$$\int dr r^{\mu}Z_{\nu}(r)\exp(ir) = i^{\mu-1}r\{[(\mu - \nu)(\mu - \nu - 1)H_{\mu-1,\nu+1}(-ir) + (-ir)^{\mu}\exp(ir)]/(2\mu + 1)\}Z_{\nu}(r) + i^{\mu+1}rH_{\mu,\nu}(-ir)Z_{\nu+1}(r). \tag{A28}$$

This result is identical to that obtained by Luke [73] using a specialized integration technique developed by McLachlan and Meyers [74] for certain integrals involving Bessel and Struve functions. Luke [73] provides formulas by which the associated Bessel functions appearing in Eq. (A28) may be evaluated.

The above example resulted in a differential equation that was recognizable. However, the technique is still applicable even if no previously known solution to the differential equation exists. We first try to obtain a particular solution to our inhomogeneous differential equation by using standard methods [75] such as the method of Lagrange or the method by Cauchy. If none of these methods proves satisfactory, we can always obtain a solution in the form of an infinite series. As an example of this, we again

return to Eq. (A23) and assume that A_1 may be expressed as

$$A_1 = \exp(ir) \sum_{m=-\infty}^{\infty} B_m r^{m+\mu}, \tag{A29}$$

where the coefficients B_m are constants to be determined. To simplify subsequent calculations, we chose the form of the expansion to be compatible with the inhomogeneous term. If Eq. (A29) is substituted into Eq. (A23) and coefficients of like powers of r are equated, the following recursion relation is obtained for the B_m:

$$(m + \mu + \nu)(m + \mu - \nu)B_{m+1} + i[2(m + \mu) - 1]B_m = \delta_{m,1}. \tag{A30}$$

We can obtain a particular solution to Eq. (A30) and, hence, to Eq. (A23) by setting $B_m = 0$ for $m>1$ and solving for the nonzero coefficients B_m, $m = 1, 0, -1, \ldots,$. The resulting descending power series representation for A_1 can be expressed in terms of a hypergeometric function as

$$A_1 = i^{\mu+1} r\{(-1)^{\mu+1}(ir)^{\mu}\exp(ir)_3F_1 \\ [1,-\mu+\nu,-\mu+\nu,-\mu-\nu;\ (1/2)-\mu;\ (1/2)ir]/(2\mu+1)\}. \tag{A31}$$

In view of Eq. (A26), it is not surprising that the quantity in brackets is identical to the series representation of $H_{\mu,\nu}(-ir)$ given by Luke [69]. The solution [Eq. (A31)] is not defined if $\mu = -1/2$. It is also not defined if μ is an odd multiple of 1/2 unless both $\mu \pm \nu$ are positive integers or zero. The solution is a terminating series if either $\mu + \nu$ or $\mu - \nu$ is a positive integer. The infinite series obtained otherwise is an asymptotic representation of A_1 that is valid for $r \to \infty$.

We can obtain a second particular solution for A_1 by setting $B_m = 0$ for $m \leq 1$ and solving Eq. (A30) for B_m, $m = 2,3,\ldots,$. The hypergeometric representation of the resulting ascending power series in r is

$$A_1 = i^{\mu+1} r \{(-ir)^{\mu+1} {}_2F_2$$

$$(1, \mu + \tfrac{3}{2}; \mu - \nu + 2, \mu + \nu + 2; -2ir)/$$

$$[(\mu - \nu + 1)(\mu + \nu + 1)]\}. \qquad \text{(A32)}$$

The quantity appearing in braces in Eq. (A32) is the series representation of the associated Bessel function $h_{\mu,\nu}(-ir)$ as defined by Luke [69]. This function is a second particular solution to the differential equation satisfied by $H_{\mu,\nu}$ and hence can be used in place of H in the solution [Eq. (28)] to the original integral.

The solution [Eq. (A32)] is a terminating series if μ is a positive odd multiple of -1/2 (other than -1/2) and if both $\mu \pm \nu$ are not positive integers. It is not defined if either $\mu + \nu$ or $\mu - \nu$ is a negative integer and μ is not a positive odd multiple of -1/2 (other than 1/2).

5. Additional Illustrative Examples.

The two previous examples illustrate the power and versatility of the current integration technique, but two objections may be raised: The first example can be handled trivially, and the second example is one involving products of Bessel functions and, hence, is amenable to the original approach proposed by Sonine. The examples that follow will serve to illustrate the applicability of the current technique to integrals that are not of the Bessel function type. Although some of these may be solved by standard techniques, they nonetheless illustrate the broad range of integrands that can successfully be handled via this technique (and to the author's knowledge, several of these integrals have not been previously tabulated).

a. Some integrals involving Legendre functions. We now consider some examples of integrals of the general form

$$I = \int dx P_\nu(x) f(x), \qquad \text{(A33)}$$

where $P_\nu(x)$ is the Legendre function of order ν and $f(x)$ has the same meaning as in Eq. (A1). We assume the integral I may be represented in the usual way as

$A(x)P_\nu(x) + B(x)P_{\nu+1}(x)$. Following the procedure outlined in Section 2, we obtain two coupled equations for A and B which can be uncoupled to yield

$$A(x) = -xB(x) + \frac{(1-x^2)}{(\nu+1)} B'(x), \tag{A34}$$

where

$$(1-x^2)B''(x) - 2xB'(x) + \nu(\nu+1)B(x) = (\nu+1)f(x). \tag{A35}$$

As a first example of an integral of the form Eq. (A33), we consider the case where $f(x) = 1$. A particular solution to Eq. (A35) for this case is $B(x) = (1/\nu)$. Equation (A34) now determines A(x) to be $A(x) = -(x/\nu)$. Substitution of A and B into the representation for I now produces

$$\int dx P_\nu(x) = -\frac{x}{\nu} P_\nu + \frac{1}{\nu} P_{\nu+1}. \qquad \nu \neq 0 \tag{A36}$$

We next consider a more challenging integrand [i.e., one which cannot be handled by direct manipulation of the recurrence relations for $P_\nu(x)$]. Let $f(x)$ be $\ln(1\pm x)$. In obtaining a particular solution to Eq. (A35) we use the inhomogeneous term as a guide and assume $B(x) = K_1 \ln(1\pm x) + K_2$, where K_1 and K_2 are undetermined constants. Direct substitution into Eq. (A35) gives $K_1 = 1/\nu$ and $K_2 = 1/[\nu^2(\nu+1)]$. Equation (A34) may next be used to show that $A(x) = \{-(x/\nu)\ln(1\pm x) \pm 1/[\nu(\nu+1)] - x/\nu^2\}$. Substitution of A and B into the representation for I results in

$$\int dx \ln(1\pm x)P_\nu(x) = \left[-\frac{x}{\nu}\ln(1\pm x) \pm \frac{1}{\nu(\nu+1)} - \frac{x}{\nu^2}\right] P_\nu(x) + \left[\frac{1}{\nu}\ln(1\pm x) + \frac{1}{\nu^2(\nu+1)}\right] P_{\nu+1}.$$

$$\nu \neq 0,-1 \tag{A37}$$

b. Some integrals involving Hermite functions. We next consider integrals of the general form

$$I = \int dx H_\nu(x) f(x), \tag{A38}$$

where $H_\nu(x)$ is the Hermite function of order ν, and once again $f(x)$ has the same meaning as was used in connection with Eq. (A1). We assume the integral of Eq. (A38) may be represented as $A(x)H_\nu(x) + B(x)H_{\nu-1}(x)$. (Note that H_ν and $H_{\nu-1}$ are used to represent the integral as opposed to H_ν and $H_{\nu+1}$. This difference is inconsequential. Any two orders separated by one integral value will be adequate to implement the procedure.) Omitting the details, we uncouple the resulting coupled set to obtain

$$A(x) = -\frac{x}{\nu} B(x) - \frac{B'(x)}{2\nu}, \tag{A39}$$

where

$$2\nu f(x) = -B''(x) - 2xB'(x) - 2(\nu+1)B(x). \tag{A40}$$

As a first example of this general form, we let $f(x) = e^{-x^2}$. [This is the usual weighting function used in the orthogonality integral for $H_\nu(x)$.] If we assume a particular solution of Eq. (A40) of the form $B(x) = Ke^{-x^2}$ (with K an undetermined constant), direct substitution gives $K = -1$. Equation (A39) gives $A(x) = 0$ so that

$$\int dx e^{-x^2} H_\nu(x) = -e^{-x^2} H_{\nu-1}(x). \tag{A41}$$

As a second example we let $f(x) = x^{-\mu}$, where for the moment μ is an arbitrary exponent. If we assume a particular solution of the form $B(x) = K_1 x^{-K_2}$, where K_1 and K_2 are constants, direct substitution into (A42) produces

$$2\nu x^{-\mu} = -K_1 K_2 (K_2+1) x^{-(K_2+2)} + 2K_1 [K_2 - (\nu+1)] x^{-K_2}. \tag{A42}$$

There are two sets of values for the constants K_1, K_2, and μ for which Eq. (A42) is satisfied: $K_1 = \frac{-2\nu}{(\nu+1)(\nu+2)}$, $K_2 = \nu+1$, $\mu = \nu+3$; and $K_1 = -\frac{\nu}{(\nu+2)}$, $K_2 = -1$, $\mu = -1$. Using the first set of values, we obtain the result

$$\int dx H_\nu(x) x^{-(\nu+3)} = \left[\frac{2x^{-\nu}}{(\nu+1)(\nu+2)} - \frac{x^{-(\nu+2)}}{(\nu+2)}\right] H_\nu(x)$$

$$- \frac{2\nu}{(\nu+1)(\nu+2)} x^{-(\nu+1)} H_{\nu-1}(x) \qquad \text{(A43)}$$

$$\nu \neq -1, -2.$$

We obtain from the second set of values

$$\int dx x H_\nu(x) = \left(\frac{1+2x^2}{2(\nu+2)}\right) H_\nu(x) - \frac{\nu x}{(\nu+2)} H_{\nu-1}(x) \qquad \text{(A44)}$$

$$\nu \neq -2.$$

For a final example involving Hermite functions, we let $f(x) = xe^{i\gamma x}$, where γ is a constant initially assumed to be arbitrary.

A particular solution to Eq. (A40) can be obtained with $B(x) = Ke^{i\gamma x}$, where K is an unknown constant. Direct substitution shows that a solution exists for $\gamma = \sqrt{2(\nu+1)}$ and $K = i\nu/\sqrt{2(\nu+1)}$. Using the resulting solution for B in Eq. (A39) to obtain A, we then have

$$\int dx x e^{i\sqrt{2(\nu+1)}x} H_\nu(x) = e^{i\sqrt{2(\nu+1)}x} \left[\left(\frac{-ix}{\sqrt{2(\nu+1)}} + \frac{1}{2}\right) H_\nu(x) + \frac{i\nu}{\sqrt{2(\nu+1)}} H_{\nu-1}(x)\right]$$

$$\nu \neq -1. \qquad \text{(A45)}$$

c. Some examples involving Laguerre functions. We now consider integrals of the general form

$$I = \int dx f(x) L_\nu(x), \tag{A46}$$

where $L_\nu(x)$ is the Laguerre function of order ν, and $f(x)$ has the same meaning as in Eq. (A1). As usual, we represent I in the form $A(x)L_\nu(x) + B(x)L_{\nu-1}(x)$ and obtain the following uncoupled equations

$$A(x) = \left(\frac{x}{\nu} - 1\right) B(x) + \frac{x}{\nu} B'(x), \tag{A47}$$

where

$$\nu f(x) = xB''(x) + (x+1)B'(x) + (\nu+1)B(x). \tag{A48}$$

As an example of this case we let $f(x) = xe^{-(\nu+1)x}$. To obtain a particular solution of Eq. (A48), we assume $B(x) = Ke^{-(\nu+1)x}$. Direct substitution gives $K = 1/(\nu+1)$. Using this value yields the integral

$$\int dx x e^{-(\nu+1)x} L_\nu(x) = \frac{e^{-(\nu+1)x}}{(\nu+1)} [-(1+x)L_\nu(x) + L_{\nu-1}(x)]$$

$$\nu \neq -1. \tag{A49}$$

As a final example, we let $f(x) = x(1+x)^{-(\nu+3)}$. A particular solution to Eq. (A48) can then be obtained assuming $B(x) = K(1+x)^{-(\nu+1)}$, where again K is an unknown constant. Direct substitution into Eq. (A48) yields $K = \nu/[(\nu+1)(\nu+2)]$so that

$$\int dx x(1+x)^{-(\nu+3)} L_\nu(x) = \frac{(1+x)^{-(\nu+1)}}{(\nu+2)} \left[\left(\frac{x-\nu}{\nu+1} - \frac{x}{1+x}\right) L_\nu(x) + \left(\frac{\nu}{\nu+1}\right) L_{\nu-1}(x)\right]$$

$$\nu \neq -1, -2. \tag{A50}$$

d. Some final results. The following is a tabulation of some additional results obtained using the integration technique described in this paper. For the sake of brevity the derivations have been omitted.

$$\int dx x e^{-x^2} H_\nu(x) H_\mu(x) = e^{-x^2} \left\{ \frac{(\mu+\nu+1)}{2[(\mu-\nu)^2-1]} H_\mu(x) H_\nu(x) + \left(\frac{\mu}{\nu-\mu+1}\right) H_\nu(x) H_{\mu-1}(x) \right.$$

$$\left. + \left(\frac{\nu}{\mu-\nu+1}\right) H_{\nu-1}(x) H_\mu(x) + \left[\frac{2\mu\nu}{(\mu-\nu)^2-1}\right] H_{\nu-1}(x) H_{\mu-1}(x) \right\}, \tag{A51}$$

where H is a Hermite function and $\mu - \nu \neq \pm 1$.

$$\int dx [P_{\frac{1}{2}}(x)]^2 = \frac{x}{2} \left[P_{\frac{1}{2}}(x)^2 + P_{-\frac{1}{2}}(x)^2\right] - P_{\frac{1}{2}}(x) P_{-\frac{1}{2}}(x) \tag{A52}$$

and

$$\left[\frac{\mu(\mu+1) - \nu(\nu+1)}{(\nu+1)}\right] \int dx P_\nu(x) x^\mu = \frac{\mu(\mu-1)}{(\nu+1)} \int dx P_\nu(x) x^{\mu-2}$$

$$- x^\mu P_{\nu+1}(x) + \left[x^{\mu+1} - \frac{\mu(1-x^2)x^{\mu-1}}{(\nu+1)}\right] P_\nu(x)$$

$$\nu \neq -1. \tag{A53}$$